REPUBLIC OF TÜRKİYE
YILDIZ TECHNICAL UNIVERSITY
GRADUATE SCHOOL OF SCIENCE AND ENGINEERING

APPLICATIONS OF ARTIFICIAL INTELLIGENCE IN ENERGY PRODUCTION

Mert Akın İNSEL

DOCTOR OF PHILOSOPHY THESIS

Department of Chemical Engineering

Program of Chemical Engineering

Supervisor

Prof. Dr. Hasan SADIKOĞLU

Co-Supervisor

Assist. Prof. Dr. Özgün YÜCEL

February, 2025

REPUBLIC OF TÜRKİYE

YILDIZ TECHNICAL UNIVERSITY

GRADUATE SCHOOL OF SCIENCE AND ENGINEERING

APPLICATIONS OF ARTIFICIAL INTELLIGENCE IN ENERGY PRODUCTION

A thesis submitted by Mert Akın İNSEL in partial fulfillment of the requirements for the degree of **DOCTOR OF PHILOSOPHY** is approved by the committee on 19.02.2025 in Department of Chemical Engineering, Program of Chemical Engineering.

Prof. Dr. Hasan SADIKOĞLU
Yildiz Technical University
Supervisor

Assist. Prof. Dr. Özgün YÜCEL
Gebze Technical University
Co-supervisor

Approved By the Examining Committee

Prof. Dr. Hasan SADIKOĞLU, Supervisor
Yildiz Technical University _____

Prof. Dr. Nil ACARALI, Member
Yildiz Technical University _____

Prof. Dr. Murat ÖZDEMİR, Member
Gebze Technical University _____

Prof. Dr. Fatma Jale GÜLEN, Member
Yildiz Technical University _____

Assist. Prof. Dr. Meral YILDIRIM YALÇIN, Member
İstanbul Aydin University _____

I hereby declare that I have obtained the required legal permissions during data collection and exploitation procedures, that I have made the in-text citations and cited the references properly, that I haven't falsified and/or fabricated research data and results of the study and that I have abided by the principles of the scientific research and ethics during my Thesis Study under the title of "Applications of Artificial Intelligence in Energy Production" supervised by my supervisors, Prof. Dr. Hasan SADIKOĞLU and Assist. Prof. Dr. Özgün YÜCEL. In the case of a discovery of false statement, I am to acknowledge any legal consequence.

Mert Akın İNSEL

Dedicated with heartfelt gratitude

to my family, whose support knows no bounds,

and to my wife, whose love enlightens my path.

ACKNOWLEDGEMENTS

I would like to express my deep respect and gratitude to my supervisors, Prof. Dr. Hasan SADIKOĞLU and Assist. Prof. Dr. Özgün YÜCEL, for their unwavering support, insightful guidance, invaluable encouragement, and steadfast dedication. Their contributions have been pivotal not only to the successful completion of this thesis but also to my academic and personal growth. I am truly grateful and honored to have been one of their students.

I'd also like to thank Prof. Dr. Nil ACARALI and Prof. Dr. Murat ÖZDEMİR for their valuable insights and contributions to the completion of this thesis as TMC members.

Finally, I'd like to express my love and appreciation to my family, who have always supported me in any endeavor I have undertaken and never doubted that I would be successful in attaining my goals.

Mert Akın İNSEL

TABLE OF CONTENTS

LIST OF SYMBOLS

c	Completeness
C	Carbon
DBI	Davies-Bouldin Index
h	Homogeneity
H	Hydrogen
MI	Mutual Information Score
RI	Rand Index
s	Silhouette Coefficient
S	Sulfur
V	V-Measure

LIST OF ABBREVIATIONS

AI	Artificial Intelligence
ANN	Artificial Neural Network
AR	Autoregressive
ARI	Adjusted Rand Index
ARIMA	Autoregressive Integrated Moving Average
ARMA	Autoregressive average
Bi-LSTM	Bidirectional Long-Short Term Memory
CHI	Calinski-Harabasz Index
CS	Classification System
ELP	Electric Load Prediction
HHV	Higher Heating Value
INFPLS	Iterative Network-Based Fuzzy Partial Least Squares
LS	Least Squares
LSSVM	Least Square Support Vector Machine
LSTM	Long-Short Term Memory
MC	Moisture Content
ML-LSTM	Multi Layer Long-Short Term Memory
MLP	Multilayer Perceptron
MSE	Mean Squared Error
MVR	Multi-variate Regression
N	Nitrogen
NARX	Nonlinear Autoregressive Exogenous Inputs
O	Oxyhen
P	Proximate Analysis
PC	Pearson Correlation
PCA	Principal Component Analysis
PRETCR	Precipitation Corrected(mm/hour)
PS	Surface Pressure(kPa)

Q2VM	Specific Humidity at 2 Meters(g/kg)
R2	Correlation Coefficient
RBF	Radial Basis Function
RF	Random Forest
RFR	Random Forest Regression
RFR	Random Forest Regression
RH2M	Relative Humidity at 2 Meters(%)
RMSE	Root Mean Squared Error
RMSE	Root Mean Squared Error
S.F.	Supporting Files
S.I.	Supporting Information
SIF	Solar Irradiance Forecasting
SL-LSTM	Single Layer Long-Short Term Memory
ST	Short Term
SVM	Support Vector Machine
SVR	Support Vector Regression
T2M	Temperature at 2 Meters(C)
T2MDEW	Dew/Frost Point at 2 Meters(C)
T2MWET	Wet Bulb Temperature at 2 Meters(C)
TF	Transfer Function
U	Ultimate Analysis
UP	Ultimate & Proximate Analysis
VST	Very Short Term
WD10M	Wind Direction at 10 Meters(Degrees)
WD50M	Wind Direction at 50 Meters(Degrees)
WF	Wind Farm
WP	Wind Power
WPF	Wind Power Forecasting
WPSDF	Wind Power, Speed, Direction Forecasting
WS10M	Wind Speed at 10 Meters(m/s)
WS50M	Wind Speed at 50 Meters(m/s)
WSF	Wind Speed Forecasting
XGB	XGBoost

LIST OF FIGURES

LIST OF TABLES

ABSTRACT

Applications of Artificial Intelligence in Energy Production

Mert Akın İNSEL

Department of Chemical Engineering

Doctor of Philosophy Thesis

Supervisor: Prof. Dr. Hasan SADIKOĞLU

Co- supervisor: Assist. Prof. Dr. Özgün YÜCEL

This thesis investigates the most prevalent applications of the key artificial intelligence methodologies in energy production. Foremostly, as a regression problem, higher heating value estimation of wastes and fuels is undertaken by utilizing artificial neural networks (ANNs). Hyperparameter optimization was carried out for the obtainment of best ANN models possible with the available data. Secondly, a clustering approach was utilized to propose a novel classification system, namely HOM-CS, to enhance the correct classification and utilization of wastes and fuels. Finally, as a time-series problem, forecasting of wind power output of wind farms is investigated since the unpredictability and instability resulting from the extensive utilization of windpower result considerable problems for maintaining the secure and consistent operation of the energy system. A generalizable wind power prediction model based on publicly available data is obtained that can succesfully estimate the wind power of any wind farm in the specified region. Overall, this thesis showcases the application of artificial intelligence in energy production by considering the most challenging problems in the subject of energy production, which makes it a comprehensive and impactful contribution to the field. By addressing critical challenges such as accurate fuel

quality assessment, informative classification, and reliable renewable energy forecasting, the thesis paves the way for enhanced efficiency and sustainability in energy production. The methodologies and models developed are versatile, scalable, and applicable globally, providing valuable tools for researchers, industry professionals, and policymakers in optimizing energy systems and advancing waste-to-energy and renewable energy solutions.

Keywords: Artificial Intelligence, Biomass, Energy Production, Wind Power

ÖZET

Enerji Üretiminde Yapay Zeka Uygulamaları

Mert Akın İNSEL

Kimya Mühendisliği Anabilim Dalı

Doktora Tezi

Danışman: Prof. Dr. Hasan SADIKOĞLU

Eş-Danışman: Dr. Öğr. Üyesi Özgün YÜCEL

Bu tez, enerji üretimindeki temel yapay zeka metodolojilerinin en yaygın uygulamalarını araştırmaktadır. Öncelikle, bir regresyon problemi olarak, yapay sinir ağları (YSA'lar) kullanılarak atıkların ve yakıtların daha yüksek ısıtma değeri tahmini gerçekleştirilmiştir. Mevcut verilerle mümkün olan en iyi ANN modellerinin elde edilmesi için hiperparametre optimizasyonu yapılmıştır. İkinci olarak, atıkların ve yakıtların doğru sınıflandırılmasını ve kullanımını geliştirmek için yeni bir sınıflandırma sistemi olan HOM-CS'yi önermek için bir kümeleme yaklaşımı kullanılmıştır. Son olarak, bir zaman serisi problemi olarak, rüzgar enerjisinin yaygın kullanımından kaynaklanan öngörülemezlik ve istikrarsızlık, enerji sisteminin güvenli ve tutarlı bir şekilde çalışmasını sürdürmek için önemli sorunlara yol açtığından, rüzgar çiftliklerinin rüzgar enerjisi çıktısının tahmini araştırılmıştır. Belirtilen bölgedeki herhangi bir rüzgar çiftliğinin rüzgar gücünü başarılı bir şekilde tahmin edebilen, kamuya açık verilere dayalı genelleştirilebilir bir rüzgar enerjisi tahmin modeli elde edilmiştir. Genel olarak, bu tez, enerji üretimi konusundaki en zorlu sorunları göz önünde bulundurarak yapay zekanın enerji üretiminde uygulanmasını sergilemekte ve bu da onu alana kapsamlı ve etkili bir katkı haline getirmektedir. Tez, doğru yakıt kalitesi değerlendirmesi, bilgilendirici sınıflandırma ve güvenilir yenilenebilir enerji tahmini gibi kritik zorlukları ele

alarak, enerji üretiminde gelişmiş verimlilik ve sürdürülebilirliğin yolunu açmaktadır. Geliştirilen metodolojiler ve modeller çok yönlü, ölçeklenebilir ve küresel olarak uygulanabilir olup, araştırmacılar, endüstri profesyonelleri ve politika yapıcılar için enerji sistemlerini optimize etme ve atıktan enerjiye dönüştürme ve yenilenebilir enerji çözümlerini geliştirme konusunda değerli araçlar sağlamaktadır.

Anahtar Kelimeler: Biyokütle, Enerji Üretimi, Rüzgar Enerjisi, Yapay Zeka

1
INTRODUCTION

1.1 Applications of Artificial Intelligence in Energy Production

The energy generation has always been a priority for nations worldwide in terms of economic and security concerns (Amin et al., 2022). Furthermore, As the urgency of climate change escalates, governments, experts, and the global public are increasingly advocating for collective action to establish a sustainable energy system, referred to as the energy transition (Q. Wang et al., 2025). Thus, innovative solutions are needed to tackle the technological, financial, and social obstacles of decarbonization as a result of the global energy transition, which is being fueled by the necessity to slow down climate change. Thus, artificial intelligence applications emerged as a promising tool to be implemented in energy production and conversion systems, especially in topics of energy demand forecasting, fault detection and diagnosis, system optimization and control, renewable energy integration, and energy storage systems.

Collectively investigated, the artificial intelligence problems in energy production can be classified into four main categories, namely regression problems, classification problems, clustering problems, and time-series problems, as illustrated in Figure 1.1. The regression problems are the cases where the output of the artificial intelligence model is a continious dependent variable that can directly be estimated from the continious or discrete inputs (independent variables). Most common application examples in energy production sector are the estimation of fuel properties and biomass content for optimized fuel utilization. The classification problems can be defined as the modeling problems that tries to estimate a discrete output (the classes) from continious or discrete inputs. The most common such problems in the energy production sector are the classification of fuels or wastes for determining the most suitable use cases, fault detection and classification in energy systems (espacially for renewable energy), and clasification of the energy storage systems (i.e. batteries) according to their quality for the best applications. Clustering problems can be regarded as the problems where there is not an output we are aiming to obtain a model for, but rather, understand the nature of the data

and see if any meaningful clusters can be formed, which can then be referred as classes following the completion of the clustering study. While there are not as many clustering problems investigated in the literature for the energy sector yet, in theory, each classification problem may be investigated in the light of clustering algorithms. Some prevalent application areas are the clustering of fuels for appropriate application areas and the clustering of countries or regions with respect to their energy sources, demands, and productions. Time-series problems, while can also be considered as special regression problems from some perspectives, are the problems that depend on time as well as on the other independent variables. Thus, it is an estimation of the future step, or trend, which differs from the regression problems since the estimated variable is, by defination, out of the range of the estimators. Furthermore, optimization of appropriate lookback period (the data collected during the former time period that effects the output in the next time step) is also crucial in accurate solutions for the time-series problems. Since there are numerous use-cases for time dependent modeling in energy production such as energy production/demand forecastings, estimation of remeaning useful life for energy storage systems, weather forecasting, etc., solving these time-series problems by the utilization of artificial inteligence algorithms have attracted significant attention, and continues to be one of the most important type of problems in the energy sector due to the natural uncertainty of the future.

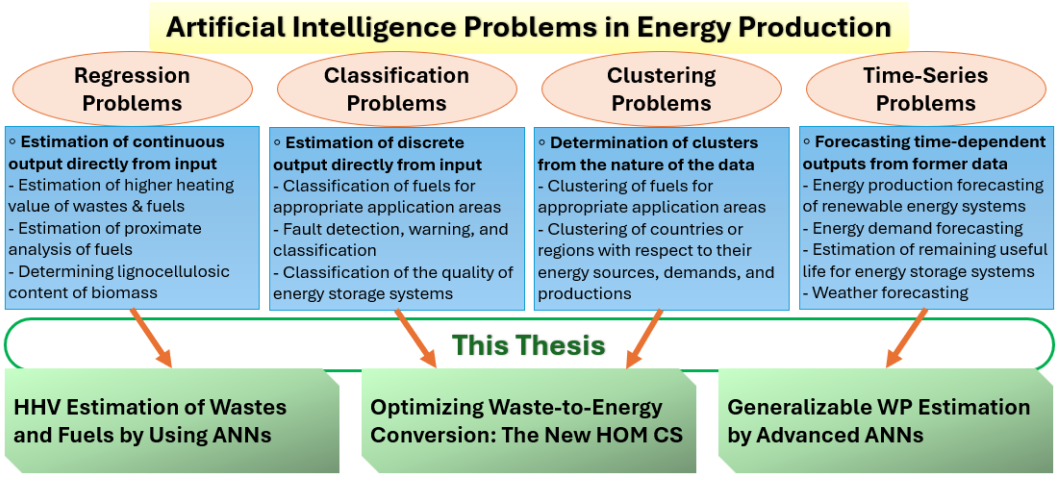

Figure 1.1 Artificial intelligence problems in energy production along with the demonstrated applications in the thesis.

In this thesis, each of these problems are challenged by selecting an important problem in the energy production sector and enhance the existing literature for that

problem, as also illustrated in Figure 1.1. In terms of regression problem, the estimation of higher heating values of wastes and fuels is studied for enhanced fuel utilization. With the same goal, a novel HOM classification system considering all fuels is proposed as a solution to a clustering and classification problem. Finaly, for a time-series problem, a generalizable wind power estimation study is carried out showcasing that the time dependent problems can be generalized in terms of location by using advanced artificial neural networks, enhancing the literature for the grid optimization and management of renewable energy systems. The methodologies presented here for each problem set is generally applicible to the remaining problems within that problem set, making this thesis an important contribution to the general body of knowledge regarding the applications of artificial intelligance in energy production.

1.2 Aim of the Thesis

The aim of this thesis is to demonstrate each of the key artificial intelligence methodologies—regression, classification, clustering, and time-series modeling—through practical and impactful applications in energy production. This research focuses on critical topics that have attained significant attention in the field, including waste-to-energy optimization and hybrid power plant performance estimation.

First, it develops highly accurate ANN-based models for predicting the higher heating values of various wastes and fuels, enabling precise evaluation of their energy potential.

Second, it introduces the HOM CS optimization model to determine the most efficient energy conversion pathway including power generation, anaerobic digestion or composting based on biomass characteristics, paving the way for improved decision-making in waste-to-energy processes.

Third, it extends the generalizability of power plant performance prediction models by creating advanced ANN frameworks tailored to production of wind power, which ensure reliable integration of renewable energy sources under diverse conditions.

By combining these methodologies with real-world applications, this research contributes to the advancement of AI in energy production, providing tools to enhance decision-making, optimize energy systems, and promote sustainable practices.

1.3 Organization of the Thesis

Firstly, in the 2nd chapter of the thesis, an overall literature review of the artificial intelligence applications in the energy sector are reported focusing on the most prevalent studies in the field.

In the 3rd chapter of the thesis, higher heating value estimation of wastes and fuels by utilizing artificial neural networks is investigated as a regression problem in the energy sector. Higher heating value (HHV) is one of the most important parameters in determining the quality of the fuels. In this study, comparatively large datasets of ultimate and proximate analysis are constructed to be used in HHV estimation of several classes of fuels, including char & fossil fuels, agricultural wastes, manure (chicken, cow, horse, sheep, llama, and pig), sludge (like paper, paper-mil, sewage, and pulp), micro/macro-algae's, wastes (RDF and MSW), treated woods, untreated woods, and others (non-fossil pyrolysis oils) between the HHV range of 4.22-55.55 MJ/kg. The relationships of carbon, hydrogen, and oxygen atomic ratios for fuel classes are illustrated by using ternary plots, and the effects of elemental composition on HHV was analyzed with the extensive dataset. Then, the ultimate (U) and ultimate & proximate (UP) datasets were utilized separately to estimate the HHV by using artificial neural networks (ANN). Hyperparameter optimization was carried out and the best performing ANNs were determined for each dataset. The results indicate that while ANNs trained by both datasets perform remarkably well, utilization of U dataset is sufficient for HHV estimation. Finally, the best performing ANN models for both U and UP datasets are given in a directly utilizable format enabling the accurate estimation of HHV of any fuel for optimization of fuel processing and waste management operations.

In the 4th chapter of the thesis, a novel classification system (the HOM classification system) is proposed by utilizing a clustering approach. This application is one of the few examples in terms of classification problems in the energy sector and, as far as we know, the only study that utilizes a clustering approach in proposing a

classification system for both wastes and fuels. The correct and informative classification of a given fuel is essential in optimizing the utilization of the fuel. While the physical properties of the fuels provide more complete information about the fuel, conventional fuel classification systems (CSs) are based on the fuels' source or origin. In this study, the novel HOM CS is proposed from the data of fuels' ultimate and proximate analysis and HHVs by utilizing k-means clustering where the number of clusters are optimized. The obtained clusters are investigated in comparison with the conventional CSs by using several methods such as contingency matrices, PCAs, ternary plots, and Van-Krevelen diagrams. Finally, the clusters are appropriately named and the HOM CS is distinctly defined. The proposed CS can be used in informative class assignment of any kind of fuel including fuel mixtures or fuels of unknown source or origin which are generally categorized vaguely as "composite-streams", "wastes", or "others" in conventional CSs. Thus, by the implementation of the new CS, these materials can now be categorized in a manner that provides insight into their specific application possibilities. This categorization can assist researchers in determining the most efficient conversion methods especially for the waste-to-energy processes including combustion, gasification, and biogas plants.

In the 5th chapter of the thesis, a generilazible wind power estimation time-series model is proposed by using deep learning models that utilize historic meteorlogical data. The unpredictability and instability caused by the widespread use of wind power (WP) poses significant challenges for ensuring the secure and consistent functioning of the electricity grid. Accurate estimation of the WP output of wind farms (WFs) will effectively mitigate these adverse effects. Thus, in this study, a comprehensive analysis of the most prevalent artificial neural network (ANN) models is conducted using the meteorological and power data of four distinct WFs situated to the west of Türkiye. The performances of these ANN models are examined by using the expanding window validation approach at three well-established WFs. The optimal ANN approach is determined based on thorough evaluation of both performance and computational load. Then, the most effective ANN model is utilized with slight modifications to obtain the generalizable model. The results indicate that the model can succesfully be employed in estimation of WP output of any WF within the region, and the methodology presented here can

easily be applied globally, enabling anyone, including third parties like goverment agencies, to estimate WP output of any WF.

In the 6th and final chapter of the thesis, the overall conclusion of all these studies are underlined and the current challenges and future directions regarding the artificial intelligence applications in energy production are highligted. The flowsheet of the thesis is given in Figure 1.2, which also higlights the individual and combined impacts of the chapters.

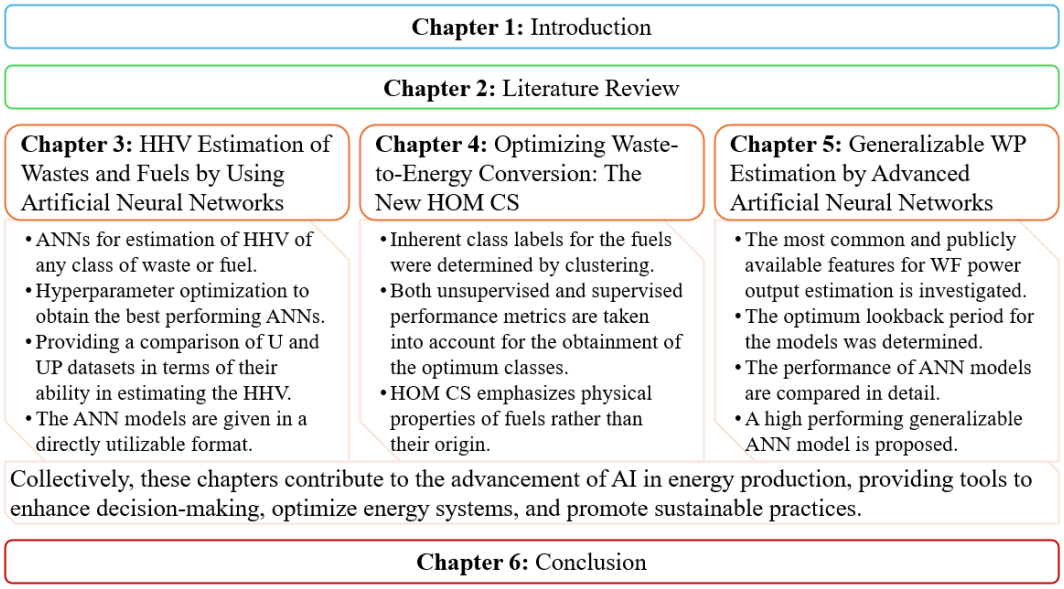

Figure 1.2 Flowsheet of the thesis along with the impacts of the chapters.

2
LITERATURE REVIEW

2.1 Applications of Artificial Intelligence in Energy Production

2.1.1 Energy Demand Forecasting

The quest for cost-effective, efficient, dependable, and secure energy sources within autonomous heterogeneous power networks has resulted in the emergence of the smart grid concept. This notion offers a multifaceted platform for the implementation of intelligent solutions from diverse viewpoints, including human-centric methodologies, technological adherence, technical coherence, and ecological sustainability. The distribution networks have been progressively decentralized because of the swift and expanding integration of renewable-powered microgrid networks. Furthermore, the digital revolution has integrated novel technologies into our daily existence, molding and influencing our preferences and personal standards. In this environment, the electricity consumption data of households has become an essential instrument for managing and regulating smart grid networks via demand response programs (Eren & Küçükdemiral, 2024). Demand response pertains to the methodologies utilized in the electrical market to regulate and equilibrate the supply and demand of electricity across various timeframes, including real-time scenarios (Mohseni et al., 2022). Demand response encompasses programs designed to incentivize users to voluntarily decrease or redistribute their electricity usage during certain timeframes, tailored to each consumption profile. Nonetheless, the comprehensive implementation of data-meter devices, along with their upkeep and online functionality, may be prohibitively expensive or impractical. Consequently, precise residential load forecasting has emerged as a prominent study subject for both local and large-scale demand response schemes.

Load forecasting can be classified into two primary types according to the temporal scope of the data. Short-term load forecasting encompass projecting power consumption over brief intervals, generally spanning minutes, hours, or days, and long-term load forecasting pertains to projections extending up to 20 years (Hippert

et al., 2001). Load forecasting mitigates the possibility of discrepancies between energy supply and demand. Through the assistance of load forecasting, a viable and dependable energy management framework may be developed utilizing demand response and demand-side initiatives. This decision-making framework benefits both electricity producers and end-users while adhering to governmental commitments and restrictions. Consequently, load forecasting is pivotal in the execution of every micro decision-making component of the smart grid.

Literature underscores the enhancement and innovation of energy management. Both utility companies and end-users can reduce operational and energy expenses as a result of this research. Owing to constraints in electrical energy generation and usage, deep learning based load forecasting methodologies have gained prominence. Data-driven load forecasting technologies are beneficial for controlling load demand and renewable energy supply. Data-driven methodologies can be employed for the integration of both supply and demand side renewables. The engagement between consumers and utility providers enables this integration. By examining usage trends, energy sources can be strategically positioned near consumers. Renewable resources can correspondingly reduce the environmental impact of conventional resources. Energy security is enhanced by the diversification of energy sources to mitigate fluctuations in fuel prices and supply interruptions. Consequently, machine learning and deep learning neural network methodologies can synchronize renewable energy generation and stabilize grid operations in real-time. The primary issue on the supply side is the immediate necessity for substantial electricity utilization. Microgrids fueled by renewable energy alleviate this limitation. Load profiles indicate that demand is variable and erratic. The primary non-linear correlations in load demand profiles arise from occupancy, seasonal variables, energy expenses, geography, and other factors. Load forecasting models must be self-adaptive, replicable, and resilient to address contingencies (Luo & Oyedele, 2022). Residential load forecasting is dynamic; hence, a load forecasting model must adjust to preference-driven trends, replicate for future forecasts, exhibit resilience to uncertainties, and undergo validation for anticipated accuracy. Artificial intelligence approaches provide effective and advantageous solutions owing to their non-linear mapping capabilities, notwithstanding the challenges posed by unpredictable load profiling. Recurrent

neural networks, Long Short-Term Memory, and Convolutional Neural Networks are the principal artificial intelligence methodologies addressing load forecasting issues (Huang et al., 2020). Combinations of these techniques have also been proposed. Hybrid and ensemble load forecasting models have been developed to enhance neural network models. A hybrid model employs two or more models to address a problem, integrating their strengths for enhanced accuracy in the solution. Hybrid models may blend a time series model, such as an autoregressive integrated moving average, with a neural network model to include both linear and non-linear data dynamics. To enhance predictions, an ensemble model trains many models on identical data and amalgamates their projections into a singular output. Ensemble models mitigate variance and bias in predictions, hence enhancing forecast precision. An ensemble model for a linear function issue may involve training many decision trees or sub-models and aggregating their predictions by voting or averaging. Table 2.1 highlights some of the most prevalent studies regarding energy demand forecasting.

In numerous countries, power networks have undergone privatization, and electricity is exchanged within the energy market (Blagrave & Furceri, 2021). Only a reliable indicator such as load forecasting can guarantee energy price stability. Consequently, load forecasting, especially short term load forecasting has emerged as a crucial component of market price control, facilitating trade-offs between the smart grid concept's increasing operational competition and consumers' need for convenient and cost-effective solutions. Load forecasting’s capacity to fulfill the requirements of both market participants by providing affordable and comfortable solutions makes it a crucial tool in energy management from both industrial and governmental perspectives.

Table 2.1 Some of the most prevalent studies in energy demand forecasting.

Reference	Aim	Performance
(Simsek et al., 2024)	The LSTM-CNN model improves by offering detailed forecasts for four vehicle categories with lower error rates.	RMSE: 2.62
(Cordeiro-Costas, Villanueva, Eguía-Oller, Martínez-Comesaña, et al., 2023)	This study lays the groundwork for improving smart building and grid analysis, optimizing production, storage, and electric vehicle integration.	nRMSE: 2.76%
(Almalaq & Edwards, 2017)	This survey aims to explore various deep learning applications in power systems and smart grid load forecasting.	RMSE: 0.25 in summer RMSE: 0.26 in winter
(Le et al., 2020)	This study presents the MEC-TLL framework for forecasting electric energy consumption in smart buildings using Transfer Learning and LSTM.	RMSE: 1.368
(Yan et al., 2024)	The article discusses various deep learning methods for predicting green energy production in different Asian countries.	RMSE: 0.2383
(Dinesh et al., 2025)	A deep learning model is proposed for fast multistep PV forecasting using minimal weather data at 15-minute intervals.	nRMSE: 0.0740
(Li et al., 2024)	This study confirms the ASTGNN-LSTM model's accuracy in predicting wind speed and solar radiation with two decades of data from Northwest China.	RMSE: 0.306 for solar radiation RMSE: 1.003 for wind speed

2.1.2 Fault Detection and Diagnosis

Fault detection and diagnosis is a study domain comprised of two components: fault detection, which seeks to activate alarms upon the emergence of a failure in a system, and fault diagnosis, which offers comprehensive insights on the fault (Ruiz-Moreno et al., 2023). The diagnostic component is bifurcated into two segments: fault isolation, which delineates the nature and location of the defect, and fault identification, which assesses its magnitude. Fault detection and diagnosis strategies can be categorized into three types (Venkatasubramanian et al., 2003): quantitative model-based methods reliant on mathematical relationships, qualitative model-based methods grounded in qualitative functions, and process history-based methods utilizing historical data. Model-based methods require mathematical models that incorporate robust assumptions and physical information, which are sometimes impractical for complex non-linear dynamic systems like nuclear power plants. Information-based approaches necessitate the prolonged collection of specialist information, which can be both time-intensive and costly. Moreover, the vast quantity and intricacy of possible failure scenarios can render the formulation of a comprehensive set of rules difficult (Fang et al., 2025). In contrast to the aforementioned methodologies, data-driven approaches adeptly employ sophisticated algorithms to conduct thorough analyses of non-linear interactions within extensive datasets and may assess system status with less specialized knowledge (Yin et al., 2023).

Fault diagnosis via artificial neural networks mirrors the architecture of model-based approaches: a collection of signals, conveying fault information, is input into a neural machine that produces a vector fault signal indicating normal or problematic system performance (Pouliezos A. D.and Stavrakakis, 1994). Artificial neural network based fault diagnostics seeks to address the limitations of model-based methodologies. These strategies necessitate mathematical process models that accurately depict the actual process. The model should not be overly complex, as calculations can quickly become time-consuming. In approaches dependent on state-variable estimation, state variables are rarely measurable, necessitating the estimation of non-measurable state variables as well. Fault detection techniques are also increasingly essential in renewable energy systems as energy companies invest in technologies to optimize the utilization of renewable energy sources, including

wind, solar, fuel cells, biomass, and geothermal, for electricity generation, where power generation failure due to a fault is more detrimental than the lack of the renewable energy source itself (Al-Sheikh & Moubayed, 2012). They provide failure prevention of components, maintenance cost reduction, and degradation detection. They offer comprehensive information regarding the performance and operation of the systems, facilitate condition-based monitoring methods, and address the issue of equipment longevity associated with unnecessary maintenance. Table 2.2 highlights some of the most prevalent studies regarding fault detection and diagnosis.

Table 2.2 Some of the most prevalent studies in fault detection and diagnosis.

Reference	Aim	Performance
(H. Wang et al., 2025)	This study compares the proposed FDD method's fault diagnosis accuracy with support vector machines and random forests.	91.9% Accuracy
(Q. Wang et al., 2024)	This study develops a deep learning approach for rail corrugation diagnosis.	89.5% Accuracy
(Masdoua et al., 2023)	This article proposes an FDD system using CNN and LSTM networks for AHU, with a hybrid database of simulation and real-world data.	96.88% Accuracy
(Y. Wang et al., 2024)	This study presents a deep CNN-based fault diagnosis method for rolling bearings, enhanced with VAEs.	96.53% Accuracy
(Chi et al., 2025)	This research presents a DCNN-based cable fault diagnosis approach with enhanced generalization through incremental learning.	~ 90% Accuracy
(Jiang et al., 2024)	This study introduces a deep learning method for precise multi-fault diagnosis using continuous wavelet transform for feature extraction.	100% Accuracy
(Sethi et al., 2024a)	This research aims to integrate convolutional neural networks with continuous wavelet transform for a hybrid diagnostic approach.	97.62% Accuracy

2.1.3 System Optimization and Control

Amid current issues related to sustainable development and energy resource efficiency, there is a growing focus on creative approaches to analyze and optimize the functioning of energy systems. Historical and contemporary evidence consistently underscores that guaranteeing secure and adequate energy availability is fundamental to economic and societal stability. Amidst escalating energy demand and global emission concerns, hybrid systems that integrate various renewable sources are becoming increasingly significant, providing opportunities for enhanced energy and cost efficiency. In recent years, numerous research have focused on analyzing various aspects of these systems, including control algorithms, thermo-economic assessments, and environmental factors.

An instance of the capability of artificial neural networks (ANNs) in predictive control is illustrated by Mohammad et al. (Zandie et al., 2023), which elaborates on the creation of a multidimensional neural network-based predictive model for the attributes of engines powered by diesel, biodiesel, and gasoline mixes. The neural network underwent training and testing using data reflecting various load, speed, and fuel ratios, which, in conjunction with sensitivity analysis and outlier detection, facilitated the removal of less effective input data. The model's extraordinary accuracy underscores its ability to predict combustion characteristics, making it a highly effective tool for optimizing the performance of internal combustion engines and regulating exhaust emissions. The research exhibited considerable adaptability and flexibility of the neural control method. Another study conducted by Yang et al. (Yang et al., 2018) discusses the performance modeling and optimization of a diesel heat recovery system utilizing an organic rankine cycle based on an artificial neural network. The research employed a genetic algorithm to enhance the precision of the predictions. The investigation assessed the impact of seven critical operating factors on the output of the organic rankine cycle. Most recently, Podlasek et al. (Podlasek et al., 2024) has proposed a deep deterministic policy gradient algorithm to obtain the best annual performance of the hybrid organic rankine power plant, surpassing other approaches by at least 13.84%. Table 2.3 highlights some of the most prevalent studies regarding system optimization and control. These studies underline the importance of artificial intelligence approaches in optimization and control of energy systems.

Table 2.3 Some of the most prevalent studies in system optimization and control.

Reference	Aim	Performance
(Napitupulu et al., 2024)	This study established four distinct frameworks for optimization control systems.	RMSE: 0.8079
(Srinivasan & Sheeba Joice, 2025)	A new approach has been proposed for predicting SOC and SOH by utilizing an optimized hybrid deep learning model that combines three different optimization techniques to improve prediction accuracy.	SOC: R^2 0.991 SOH: R^2 0.996
(P. Wang et al., 2025)	This research introduces the MTE-BDRL framework, developed to optimize machining parameters by considering the interdependencies between multiple objectives within specific intervals.	RMSE: 0.067
(Qiu et al., 2025)	A novel noise-handling approach is integrated into a multi-objective evolutionary algorithm in this study, with a deep learning-based surrogate model replacing the costly simulation model.	R^2: 0.98
(Karthikeyan et al., 2025)	This research presents a new Deep Learning Neural Network (DLNN) model, optimized through the Artificial Bee Colony (ABC) algorithm, to enhance voltage management and stabilization in smart microgrids incorporating electric vehicles (EVs).	RMSE: 0.048
(Lakshmanaprakash et al., 2025)	A Deep Optimized Network model is introduced in this work, creating an intelligent, automated edge computing framework for healthcare monitoring and disease diagnosis, enabled by IoMT.	Accuracy: 99%
(Sethi et al., 2024b)	A novel optimizer, the Deep Reinforcement Learning-Enhanced Hybrid African Vulture and Aquila, is proposed in this research, optimizing dynamic clustering and energy-based parameters in real-time.	R^2: 0.91

2.1.4 Renewable Energy Integration

Globally, renewable and sustainable energy systems and regulations have been advocated to shift from fossil fuel sources to ecologically friendly alternatives, including wind power, solar energy, and fuel cells. Wind and solar energy sources are inconsistent and challenging to integrate into renewable energy systems; thus, caution is required in the implementation of these systems and policies. Currently, the renewable energy integration research by artificial intelligence is mainly carried out for forecasting studies that estimates the power output of the renewable energy system in the next minutes (very short term prediction), next hours to several days (short term prediction), next weeks to a month (medium term prediction), and next months to years (long term prediction) (Gaboitaolelwe et al., 2023). While the very short term and short term predictions are important for optimizing energy efficiency and economics for the systems, the medium term and long term predictions play a crucial role in planning policies and future investments for the energy sector. Table 2.4 highlights some of the most prevalent studies regarding renewable energy integration. These studies showcase that the artificial intelligence approaches are well-established in estimating the power output of various energy systems, especially in the case of solar and wind since they are the most unpredictable via the conventional approaches, however the generalizability of these models still needs to be further investigated.

2.1.5 Energy Storage Systems

Notwithstanding the presence of two-way communication systems and advanced metering infrastructure, the effective management of electrical energy across appliances and resources lags behind the swift increase in power consumption . The contemporary lifestyle of consumers has led to a significant growth in the utilization of electrical appliances. The extensive integration of renewable resources and energy storage systems is crucial for alleviating electrical energy demand while minimizing carbon emissions (Alam et al., 2022). Energy storage system technology may instantaneously convert and store electrical energy from the power grid and reinject it according to the specified scheme or when the primary units are unavailable for generation. Building energy efficiency can be enhanced by 30% without structural modifications through the optimization of load operations and distributed energy resources(L. Yu et al., 2021). The battery is identified as a crucial

component for the real-time balancing of energy supply and demand in buildings and is anticipated to increase its annual growth rate in the forthcoming years (Ali et al., 2021). Precise predictive energy modeling of loads and production in buildings is crucial for the proper functioning of the storage system, thereby impacting energy efficiency enhancements. Conventional modeling techniques, such as physical representations or mathematical programming methods, exhibit challenges related to computational cost and accuracy, hindering their adaptability to contemporary requirements (Cordeiro-Costas, Villanueva, Eguía-Oller, & Granada-Álvarez, 2023). Consequently, in an environment where intelligent devices, like smart meters, continuously generate substantial data, there is an opportunity alongside a necessity to employ efficient and precise models, such as artificial intelligence techniques.

Table 2.4 Some of the most prevalent studies in renewable energy integration.

Reference	Aim	Performance
(Arun et al., 2024)	This research proposes an enhanced LSTM-based energy management system for home micro-grids with PV systems and battery storage (OHM-GEM).	R^2: 0.92
(Mishra et al., 2024)	This research presents a sophisticated neural network model for estimating renewable asset values.	RMSE: 0.0049
(Ha et al., 2024)	Combining stochastic and deterministic algorithms, this study develops deep-learning frameworks, proposing a stochastic techno-economic assessment (TEA) for evaluating national energy policies in a case study.	R^2: 0.998
(Adomako et al., 2024)	This research utilizes sophisticated deep learning (DL) methods to adjust WRF model outputs, enhancing the accuracy of wind and solar energy predictions for East and West Malaysia.	RMSE: 0.97
(Kim et al., 2024)	Focusing on a 400-MW offshore wind farm, this study analyzed the effects of various input features on short-term wind power forecasting.	RMSE: 0.122

Another major branch of artificial intelligence applications for the energy storage systems is the estimation of battery life cycles (or battery quality classifications in a more general sense). Here, the accurate classification of battery quality and the forecasting of battery lifespan prior to factory departure yields economic and safety advantages. Electric vehicles are becoming more and more popular as a result of the recognition in recent years that gasoline and diesel vehicles are significant contributors to air pollution and global warming (Schmuch et al., 2018). Lithium-ion batteries are preferred for electric vehicles because of their cost-effectiveness, elevated power and energy density, and extended longevity. Nonetheless, apprehensions over battery quality, namely in terms of energy and power density, longevity, and safety, persist . Consequently, quality control is an essential component of battery manufacturing. Monitoring metrics associated with battery quality prevents defective or inferior battery products from exiting production lines and supplies critical information for battery scientists and engineers to implement necessary adjustments for product optimization. Presently, advanced techniques, such as capacity testing and resistance measuring, are extensively employed at the end-of-line testing in battery manufacturing (Kampker et al., 2023). These studies offer insights into the electrical behavior of batteries; nevertheless, they necessitate supplementary testing apparatus and time, and frequently fail to deliver exhaustive information regarding battery aging and longevity. To save expenses and time related to end-of-line testing while enhancing the precision of quality assessment and longevity forecasting, there is an increased emphasis on analyzing and leveraging data from production processes such as battery generation (Zou et al., 2024). A battery is deemed to have reached its end of life when its capacity diminishes by 20%. The remaining useful life is a crucial parameter for assessing the battery's health status. Predicting the remaining useful life is difficult due to intricate battery aging mechanisms and variable usage patterns (Harris et al., 2017). This problem is exacerbated by the reality that only current and voltage are often measured in practical battery management systems (Ma et al., 2024). Driven by the swift advancement of artificial intelligence across several domains, data-driven methodologies have also garnered heightened interest in the prediction of remaining useful life of the batteries. Thus, artificial intelligence methods have been succesfully utilized in determining remaining useful life or classifying the quality

of the batteries. The Table 2.5 showcases some of the most prevalent studies regarding energy storage systems.

Table 2.5 Some of the most prevalent studies regarding energy storage systems.

Reference	Aim	Performance
(Lv et al., 2024)	Experiments explored hydrate formation in gas-saturated oil-in-water systems, with a 1D CNN model applied to predict hydrate volume fractions.	RMSE: 0.1564
(Cordeiro-Costas, Villanueva, Eguía-Oller, & Granada-Álvarez, 2023)	This study utilizes Standard Neural Networks to predict electricity consumption and PV generation, aiming to minimize energy waste through storage management via Reinforcement Learning.	nRMSE: 6-7%
(Ramesh et al., 2023)	A novel approach is proposed in this study to analyze communication data within renewable energy storage systems based on VANET.	Accuracy: 98%
(H. Lee et al., 2020)	A framework leveraging deep learning is introduced in this paper to detect unreliable battery sensor data.	Accuracy: 100%
(H. Liu, Liu, et al., 2023)	This study examines peak shaving and valley filling in office building HVAC energy storage systems.	R^2: 0.793
(Balakumar et al., 2023)	The presented study is a framework based on LSTM-driven RNNs, designed to forecast EPC and REG at 1-minute and 5-minute intervals, supporting the development of the DSM program.	R^2: 0.9969
(Duhirwe et al., 2021)	Utilizing deep learning, this article presents an integrated PV-ESS-EHP system with a scheduling algorithm that predicts EHP electricity consumption and PV energy generation, optimizing renewable energy usage and minimizing electricity costs.	R^2: 0.95

2.2 Hıgher Heatıng Value Estimation of Wastes and Fuels by Using Artificial Neural Networks

The higher heating value (HHV) of a fuel is defined as the heat emitted when a unit weight of the fuel is entirely combusted, and the combustion products are cooled to a standard temperature of 298 K (Majumder et al., 2008). This measure is crucial for assessing fuel quality and its applicable domains, as it indicates the fuels' high energy content (Cordero et al., 2001). Numerous research on fuel usage and waste management have employed the Higher Heating Value (HHV) of the fuel as the performance indicator for selecting the suggested fuel (Guo et al., 2019; Subhash et al., 2021; S. Wang et al., 2022). Higher heating value (HHV) is determined experimentally using a bomb calorimeter (Uzun et al., 2017). The experimental produce is uncomplicated, although it is labor-intensive and may not be accessible to many (Khan et al., 2023; Xing et al., 2019a). Consequently, the acurate determination of HHV by more accessible methodologies, such as ultimate and proximal analysis, has become significant (Dodo et al., 2022).

Recently, artificial intelligence has been utilized as a data-driven approach to improve the efficiency of biofuel and waste systems (Ullah et al., 2022). This strategy aligns with environmental, social, and governance (ESG) standards, successfully addressing environmental challenges and fostering sustainable behaviors inside the organization (Naveed et al., 2024). Numerous research offer models for estimating HHV based on ultimate analysis (U), proximate analysis (P), or a combination of both (UP) datasets. In 2017, Ghugare and Tambe employed genetic programming (GP) to estimate the higher heating value (HHV) of coals from the UP dataset (Ghugare & Tambe, 2017). In 2018, Hosseinpour et al. employed the P dataset and principal component analysis integrated with iterative network-based fuzzy partial least squares (PCA-INFPLS) methodology to estimate the higher heating value (HHV) of biomass (Hosseinpour et al., 2018). The U and UP datasets are employed for the estimation of the higher heating value (HHV) of biomass through various methodologies, including Gaussian processes (GP), multivariate regression (MVR), artificial neural networks (ANNs), support vector machines (SVMs), multilayer perceptron artificial neural networks (MLP-ANNs), genetic algorithm-adaptive neuro fuzzy inference systems (GA-ANFIS), differential evolution-ANFIS (DE-ANFIS), GA-radial basis function (GA-RBF),

and least squares support vector machines (LSSVMs) (Boumanchar et al., 2019a; Çakman et al., 2021; Ighalo et al., 2021; Noushabadi et al., 2021; Xing et al., 2019a). Çakman et al. employed artificial neural networks for the estimation of higher heating value of biochar. In 2022, the higher heating value (HHV) of all fuels was evaluated using machine learning algorithms, including decision tree regression (DTR), support vector regression (SVR), Gaussian process regression (GPR), and random forest regression (RFR), applied to a substantial dataset of 1,526 fuel samples. (Yaka et al., 2022). Dodo et al. employed MLR, ANFIS, ANN, and SVM techniques for the estimate of HHV in biomass (Dodo et al., 2022). The most recent research on HHV estimate, undertaken by Büyükkanber et al., employed MLR, DTR, RFR, and ANN methodologies for the estimation of coals (Büyükkanber et al., 2023). A recent study demonstrated that ensemble classifiers combined with RF and MLP can enhance the prediction of HHV of biochars (Dubey & Guruviah, 2023). Kocer (2024) recently evaluated the U and P datasets in HVV estimation using machine learning techniques, demonstrating that the U dataset produces superior models compared to the P dataset. The subsequent table provides a summary of our literature analysis.

All models derived from the aforementioned studies can effectively predict the HHV of coal, charcoal, trash, or biomass independently. A model capable of accurately estimating the HHV of various fuels—encompassing char, fossil fuels, agricultural residues, manure, sludge, treated and untreated wood, as well as solid, liquid, and gaseous wastes—is essential for assessing the HHVs of innovative fuels and fuel mixes. The ambiguity in dataset selection (U or UP) must be resolved comprehensively to ensure that future studies utilize the most suitable dataset. To our knowledge, no literature exists that employs artificial neural networks for the assessment of the higher heating value of any fuel type. Consequently, the acquisition of these models is essential for forthcoming research on the topic.

Table 2.6 Most prevalent AI models in HHV estimation of wastes and fuels.

Data Size	Dataset	Method	Fuel Class	Validation Method	Performance Metrics	Ref.
7682	UP	GP	Coal	Train/Val./Test = 75%/15%/10%	R^2=0.998 RMSE=0.261 MAPE=0.79%	(Ghugare & Tambe, 2017)
131	P	ANN	Biomass	Holdout (66%/33%)	R^2= 0.963 RMSE=0.375 MAE=0.328	(Uzun et al., 2017)
350	P	PCA-INFPLS	Biomass	Train/Val./Test = 70%/15%/15%	R^2>0.96, MSE<0.51	(Hosseinpour et al., 2018)
171	U	GP, MVR	Biomass	Holdout (75%/25%)	MAPE>4.25%	(Boumanchar et al., 2019a)
737	UP	ANN, SVM, RF	Biomass	Holdout + 10-Fold Cross Validation	0.90<R^2<0.95	(Xing et al., 2019a)
210	UP	MLP-ANN	Biomass	Train/Val./Test = 85%/10%/5%	R^2=0.9249 MSE=0.88097 RMSE=0.8998	(Ighalo et al., 2021)
535	U	MLP-ANN, LSSVM, ACO-ANFIS, PSO-ANFIS, GA-RBF	Biomass	Train/Val./Test = 70%/15%/15%	R^2=0.96 MSE=0.76 RMSE=0.87 MAE=0.64 MAPE=3.45%	(Noushabadi et al., 2021)
129	P	ANN	Biochar	Holdout (70%/30%)	R^2=0.9651 RMSE=0.8064	(Cakman et al., 2021)
1566	U	MLR, DTR, SVR, GPR, RFR	All Fuels	10-Fold Cross Validation	R^2=0.9814 RMSE=0.7133	(Yaka et al., 2022)
474	UP	MLR, ANFIS, ANN, SVM	Biomass	10-Fold Cross Validation	R^2=0.9371 NMSE=0.0029	(Dodo et al., 2022)
88	UP	MLR, DTR, RFR, ANN	Coal	5-Fold Cross Validation	R^2=0.968 MAE=1.101	(Büyükkanber et al., 2023)
1140	P	Ensables with RF and MLP	Biochar	10-Fold Cross Validation	R^2=0.984 RMSE=1.4204	(Dubey & Guruviah, 2023)
617	U	SVM, RF, XGB, MLP	Biomass	10-Fold Cross Validation	R^2=0.826 RMSE=1.1813	(Kocer, 2024)
329	P	SVM, RF, XGB, MLP	Biomass	10-Fold Cross Validation	R^2=0.637 RMSE=1.0885	(Kocer, 2024)

2.3 Optimizing Waste-to-Energy Conversion: The New HOM Classification System

In literature, fuels are often categorized according to their origin or source. Ross et al. classified microalgae as a fuel and examined its thermochemical properties (Ross et al., 2008). Zhou et al. employed ultimate and proximal analysis, together with thermogravimetric features, to classify 26 samples of municipal solid trash (Zhou et al., 2015). Duca et al. employed a soft independent modeling technique for the swift differentiation of hardwood and softwood (Duca et al., 2016). Elmaz et al. examined the classification efficacy of machine learning algorithms in accurately categorizing solid fuels based on their proximal analysis (Elmaz et al., 2020). These traditional categorization methods yield many class labels, including hardwood, softwood, biomass, fossil fuel, manure and sludge, and algae. Two prevalent classification systems (CSs) that standardize fuel class labels are the ECN Phyllis CS and the NTA 8003 CS (Better Biomass, 2019; Netherlands Enterprise Agency, 2019; Phyllis2, 2023). The class labels of these CSs offer information into the sources and methods of fuel acquisition, although they may be inadequate for assessing its consumption. Moreover, they are typically insufficient for identifying the classification of a fuel of unknown origin, as several fuel kinds may exhibit identical physical features. Furthermore, the amalgamations of various fuels cannot be precisely categorized by these classification systems due to the definitions of the classes, which are articulated as "others" or "composite streams." To our knowledge, there is no categorization system based directly on the physical features of fuels, despite the fact that fuels are often categorized according to their physical characteristics, such as ultimate or proximate analysis. A comprehensive study might yield essential information on the unique application areas of fuels by elucidating the features of each fuel type.

Ultimate analysis of a fuel ascertains its elemental composition, whereas proximate analysis provides data on moisture content and ash percentage, both of which are crucial for evaluating the energy content of the examined fuel (Nunes et al., 2018; Shadangi et al., 2023). Ultimate and proximate analyses are commonly employed to predict the higher heating value (HHV) of fuels, as the determination of HHV is both time-intensive and costly, yet critically significant (Dashti et al., 2019; Noushabadi et al., 2021; Xing et al., 2019b; Yaka et al., 2022). Xing et al. utilized

machine learning techniques to predict the higher heating value (HHV) of biomass fuels based on both ultimate and proximate analyses (Xing et al., 2019b). Dashti et al. employed just proximate analysis to assess the higher heating value (HHV) of biomass samples. (Dashti et al., 2019) Noushabadi et al. also calculated the higher heating value (HHV) of biomass fuels based on their final study, utilizing an enhanced equation (Noushabadi et al., 2021). Recently, Yaka et al. employed several machine learning methodologies to identify the optimal model for estimating the higher heating value (HHV) of all types of fuels (Yaka et al., 2022). The application of ultimate and proximate analysis extends beyond the assessment of HHV. Multiple research concerning fuel categorization also include the ultimate and proximal analyses of the examined fuels (Laszakovits & MacKay, 2022; Poudel et al., 2018; Ross et al., 2008; Zhou et al., 2015). The objective is to ascertain whether the examined fuels exhibit any clustering on the Van-Krevelen diagrams or ternary plots. Although these studies do categorization, they typically compare experimentally examined fuels to established fuel categories instead of introducing a new classification system.

Clustering algorithms are typically employed in the literature for the creation of fresh classes and new labels straight from the data. Clustering is described as the process of grouping related elements into a cluster while segregating dissimilar ones (Tiwari & Kumar, 2018). It is employed to categorize items defined by a collection of variables into groups (Vandeginste et al., 1998). Examples of clustering applications encompass the diagnosis of multi-component degradation in aircraft fuel systems (H. Liu et al., 2023), durability assessment of polymer electrolyte fuel cells (Hissel et al., 2007), and estimation of aircraft fuel consumption and carbon dioxide emissions based on path profiles (Pagoni & Psaraki-Kalouptsidi, 2017), among others. A study conducted by Sancho et al. utilized k-means clustering analysis on the physicochemical parameters of crude oils to enhance the categorization of these oils (Sancho et al., 2022). K-means clustering is a technique that partitions observations into a certain number of groups based on their proximity to designated center locations known as cluster centroids (Deka & Saha, 2023). The optimal number of clusters may be established by both unsupervised and supervised approaches by employing several performance criteria (Pedregosa et al., 2011; Rand, 1971; Rosenberg & Hirschberg, 2007; Steinley, 2004).

2.4 Generalizable Wind Power Estimation from Historic Meteorological Data by Advanced Artificial Neural Networks

Numerous recent research have been undertaken to enhance wind power forecasting. The models utilized in these investigations are often classified as physical models, statistical models, and machine learning models. Physical models predominantly employ numerical weather prediction (NWP) techniques to provide wind energy predictions by resolving differential equations grounded in the concepts of wind energy conversion and meteorological expertise (Nielsen et al., 2007; L. Wang et al., 2013). Statistical models often utilize previous data to forecast WP. Conventional statistical approaches, including time series models such as autoregressive (AR), autoregressive moving average (ARMA), and autoregressive integrated moving average (ARIMA), utilize previous WP data to forecast future WP (Karakuş et al., 2017). Nonetheless, their performance is significantly influenced by meteorological circumstances (Liao et al., 2023).

Recent advancements in artificial intelligence (AI) techniques have led to the utilization of diverse machine learning algorithms, including artificial neural networks (ANN), support vector machines (SVM), and long short-term memory networks (LSTM), for the prediction of WP (Yu et al., 2019; H. Zhang et al., 2014). These models are employed to compute WP utilizing numerical weather forecast and historical power data. A study introduced an enhanced radial basis function neural network model incorporating an error feedback mechanism to predict short-term wind speed and power. Numerical experiments conducted on a wind farm demonstrated that the proposed method achieves superior accuracy while preserving computational efficiency (Rajagopalan & Santoso, 2009). Khosravi et al. integrated decision trees with SVM, resulting in a 37% improvement in prediction performance, while the computation time was reduced compared to using SVM alone (Khosravi et al., 2018). Zhang et al. employed LSTM to forecast wind turbine power with numerical weather predictions and historical power data (J. Zhang et al., 2019). A Gaussian mixture model was employed to assess the uncertainty of WP. The efficacy of the suggested model was validated using numerical tests performed in an actual power plant.

Recent research on WP prediction highlight the benefits of sophisticated Artificial Neural Network (ANN) models, including the Nonlinear Autoregressive with Exogenous Inputs (NARX) model, Elman model, and Long Short-Term Memory (LSTM) model. Cadenas et al. evaluated the univariate ARIMA model against the multivariate NARX model for wind speed forecasting and concluded that the NARX model outperformed ARIMA (Cadenas et al., 2016). Gu et al. demonstrated that the LSTM model they created had superior wind power forecast accuracies at 4-hour, 24-hour, and 72-hour intervals compared to other evaluated models (Gu et al., 2021). Cui et al. introduced a sophisticated hybrid model employing Long Short-Term Memory (LSTM) to account for wind power ramp events (WPREs). The suggested model's findings surpassed those of previous approaches (Cui et al., 2023). Liao et al. introduced a novel short-term wind power probabilistic prediction model utilizing MTGP and the concept of multi-task learning. The model indicated that Gaussian Processes excel in wind power forecasting when enough training data is accessible (Liao et al., 2023). Gidom et al. gathered data from a power plant in Kocaeli, Türkiye, demonstrating the superior efficacy of the NARX model in power forecasting for this facility (Gidom et al., 2024). Liu et al. demonstrated the efficacy and complexity of the Elman neural network model in forecasting wind power, achieving superior prediction accuracy relative to other models (S. Liu et al., 2024). The subsequent Table 2.7 provides a summary of our literature analysis.

All these studies underscore that accurate and precise assessment of wind power generation from wind farms is essential for grid stability and optimization. Nonetheless, our literature evaluation indicates that substantial research gaps continue to pose obstacles. Certain features necessary for predicting the WP production are challenging to acquire or accessible just to the management of the specific WF, therefore compromising the joint endeavor for grid stability and optimization. The lookback period, defined as the historical time frame of data utilized by the model for predictions, remains undetermined in the literature. No universally applicable model has been presented for use by anybody for any WF within an area. This compels each WF to derive their predictive models using their own data, which may provide difficulties for existing WFs and is unattainable for newly-formed WFs.

Table 2.7 Most prevalent AI models in WP estimation.

Aim	Utilized Models	Data Type / Size	Prediction Interval	Validation Method	Model Performances	Ref.
WPF	SVR	3min / 5 days	VST	Cross Validation	RMSE=1.0887 MAE=0.6336 RMAE=0.064	(H. Zhang et al., 2014)
WSF	NARX, ARIMA	10 min, Hourly /16 months	VST & ST	Holdout Validation	MAE=0.43 MSE=0.34	(Cadenas et al., 2016)
WPF	PAR, ANN-ANFIS	Hourly /1-2 years	ST	Holdout Validation	NRMSE=0.050 NMAPE=3.96	(Karakuş et al., 2017)
WPSDF	MLFFN, SVR-RBF, ANFIS-PSO	5-60 min /1 years	VST & ST	Holdout Validation	RMSE=0.3651 MSE=0.1333	(Khosravi et al., 2018)
WPF	LSTM-EFG	10min /3 years	VST	Holdout Validation	MSE=5.5311	(R. Yu et al., 2019)
WPF	LSTM-GMM	15min /3 months	VST	Holdout Validation	RMSE=6.37	(J. Zhang et al., 2019)
WPF	LSTM, SVR&GPR	10min, Hourly /1 year	VST / ST	Holdout Validation	R^2=0.89	(Gu et al., 2021)
ELP	NARX, ARMA, ELMAN	Hourly/1 years	ST	Holdout Validation	MAPE=3.42%	(Alhmoud & Nawafleh, 2021a)
WPF	MTGP	Hourly /100 days	ST	Holdout Validation	RMSE=0.1255 MAE=0.0936	(Liao et al., 2023)
WPF	LSTM-WPRE	15min /2 years	VST	Holdout Validation	MAPE=0.094 rRMSE=0.112	(Cui et al., 2023)
WSF	NARNN, NARXNN	Hourly /1 year	ST	Holdout Validation	MSE=0.2253 R^2=0.904	(Gidom et al., 2024)
WPF	Elman	Hourly /1 year	ST	Holdout Validation	MSE=4.7141 MAPE=11.777	(S. Liu et al., 2024)
SIF	HFF based SA-CNN-LSTM	Hourly /3,4,5 years	ST	Sliding Window Validation	RMSE=42.132 MAE=20.412 R^2=0.979	(Xiao et al., 2024)

3
HIGHER HEATING VALUE ESTIMATION OF WASTES AND FUELS BY USING ARTIFICIAL NEURAL NETWORKS

3.1 Introduction

Energy generation has always been a priority for nations worldwide in terms of both economic and security concerns (Amin et al., 2022). Recently, there have been several discussions on selection of fuels in households and industrial use due to both raising environmental concerns and increasing instabilities in the energy sector (Acharya & Marhold, 2019). To this end, several kinds of wastes, biomass, and fuel blends that contain some amount of these, have been considered and discussed in the literature as applicable alternative energy sources, in line with the 7th sustainable development goal (SDG-7), which encompasses the accessibility of affordable, reliable, sustainable, and modern energy for all (J. Lee et al., 2022; United Nations, 2015; Xue et al., 2022).

Higher heating value (HHV) (also termed as gross calorific value (GCV)) of a fuel is defined as the amount of heat released when a unit weight of the fuel completely combusted and the combustion products are cooled down to the standard temperature of 298 K (Majumder et al., 2008). It is one of the most important parameters in determining the fuel's quality and application areas since it provides information about the high energy content of the fuels (Cordero et al., 2001). Several studies in the topic of fuel utilization and waste management have used the HHV of the fuel as the performance metric in selection of the recommended fuel (Guo et al., 2019; Subhash et al., 2021; S. Wang et al., 2022). HHV is experimentally measured via a bomb calorimeter (Uzun et al., 2017). While the experimental produce is simple, it is time consuming and may not be available for everyone (Khan et al., 2023; Xing et al., 2019b). Hence, the accurate estimation of HHV from more convenient methods, such as ultimate and proximate analysis, has gained importance (Dodo et al., 2022).

Artificial intelligence has recently been employed as a data-driven methodology to enhance the efficiency of biofuel and waste systems (Ullah et al., 2022). This

strategy is in accordance with environmental, social, and governance (ESG) standards, effectively resolving environmental issues and promoting sustainable practices within the business (Naveed et al., 2024). When the literature is examined, there are several studies that provide models for HHV estimation from ultimate analysis (U), proximate analysis (P), or both (UP) datasets. In 2017, Ghugare and Tambe used genetic programing (GP) in order to estimate the HHV of coals from UP dataset (Ghugare & Tambe, 2017). In 2018, Hosseinpour et al. used P dataset and primary component analysis coupled with iterative network-based fuzzy partial least squares (PCA-INFPLS) method to estimate HHV of biomass (Hosseinpour et al., 2018). Then, U and UP datasets are utilized for HHV estimation of biomass by utilizing several approaches such as GP, multi-variate regression (MVR), artificial neural networks (ANNs), support vector machines (SVMs), multilayer perceptron artificial neural networks (MLP-ANNs) genetic algorithm-adaptive neuro fuzzy inference system (GA-ANFIS) differential evolution-ANFIS (DE-ANFIS), GA-radial basis function (GA-RBF), least square support vector machines (LSSVMs) (Boumanchar et al., 2019b; Cakman et al., 2021; Ighalo et al., 2021; Noushabadi et al., 2021; Xing et al., 2019b). Çakman et al. utilized ANN for HHV estimation of biochar as well. Then, in 2022, HHV of all fuels are estimated by the utilization of machine learning algorithms such as decision tree regression (DTR), support vector regression (SVR), gaussian process regression (GPR), and random forest regression (RFR) approaches by using a large U dataset with 1526 fuel samples. (Yaka et al., 2022). Dodo et al. also utilized MLR, ANFIS, ANN, and SVM methods for HHV estimation of biomass (Dodo et al., 2022). Currently, the latest research known to us about the subject of HHV estimation was conducted by Büyükkanber et. al. who used MLR, DTR, RFR, and ANN methods for HHV estimation of coals (Büyükkanber et al., 2023). One recent study showcased that ensemble classifiers coupled with RF and MLP can improve the prediction of HHV of biochars (Dubey & Guruviah, 2023). Most recently, (Kocer, 2024) compared the U and P datasets in HVV estimation by using machine learning algorithms, showing that utilization of U dataset yields superior models than utilization of P dataset.

All the models obtained in the above mentioned previous studies can successfully be utilized to estimate HHV of coal, biochar, wastes, or biomass individually. However, a model that can successfully estimate the HHV of any kind of fuel -

including char and fossil fuels, agricultural wastes, manure, sludge, treated and untreated woods, and wastes in solid, liquid, and gaseous form - is crucial for estimation of HHVs of novel fuels and fuel blends. In addition, the ambiguity in the selection of dataset (U or UP) should be addressed in a comprehensive approach, so that future studies can be focused on utilizing the most appropriate dataset. As far as we know, there is no study in literature that utilizes ANNs in estimation of HHV of any kind of fuel. Thus, the obtainment of these models is crucial for future studies about the subject. Consequentially, the main objectives of this study can be listed as:

- To analyze the extensive dataset by ternary analysis of carbon, oxygen, hydrogen atomic ratios with respect to HHVs for all fuel classes.
- To utilize ANNs in estimation of HHV for all classes of fuels - including char and fossil fuels, agricultural wastes, manure, sludge, treated and untreated woods, and wastes in solid, liquid, and gaseous form by using the constructed comparatively large datasets.
- To carry out hyperparameter optimization for the obtainment of the best performing ANNs.
- To compare the utilization of U and UP datasets in terms of their ability in estimating the HHV.
- To present the best performing ANN models are given in a directly utilizable format.

In this study, novel U and UP datasets are constructed that include 1526 and 743 fuel samples. These fuels are separated into seven classes: char & fossil fuels, agricultural wastes, manure & sludge, wastes, treated woods, untreated woods, and others. The elemental composition of these classes are investigated by utilizing ternary plots. The effects of the carbon, hydrogen, and oxygen atomic ratios on the HHV is also investigated. Then, hyperparameter optimization is conducted by utilizing bayesian optimization (BO) algorithm for each ANN type and number of layers. In this way, 1200 ANN models are constructed for HHV estimation from U and UP datasets. The best methods are determined by the models' 5-fold cross validation performances. The performance metrics (RMSE CV, RMSE Test, MSE, and R^2) of the best performing models are evaluated, compared, and reported accordingly. Finally, the performances of best ANNs that estimate HHV from U

and UP datasets are specifically compared with each other and the studies found in the literature. The novelties of this study can be listed as:

- Ternary analysis of carbon, oxygen, hydrogen atomic ratios for all fuel classes with respect to HHVs is conducted with the extensive dataset.
- ANNs are directly used in estimation of HHV for all classes of fuels by using comparatively large datasets.
- Hyperparameter optimization is carried out to obtain the best performing ANNs, and the effects of hyperparameters on the model performances discussed in detail.
- The utilization of U and UP datasets for HHV estimation are compared in a rigorous manner.
- The best performing ANN models are given in a directly utilizable format with no coding experience needed.

This study reports accurate and reliable ANN models in estimation of HHV of any class of fuel, including biomass and wastes for sustainable energy applications alongside the utilization of fossil fuels and coal. It also provides insight into the hyperparameters of the best ANNs that estimate HHV of fuels. Finally, it compares the usage of U and UP datasets and conclusively reports the performance of models trained by these datasets. The results of this study are useful for researchers that aim to estimate HHV of any class of fuel from U or UP dataset to optimize the waste management processes.

3.2 Methodology

3.2.1 Data Obtainment and Processing

Both the ultimate analysis and proximate analysis data are obtained from Phyllis2 database, which are used in creation of a dataset containing 1526 different fuel samples. 743 of these samples included both ultimate and proximate analysis. Hence, in this study, two distinct datasets U and UP are constructed. The dataset U contains only ultimate analysis and respective HHV values of the samples. A subset of the clean data containing 100 samples for U and UP datasets is made available in A.S.F.E.1. The dataset UP contains both the ultimate and proximate analysis data along with the HHV values. Table A.S.I.1 and Table A.S.I.2 shows statistical

information of the datasets U and UP, respectively, providing insight into the structure of the data and the range of this study. Table 3.1 provides further information about the classes of fuel samples. The specific contents of these classes may be obtained from our previous study (Yaka et al., 2022). The correlation heatmap of the features is presented for both U and UP datasets in Figure A.S.I.1, which proves that the features are independent. In this study, MATLAB R2022a is used to construct and validate ANNs, conduct hyperparameter optimization, and visualize the results.

Table 3.1 Classes of fuels included in the U and UP datasets.

Fuel Class	Size in U	Size in UP
Char & Fossil Fuels	253	66
Agricultural Wastes	453	229
Manure & Sludge	73	68
Wastes	205	129
Treated Woods	81	44
Untreated Woods	397	192
Others	64	15
Total	1526	743

3.2.2 Artificial Neural Networks

ANNs are considered to be one of the strongest modeling tools available, which are based on studies of the brain and nervous system (Walczak & Cerpa, 2003). They consist of neurons and weights that connect these neurons. As the ANN is trained by the training set, the weights are updated with respect to the performance metric after each iteration. This is done by a training function. There are several training functions available in the literature, however, the Levenberg-Marquardt backpropagation algorithm is shown to be superior to the others for various applications, including HHV estimation (Güleç et al., 2022; MathWorks, 2022c). This agrees with the pre-study trials of this work; hence, the Levenberg-Marquardt backpropagation algorithm is utilized in this study as the transfer function.

There are several parameters that affect the performance of obtained artificial intelligence models. These are termed hyperparameters. For ANNs trained by Levenberg-Marquardt backpropagation algorithm, the most crucial hyperparameters are depth of the network, ANN type, layer size, and transfer function of the layers (see Figure 3.1a). Depth of the network is the number of layers present in the ANN. The ANN type classifies how the layers are connected. In terms of investigation of the single layer neural networks, even a single hidden layer in an ANN can model complex nonlinear relationships if it uses nonlinear activation functions. This ability allows ANNs to capture and model complexities that simple linear regression cannot. Layer size is the number of neurons present in each layer. Transfer function is the function that collects and transforms the output of each layer. The structure of the feed forward and cascade forward type ANNs are illustrated in Figure A.S.I.2 in order to clarify the terminology of this study. Figure 1 illustrates an example ANN structure utilized in this study. Throughout this study, ANN labels are formulated as presented in Figure 1b and the ANN label of the presented network in Figure 1 is given in Figure 3.1c.

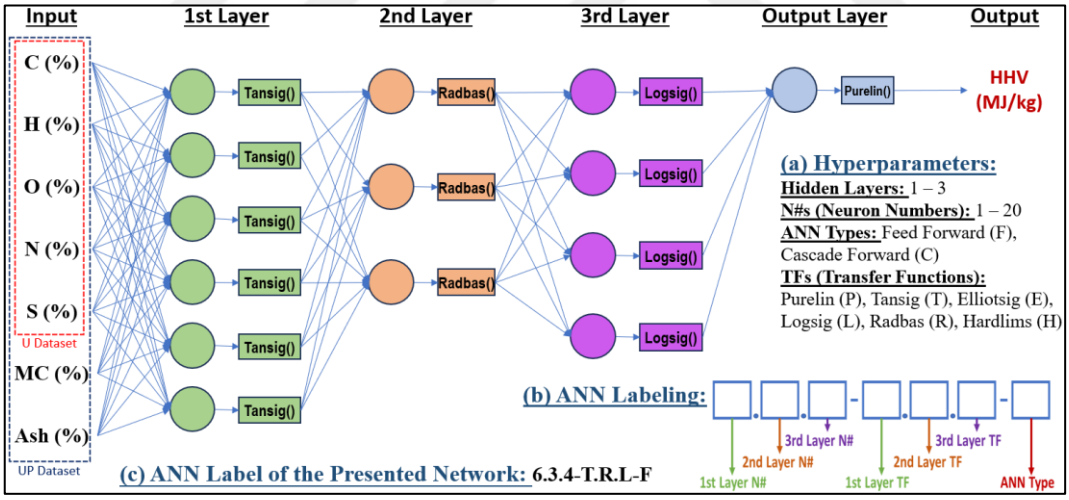

Figure 3.1 An example structure of ANNs utilized in this study with hyperparameters (a), label formulation utilized in this study (b), and the ANN label of the presented example ANN (c).

3.2.3 Validation Methods

There are several validation methods available in the literature (MathWorks, 2022a). The k-fold cross validation and hold-out validation methods are the most common ones in applications (Yaka et al., 2022). The principles of these methods

are illustrated in Figure 3.2. The k-fold cross validation divides the data into k subsets and uses one set for testing and the remaining sets for training. It trains k models and evaluates the performance of each model. Finally, the average of all errors is taken, yielding the cross validation performance. The hold-out validation separates the data into three sets: train, validation, and test. While the hold-out approach evaluates the validity of a set that it hasn't observed during training, it decreases the size of the training set which may result in reduced performance. In addition, the performance of the hold-out validation method may be altered by the selection of train and test sets. The k-fold cross validation method provides an unbiased performance evaluation by using the whole data as train and test sets but is costly in terms of time since it trains several models. Furthermore, it is able to detect overfitting since it computes an overall performance metric from different train and test datasets (Yates et al., 2023). In this study, these approaches are combined. Firstly, 5-fold cross validation is used on 90% of the data to determine the best models by hyperparameter optimization. Then, the test performance of the best models are evaluated by the remaining 10% of the data to make the results comparable with the literature. This combined approach is illustrated in Figure 3.2c. The final models presented in this study are trained with the whole data in order to provide the most accurate tools possible to be used in estimation of HHV.

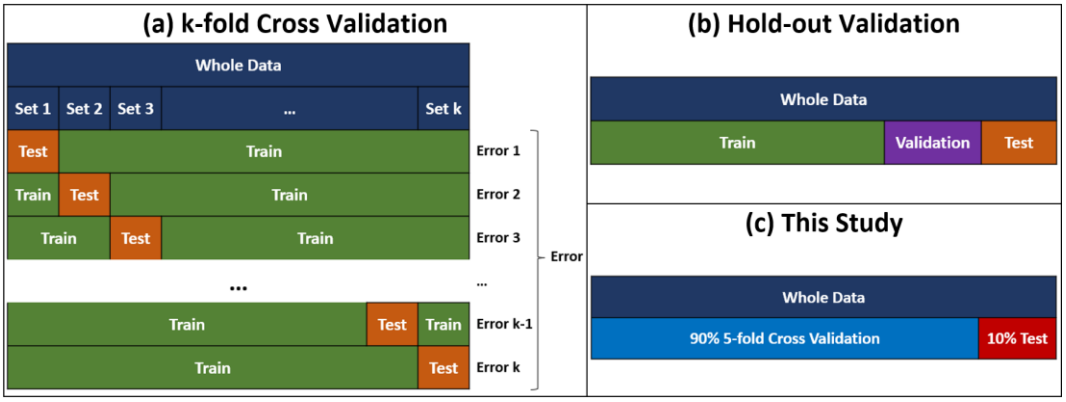

Figure 3.2 The principles of k-fold cross validation (a), hold-out validation (b), and combined validation method used in this study (c).

3.2.4 Hyperparameter Optimization

Hyperparameter optimization is one of the most crucial parts of conducting ANN research, since different ANN structures may yield significantly varying results. To obtain the best performing ANNs for HVV estimation in this study, the hyperparameters and their values are selected for the optimization as represented in Figure 2.1a and also in Table A.S.I.3.

In this study, BO algorithm is utilized to determine the best performing hyperparameters for the ANN structure due to its superior performance when the computational complexity is high and the objective function is unknown (Sezer et al., 2022). The acquisition function for BO is chosen as "expected improvement plus" to avoid overexploitation (MathWorks, 2022b). 100 maximum iteration is allowed for each ANN type and number of layers. Hence, the performance of 600 ANN is measured by 5-fold cross validation separately for the datasets of U and UP. Then, the ANNs are listed according to their performances, and the best three ANN for each case are comparatively examined in detail.

3.2.5 Performance Metrics

In developed studies, several performance metric definitions are used in evaluating reliability and accuracy of the models proposed. These metrics provide a means for determination of applicability of the models and allows comparison with other modeling approaches. The correlation coefficient (R^2) measures the strength of the relationship between the variables (Ricci & Martínez, 2008). Mean squared error (MSE) and root mean squared error (RMSE) provide positive values and are commonly used in evaluating the accuracy of the models (W. Wang & Lu, 2018). The equations used in evaluating these metrics are given as follows:

$$R^2 = 1 - \left[\frac{\sum_{i=1}^{m}(y_i - \hat{y}_i)^2}{\sum_{i=1}^{m}(y_i - \bar{y}_i)^2}\right] \tag{3.1}$$

$$MSE = \frac{\sum_{i=1}^{m}(y_i - \hat{y}_i)^2}{m} \tag{3.2}$$

$$RMSE = \sqrt{\frac{\sum_{i=1}^{m}(y_i - \hat{y}_i)^2}{m}} \tag{3.3}$$

3.3 Results and Discussion

3.3.1 Ternary Analysis of Atomic Ratios

In this study, large U and UP datasets are constructed to estimate HHV of fuels by using ANNs. Prior to investigating these advanced models, however, it is crucial to analyze the data in a rigorous manner to clearly indicate the range of this study and obtain insight about the composition and HHV of different classes of fuel. Hence, in this section, the ternary plots of carbon, hydrogen, and oxygen atomic ratios (see Figure 3.3), which are computed from mass ratios obtained for 1526 fuel samples in U dataset, are analyzed. In Figure 3.3a, the different classes of fuels are indicated with different colors and the size of the datapoints are correlated with the HHV of samples. Here, it can be observed that the data is collected in a wide composition range for all classes of fuel. In line with the literature, the samples belonging to the char & fossil fuels class contain large amounts of carbon and hydrogen. The samples belonging to the agricultural wastes, wastes, and manure & sludge contain more oxygen due to the present impurities. In order to observe the effect of composition with the HHV more clearly, the ternary surface plot with respect to the HHV is illustrated in Figure 3.3b. These figures clearly indicate that the HHV is inversely correlated with the amount of oxygen, and correlated with the amount of carbon and hydrogen, as expected.

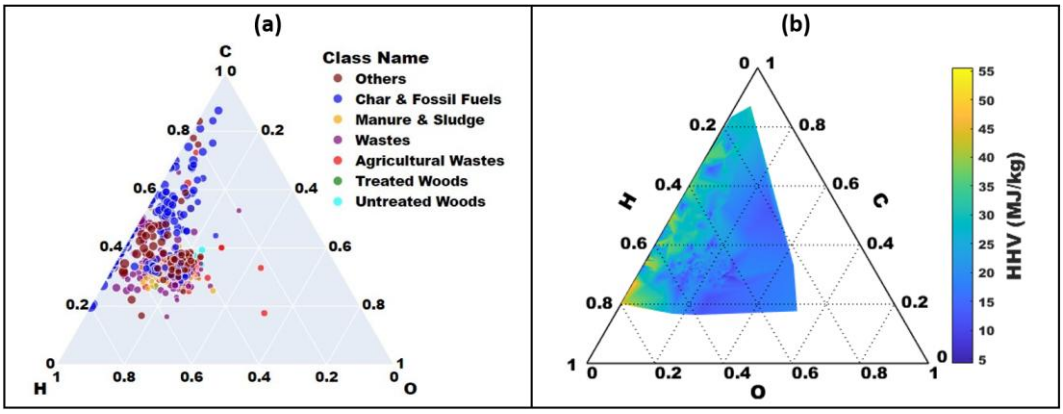

Figure 3.3 Ternary plots of carbon, hydrogen, and oxygen atomic ratios for fuels with respect to classes (a) and HHV (b). The datapoint sizes in (a) is correlated with the HHV as well.

While the ternary plots presented in Figure 2.3 successfully illustrates the effect of the carbon, hydrogen, and oxygen atomic ratio on HHV and provides insight

regarding the classification of fuels, they also confirm that the extensity of this study, which includes a large number and high variety of fuel samples.

3.3.2 HHV Estimation from only Ultimate Analysis

In this section, U dataset containing 1526 samples is utilized to estimate HHV (MJ/kg) of fuels from ultimate analysis, using the features C (%), H (%), O (%), N (%), S (%). Hyperparameter optimization is carried out as explained in section 2.4, and the structure and performances of each ANNs trained in BO steps are given in A.S.F.E.2. These stepwise results are listed with respect to the RMSE CV, and the best three performing ANNs for each ANN structure are presented in Table A.S.I.4. Here, it may be observed that as the complexity of the ANN increase, computation time increases, as expected. When the cross validation results are examined, the best performing ANN is observed to be 4-L-F with RMSE CV of 1.2428. However, the much complex ANN 13.2.4-P.P.E-C yielded a significantly lower RMSE Test, which suggest the existence of a generalization error in 4-L-F. Overall, the RMSE values are observed to be similar for all best performing ANNs. Furthermore, all the best performing 3 layer ANNs have obtained purelin as transfer function in their former layers. Hence it can be concluded that increasing the depth of the ANNs does not significantly improve the ANN performance for HHV estimation from U data. In addition, these findings suggest that the network type has no substantial impact on performance, and feed forward networks are adequate for HHV estimation.

The other performance metrics of the best performing ANNs for each ANN structure are also evaluated by using the whole dataset, which are presented in Table A.S.I.5. According to these tables, the best performing ANN for U dataset is determined to be 4-L-F, which has the one of the lowest MSE and the highest R^2 values. 20.1.1-P.T.E-F has yielded the lowest MSE, but the correlation is weaker than 4-L-F. The other ANNs also performed well, with slightly worse performances. The elliotsig transfer function was observed to be most common in the last layer of multi-layered ANNs among the best performing ANNs. All the best performing ANN models that are represented in Table A.S.I.5 are also given in a directly utilizable format in A.S.F.E.3. The loss convergence curves for training, validation, and test sets are also obtained for these ANN models by splitting the data 80%/10%/10% train/validation/test sets (see Figure A.S.I.3). Here, it is shown

that there is no overfitting of the data as the learning is stopped at minimum errors. The models have reached the stop conditions at relatively low epoch numbers as the number of features is low and the Levenberg-Marquardt backpropagation algorithm is highly efficient. Moreover, if the training dataset is much larger and more varied than the validation or test sets, it might inherently have a higher MSE simply due to the greater diversity and complexity in the data.

The observed vs. estimated HHVs are illustrated in Figure 3.4 for each best performing ANN with respect to the different classes of fuels. Here, it is observed that different types of ANNs represent different classes slightly better than others. The HHVs of char & fossil fuels and treated woods are best estimated by 1.2-L.E-C. Some HHV data of agricultural wastes are significantly underestimated by feed forward type ANNs. HHVs of manure & sludge class are slightly overestimated by all ANNs while the best estimation is provided by 4-T-C. ANN 13.2.4-P.P.E-C performed best in estimating the HHVs of wastes. HHVs of untreated woods are best estimated by ANNs 1.2-L.E-C or 13.2.4-P.P.E-C. Overall, it is shown that all the ANNs presented successfully estimate HHV of any fuel successfully from ultimate analysis.

3.3.3 HHV Estimation from Ultimate and Proximate Analysis

Even though conducting both ultimate and proximate analysis is more expensive and time consuming, there are considerable number of studies that estimate HHV from UP data. In order to deterministically finalize the discussion on the obtainment of the additional proximate analysis features necessary for accurate estimation of HHV by using ANNs, the UP dataset containing 743 samples is also analyzed in the same manner. Note that the decrease in the number of samples (from 1526 in U dataset to 743 in UP) stem from the fact that the additional features are not available for some of the fuels. This situation actually improves the simulation of the comparison of utilization of U and UP, since obtainment of U data is significantly more convenient than obtainment of UP data.

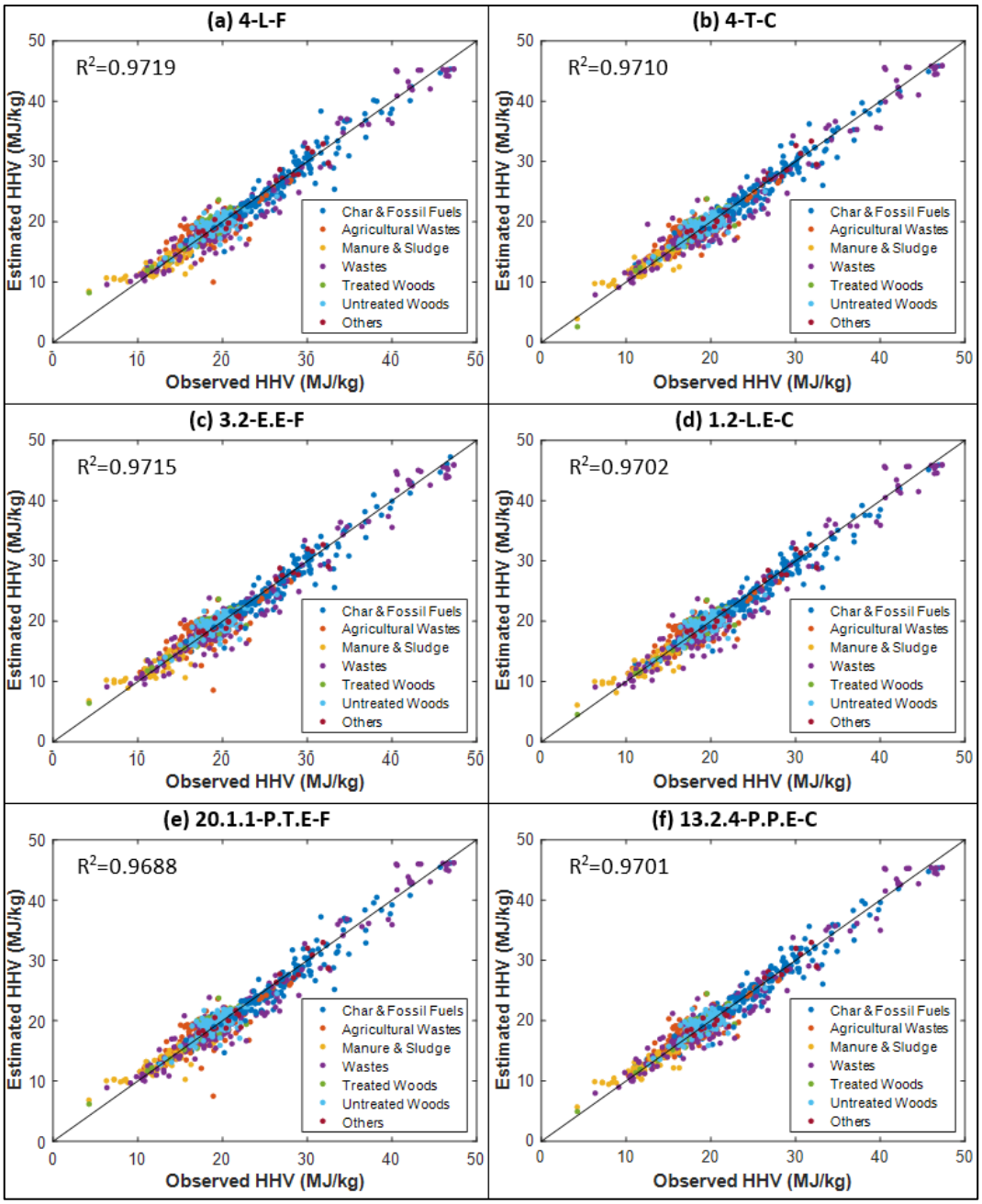

Figure 3.4 Estimated vs. observed HHV values for the best performing ANNs with respect to fuel classes for U dataset.

In this section, in addition to the above mentioned ultimate analysis features, MC (%) and Ash (%) features are included in the estimation of HHV. Similarly, hyperparameter optimization is conducted, and the results are reported in the A.S.F.E.4. The best three performing ANNs for each ANN structure and their performances are given in Table A.S.I.6. Here, the best performing ANN with lowest RMSE CV value is observed to be 1.2854 by the ANN 18.1-P.E-F. The ANNs 1.1.1-P.P.E-F and 7.12.2-P.P.T-F also obtained similar RMSE CV values.

However, the best RMSE test value is obtained by the ANN 1-L-F, which suggest the presence of memorization error by the aforementioned ANNs. Comparable to the estimation of HHV with the U dataset, all the best performing ANNs yielded similar performance metrics, and all the best performing 3 layer ANNs obtained purelin as transfer function in their former layers, indicating that the increase in the hidden layer size of the ANNs does not significantly improve the performance of the models. Furthermore, these results also indicate that the network type also does not affect the performance significantly and feed forward networks are sufficient for HHV estimation.

The remaining performance metrics are also evaluated by using the whole data for the best performing ANNs for each ANN type and presented in Table A.S.I.7. Here, the ANN 1.1-R.L-C yielded the best MSE and R^2 values while the metrics for all ANNs are quite similar. Once again, the elliotsig transfer function is observed to be present in the last layer of the best performing ANNs for HHV estimation. The observed vs. estimated HHVs are illustrated in Figure 3.5 for each best performing ANN with respect to the different classes of fuels. The HHVs of char & fossil fuels class is observed to be estimated the best by ANN 1.1-R.L-C. The HHVs of agricultural wastes are better estimated by using ANN 1-E-C. In estimation of HHVs of manure & sludge, all best ANNs may successfully be utilized. For estimation of HHVs wastes, the ANN 1.1-R.L-C is observed to yield the best fit. The HHVs of treated and untreated woods is best estimated by 1-E-C. Overall, the cascade forward type ANNs are observed to be more successful in estimating HHVs from UP dataset. This may be due to the increased number of features in UP dataset, since cascade forward type ANNs are more connected and may assign more weights to the features. Overall, it is shown that all the ANNs presented successfully estimate HHV of any fuel successfully from ultimate and proximate analysis. All the best performing ANN models that are represented in Table A.S.I.7 are also given in a directly utilizable format in A.S.F.E5. The loss convergence curves for training, validation, and test sets are also obtained for these ANN models by splitting the data 80%/10%/10% train/validation/test sets (see Figure A.S.I.4). Here, similarly to the ANNs trained by the utilization of U dataset, it is shown that there is no overfitting of the data as the learning is stopped at minimum validation errors.

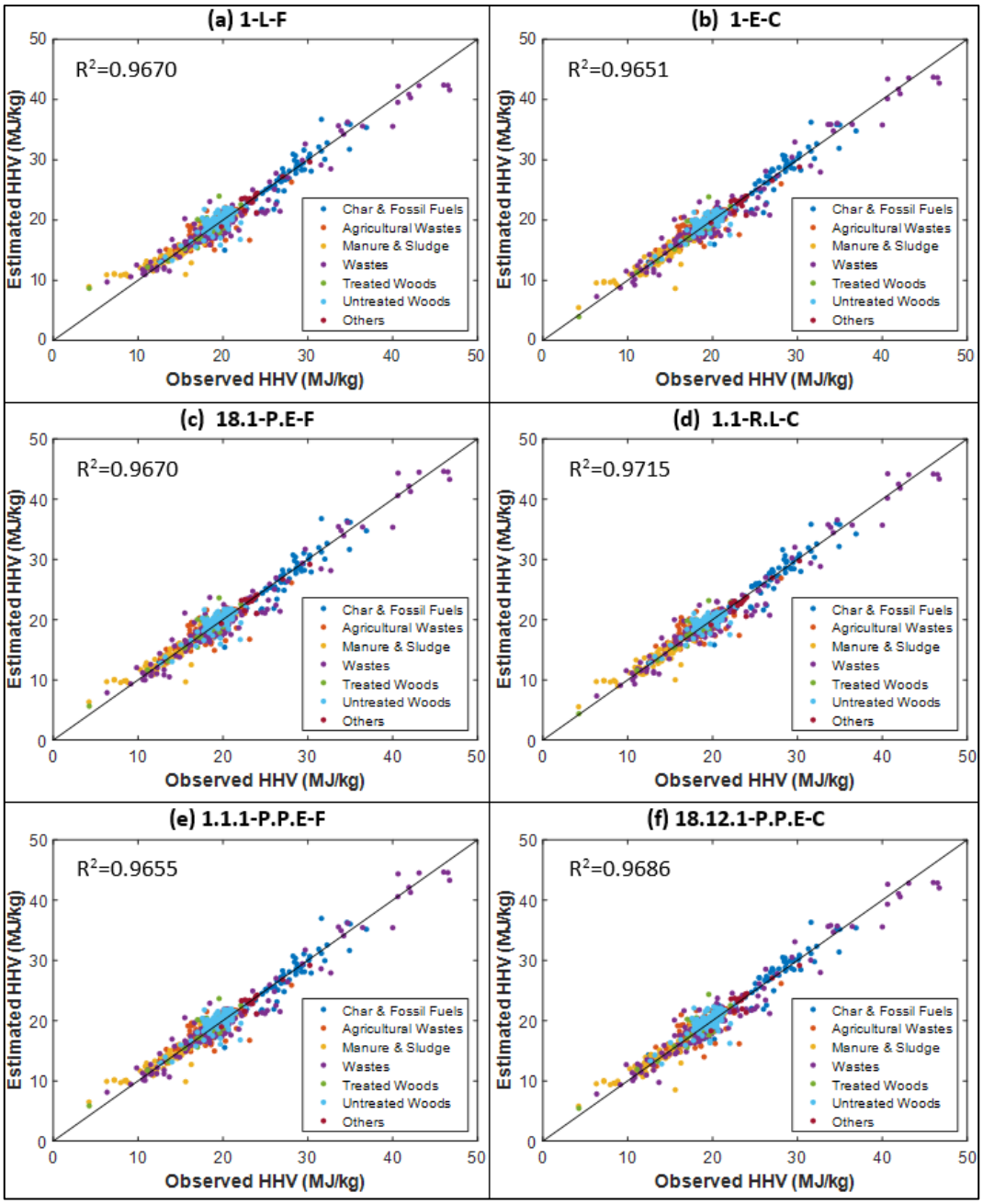

Figure 3.5 Estimated vs. observed HHV values for best performing ANNs with respect to fuel classes for UP dataset.

3.3.4 Overall Comparison

In this section, the results of this study and the results obtained by previous studies are chronologically summarized and compared with each other. Table 3.2 provides a summary of the most significant studies. Here, it can be seen that there is an ambiguity in selection of dataset, where some studies utilize a U, some P, and others UP datasets. One recent study (Kocer, 2024) compared the U and P datasets, showing that utilization of U dataset yields superior models than utilization of P dataset. In this study, one of the aims was to determine if the additional features from the proximate analysis is really necessary or not. From Table 3.2 and sections 3.1 and 3.2, it is clear that the HHV estimation from U is sufficient, and even slightly better performance metrics are obtained by using only U dataset. This may stem from the fact that obtainment of U data is significantly more convenient than obtainment of both UP data since these data is obtained experimentally. In fact, this study also simulates the effects of the difficulties of data collection by utilizing the maximum attainable data for each dataset (1526 data for U dataset and 743 data for UP dataset) from the Phyllis2 database. Furthermore, the ANNs trained by UP dataset need both ultimate and proximate analysis data to estimate the HHV of a new fuel whilst the ANNs trained by U dataset only need ultimate analysis data, which makes utilization of the ANNs trained by U dataset much more convenient. To further validate this claim, ReliefF feature ranking algorithm (MathWorks, 2022; Robnik-Sikonja & Kononenko, 2003) is also utilized to clearly observe how these additional features contribute to the overall accuracy of the models (see Figure A.S.I.5). Here, it can be observed that the importance of the features can be ordered from most important to least as C (%), O (%), H (%), Ash (%), N (%), S (%), and MC (%). While the Ash (%) is 4th in this ordered list, the MC (%) is last with a significantly lower feature importance score. Since obtainment of the proximate analysis data requires extra experimental effort and does not significantly increase the performance of the models as can be observed from Table 3.2, we conclude that utilization of models trained by U dataset is preferable for estimation of HHV of fuels.

Table 3.2 Comparison of the ANNs obtained in this study and the literature.

Data Size	Dataset	Method	Fuel Class	Validation Method	Performance Metrics	Ref.
7682	UP	GP	Coal	Train/Val./Test = 75%/15%/10%	R^2=0.998 RMSE=0.261 MAPE=0.79%	(Ghugare & Tambe, 2017)
131	P	ANN	Biomass	Holdout (66%/33%)	R^2= 0.963 RMSE=0.375 MAE=0.328	(Uzun et al., 2017)
350	P	PCA-INFPLS	Biomass	Train/Val./Test = 70%/15%/15%	R^2>0.96, MSE<0.51 MAPE<2.51%	(Hosseinpour et al., 2018)
171	U	GP, MVR	Biomass	Holdout (75%/25%)	MAPE>4.25%	(Boumanchar et al., 2019a)
737	UP	ANN, SVM, RF	Biomass	Holdout + 10-Fold Cross Validation	0.90<R^2<0.95	(Xing et al., 2019a)
210	UP	MLP-ANN	Biomass	Train/Val./Test = 85%/10%/5%	R^2=0.9249 MSE=0.88097 RMSE=0.8998	(Ighalo et al., 2021)
535	U	MLP-ANN, LSSVM, ACO-ANFIS, PSO-ANFIS, GA-RBF	Biomass	Train/Val./Test = 70%/15%/15%	R^2=0.96 MSE=0.76 RMSE=0.87 MAE=0.64 MAPE=3.45%	(Noushabadi et al., 2021)
129	P	ANN	Biochar	Holdout (70%/30%)	R^2=0.9651 MSE=0.6502 RMSE=0.8064	(Cakman et al., 2021)
1566	U	MLR, DTR, SVR, GPR, RFR	All Fuels	10-Fold Cross Validation	R^2=0.9814 RMSE=0.7133	(Yaka et al., 2022)
474	UP	MLR, ANFIS, ANN, SVM	Biomass	10-Fold Cross Validation	R^2=0.9371 NMSE=0.0029	(Dodo et al., 2022)
88	UP	MLR, DTR, RFR, ANN	Coal	5-Fold Cross Validation	R^2=0.968 MAE=1.101	(Büyükkanber et al., 2023)
1140	P	Ensables with RF and MLP	Biochar	10-Fold Cross Validation	R^2=0.984 RMSE=1.4204	(Dubey & Guruviah, 2023)
617	U	SVM, RF, XGB, MLP	Biomass	10-Fold Cross Validation	R^2=0.826 RMSE=1.1813	(Kocer, 2024)
329	P	SVM, RF, XGB, MLP	Biomass	10-Fold Cross Validation	R^2=0.637 RMSE=1.0885	(Kocer, 2024)
1526	U	ANNs	All Fuels	90% (5-Fold Cross Validation) + 10% Test	R^2=0.9719 RMSE=1.2750 MSE=0.8630	**This Study**
743	UP	ANNs	All Fuels	90% (5-Fold Cross Validation) + 10% Test	R^2=0.9715 RMSE=1.4555 MSE=1.0677	**This Study**

As seen from Table 3.2, the combined validation method utilized in this study is also unique for estimation of HHVs, which keeps the advantages of both holdout and cross validation approaches, as discussed in section 2.3. By the utilization of 5-fold cross validation, it is also confirmed that there is no overfitting problem with the ANNs up to three hidden layers. By keeping a 10% test set that is separate from the cross validation training sets, we ensure the predictive performance of the model for truly unknown dataset. Furthermore, obtainment of both cross validation and holdout validation performance metrics allows the comparison of this study by a broader range of studies. The RMSE presented for this study in Table 3.2 is the RMSE of the test data, and the R^2 and MSE values are obtained from the whole data in order to provide a comparison with the other studies. Among other studies that estimated HHV by using ANNs, this study yielded the best results by utilizing hyperparameter optimization for both U and UP datasets.

Most notably, while other studies are mainly conducted for specific classes of fuels (see Table 3.2), this study provides ANN models for all fuels. This ensures that the ANNs obtained in this study are utilizable in estimation of fuels of any kind, even of fuels with unknown origin. Furthermore, individual best performing ANNs are also determined for each fuel type, whose utilization is suggested if the fuel type is known. These suggestions are summarized in Table 3.3 for the convenience of the readers. Here, the selections are made considering Figure 2.4 and Figure 2.5 from the best performing ANNs given in Table A.S.I.5 and Table A.S.I.7 for U and UP datasets, respectively. It is observed from Table 3.3 that the cascade forward type ANNs predicts the individual classes more successfully than the feed forward type in general. This may stem from the fact that the cascade forward net is more connected and it has more weights to be optimized when compared to the feed forward net. It should also be emphasized that while increasing the hidden layer size does not increase the estimation performance with respect to the whole data, some specific fuel classes are observed to be better estimated with different sized ANNs. This result can be explained by the fact that even linear layers can sometimes learn different aspects of the data in practice due to how weights are initialized and updated during training. For example, different initializations can lead to different gradient descent paths, affecting the final learned function. Thus,

the capabilities of a multilayer network can exceed those of a simple single layer network.

Table 3.3 Summary of the best ANN structures for U and UP datasets.

Classes	Best ANN Structures	
	For U Dataset	For UP Dataset
Char & Fossil Fuels	1.2-L.E-C	1.1-R.L-C
Agricultural Wastes	4-T-C	1-E-C
Manure & Sludge	4-T-C	1.1.1-P.P.E-F
Wastes	13.2.4-P.P.E-C	1.1-R.L-C
Treated Woods	1.2-L.E-C	1-E-C
Untreated Woods	13.2.4-P.P.E-C	1-E-C

3.4 Limitations

As in common with all regression studies, the ANN models obtained here should be utilized within the range of the datasets, whose statistical information is presented in Table A.S.I.1 and Table A.S.I.2. In addition, the hyperparameter optimization was caried out in a space 2×3×6×6×6×20×20×20, where a total of 10,368,000 hyperparameter choices is present for the ANNs. By using the BO, the best performing ANNs were determined by computing the cross validation metrics of only 600 of these possibilities. Thus, optimization may not have found the global minima. However, as far as we know, this study is the only study that performs this kind of methodological hyperparameter optimization for ANNs in HHV estimation of fuels, and the best performing ANNs given in this study are shown to be highly successful. Finally, the utilization of datasets U and UP are discussed here, but these datasets are of different size. The dataset U contains 1526 samples whereas the dataset UP contains 743 samples. Thus, it is possible that increasing the size of UP dataset may increase the performance of the trained models. However, obtainment of U data is more convenient than obtainment of UP data, and this fact is also simulated in this study, by obtaining the maximum usable data for both datasets from the Phyllis2 database.

3.5 Conclusion

In this study, firstly the ternary plots are utilized in order to gain insight into the elemental composition of fuel classes and clearly present the effects of carbon, hydrogen, and oxygen atomic ratios on HHV of fuels. Then, U and UP datasets are utilized separately to estimate HHV of any class of fuels. The models obtained performed remarkably well, with comparatively high R^2 and low MSE and RMSE values. These models can successfully be utilized in determination of fuel quality for sustainable energy production. In the present work, the performance of the models are also examined in detail. ANNs trained by both U and UP datasets yielded similar performance metrics, hence we conclude that the obtainment of proximate analysis data is not necessary for HHV estimation. The best ANN models yielded high correlation coefficient and low error values when compared to the literature, which proves their ability in accurate HHV estimation. The best performing ANN models for U and UP datasets are also included in a directly utilizable format in A.S.F.E.3 and A.S.F.E.5, respectively. The ANN models given here can be utilized directly by using MATLAB, without needing any coding experience. Furthermore, different ANNs are observed to estimate the HHV of different classes of fuels variously. Hence, the utilization of appropriate ANNs for respective fuel classes enables the most accurate HHV estimation of the fuels. Moreover, the HHV of wastes, novel fuels, and fuel blends can be estimated by using the proposed ANNs in the most meticulous manner since the ANNs are constructed by utilizing the whole dataset of fuels including char & fossil fuels, agricultural wastes, manure & sludge, wastes, treated woods, untreated woods, and others. This study also contributes to the technological readiness of the ANNs in HHV estimation applications, clearly demonstrating the ability of ANNs models in HHV estimation. With the directly utilizable models that can be used, the technology readiness level of the technology can be said to be between 6 and 7, according to the definitions given in Europe Union's "Technology Readiness Level: Guidance Principles for Renewable Energy Technologies" report (Antonio De Rose et al., 2017). Overall, the results of this study are useful to researchers and managers for the optimization of the respective fuel processing and waste management processes by enabling the computation of the most accurate HHV of fuels of any kind.

4
OPTIMIZING WASTE-TO-ENERGY CONVERSION: THE NEW HOM CLASSIFICATION SYSTEM

4.1 Introduction

In all fuel based energy applications, the type of fuel is an essential information to properly process the material and optimize the results (Elmaz et al., 2020; Zhu et al., 2014). The correct and informative assessment of the fuel type is crucial to check the compliance of the declarations of the producers (Duca et al., 2016). Choosing the correct fuel or fuel mixture for a given process may increase the energy efficiency of the process or reduce the greenhouse gas emissions (Elgowainy et al., 2014), which are beneficial to both executives and the environment. By using low-carbon and renewable fuels, such as natural gas instead of coal and oil, and giving priority to energy-efficient technologies, emissions can be greatly reduced (Bordass, 2020). In addition, it is crucial to advocate for the promotion of sustainable biomass and biofuels, considering the emissions during their whole lifecycle (Muench & Guenther, 2013). Furthermore, the fuel demand can also be supplied by composite streams or wastes if these are sufficiently classified, enabling the utilization of unrecyclable resources for energy production (Gerassimidou et al., 2020; Vounatsos et al., 2016). The environmental perspective is further emphasized throughout literature due to the urgent necessity of low emissions for attaining the specific sustainability targets prioritized by the policy makers in the perspective of the 7th sustainable development goal (Insel et al., 2022; United Nations, 2015).

In literature, fuels are conventionally classified by their origin or source. Ross et al. reported the classification of microalgae as a fuel and investigated its thermochemical behavior (Ross et al., 2008). Zhou et al. utilized ultimate and proximate analysis and thermogravimetric characteristics of 26 municipal solid waste samples for classification (Zhou et al., 2015). Duca et al. used a soft independent modeling approach for rapid discrimination between hardwood and softwood (Duca et al., 2016). Elmaz et al. investigated the classification performance of the machine learning algorithms to correctly classify the solid fuels from their proximate analysis (Elmaz et al., 2020). These conventional

classification approaches result in various class labels such as hardwood, softwood, biomass, fossil fuel, manure & sludge, algae etc. Two of the most common classification systems (CSs) that provide a standardization for the class labels of fuels are ECN Phyllis CS and NTA 8003 CS (Better Biomass, 2019; Netherlands Enterprise Agency, 2019; Phyllis2, 2023). While the class labels of these CSs provide insight into where and how the fuel is obtained, they can be insufficient whilst determining its utilization. Furthermore, they are usually inadequate for determining the class of a fuel of unknown origin since different fuel types may show the same physical properties. Moreover, the mixtures of several fuels cannot be distinctly classified by these CSs due to the definitions of the classes are stated in a manner like "others" or "composite streams". To the best of our knowledge, there is no CS based directly on the physical properties of the fuels even though the classification of fuels are most commonly investigated according to their physical properties such as ultimate or proximate analysis. Such a CS could provide crucial information about the fuels' specific application areas by providing insight into the characteristics of each fuel category.

Ultimate analysis of a fuel determines the elemental composition of the data while proximate analysis gives information of moisture content and ash percentage of the fuel, making them essential in determining the energy content of the investigated fuel (Nunes et al., 2018; Shadangi et al., 2023). Both ultimate and proximate analysis are generally utilized in prediction of HHV of fuels since determination of the higher heating value (HHV) is both time consuming and expensive while being of utmost importance (Dashti et al., 2019; Noushabadi et al., 2021; Xing et al., 2019a; Yaka et al., 2022). Xing et al. estimated the HHV of biomass fuels from both ultimate and proximate analysis of the fuels by machine learning approaches (Xing et al., 2019a). Dashti et al. used only proximate analysis to estimate the HHV of biomass samples. (Dashti et al., 2019) Noushabadi et al. also estimated the HHV of biomass fuels from their ultimate analysis with the inclusion of an improved equation (Noushabadi et al., 2021). Most recently, Yaka et al. utilized all machine learning approaches to determine the best performing model to be used in estimation of the HHV of fuels of any kind (Yaka et al., 2022). However, the use case of ultimate and proximate analysis is not limited to the estimation of HHV. Numerous studies about the classification of the fuels also report the ultimate and

proximate analysis of the investigated fuels (Laszakovits & MacKay, 2022; Poudel et al., 2018; Ross et al., 2008; Zhou et al., 2015). They aim to determine if the fuels investigated form any clusters on the Van-Krevelen diagrams or ternary plots. While these studies perform classification, they generally compare experimentally investigated fuels to the conventional fuel classes rather than proposing a novel class system.

For the construction of novel classes and new labels directly from the data, clustering algorithms are generally used in literature. Clustering can be defined as the scheme of collecting similar items in a cluster and separating the dis-similar ones (Tiwari & Kumar, 2018). It is utilized to classify objects that are characterized by a set of variables into groups (Vandeginste et al., 1998). Some examples of clustering applications include the diagnosis of multi-component degradation in aircraft fuel systems (H. Liu, Zhao, et al., 2023), durability diagnosis of polymer electrolyte fuel cells (Hissel et al., 2007), estimation of aircraft fuel consumption and carbon dioxide emissions based on path profile (Pagoni & Psaraki-Kalouptsidi, 2017) etc. One particular study by Sancho et al. has performed k-means clustering analysis on the data of physicochemical properties of crude oils to better group crude oils (Sancho et al., 2022). K-means clustering is a method that divides the observations into a specified number of clusters according to their closeness to determined center points termed as cluster centroids (Deka & Saha, 2023). Here, the optimum number of clusters can be determined in both unsupervised and supervised manner by the utilization of several performance metrics (Pedregosa et al., 2011; Rand, 1971; Rosenberg & Hirschberg, 2007; Steinley, 2004).

In this study, ultimate and proximate analysis of 1139 various fuel samples are collected along with HHV values of 929 these samples. The HHV of remaining 152 fuel samples are calculated from their ultimate analysis by using the random forest regression constructed by Yaka et al. (Yaka et al., 2022). Then, the k-means clustering is carried out to determine the inherent class labels for the fuels and construct the HOM (acronym of the authors' names) CS. Firstly, the features are determined as ash (dry basis, wt. %), moisture content (MC, wt. %) from proximate analysis, carbon (C, wt. %), hydrogen (H, wt. %), oxygen (O, wt. %), nitrogen (N, wt. %), sulfur (S, wt. %), and HHV (MJ/kg) of the fuels, which are then shown as

important variables in determination of the fuel classes. The class labels according to ECN Phyllis and NTA 8003 is utilized in the hyperparameter optimization of the k-means clustering, where both unsupervised and supervised performance metrics are evaluated. Then, according to the optimization result, proposed clusters are analyzed in detail by utilizing binary plots, decision tree classification and illustration, contingency matrices, principal component analysis (PCA), ternary plots, and Van-Krevelen diagrams. After all the analysis of the clusters in comparison with the conventional CSs, the HOM CS is proposed with appropriate labels assigned to determined clusters. All these steps are illustrated in Figure 4.1. The proposed HOM CS is shown to be superior to the conventional CSs since it classifies the fuels with respect to their physical properties rather than source or origin. This enables classification of any kind of fuel, including fuels vaguely labeled as "composite stream," "wastes," or "others" in other CSs. Novel to this study, a large dataset of 1139 fuel samples that contain ultimate and proximate analysis and HHV data is constructed and the new HOM CS is proposed by using k-means clustering algorithm which emphasizes physical properties of fuels rather than their origin. The proposed HOM CS will enable researchers and engineers to assign suitable labels for the given fuel directly from its physical properties, even if the fuel's source or origin is unknown or unattainable. Thus, it will enable the determination of the most efficient conversion methods for any fuel-to-energy process, including the crucial waste-to-energy processes.

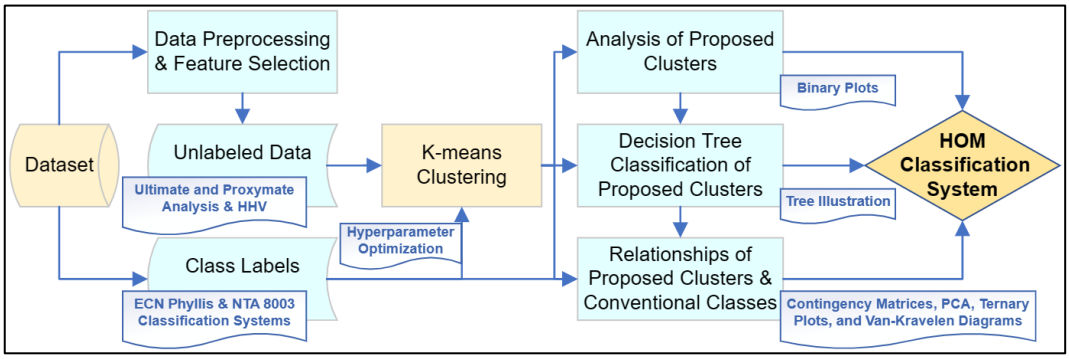

Figure 4.1 Flowsheet of this study: Optimizing Waste-to-Energy Conversion: the New HOM Classification System.

4.2 Methodology

4.2.1 Data

All the data used in this study is obtained from Phyllis database (Phyllis2, 2023). The ultimate and proximate analysis of 1081 fuel samples of sixteen different fuel classes is utilized for the clustering analysis and classification. The statistical information regarding all the data collected for utilization in this study is presented in Table 4.1. The class distribution of these samples according to ECN Phyllis and NTA 8003 CSs are given in Table 4.2. Furthermore, HHV of these samples are also utilized for the most accurate classification. While the HHV of only 929 fuel samples were present in the data, HHV of the remaining 152 fuel samples is computed by random forest regression (RFR) model obtained from (Yaka et al., 2022). The RFR model proposed by (Yaka et al., 2022) is further validated in this study with 929 fuel samples before its utilization.

Table 4.1 Statistical information regarding all the data utilized in this study.

index	MC (%)	ASH (%)	C (%)	H (%)	O (%)	N (%)	S (%)	HHV (MJ/kg)
count	1081	1081	1081	1081	1081	1081	1081	929
mean	16.20	10.13	48.60	5.72	31.84	1.28	0.30	20.18
std	18.75	13.23	11.28	1.78	14.13	1.95	0.65	5.54
min	0.00	0.00	3.97	0.00	0.00	0.00	0.00	4.22
25%	5.30	1.83	44.20	5.20	23.53	0.30	0.03	18.06
50%	9.29	4.86	48.30	5.80	38.02	0.64	0.10	19.37
75%	16.70	12.20	51.27	6.11	42.02	1.43	0.27	20.79
max	93.04	92.00	89.80	25.13	59.59	21.56	8.90	55.55

Table 4.2 Class distribution of the collected fuel samples according to ECN Phyllis and NTA 8003 CSs.

CS	Class #	Class Name	Data Size
ECN Phyllis	1	Other	37
	2	Fossil Fuel	84
	3	Grass/Plant	145
	4	Husk/Shell/Pit	69
	5	Manure	29
	6	Algae	13
	7	Non-organic Residue	29
	8	Organic Residue	110
	9	RDF and MSW	30
	10	Sludge	60
	11	Straw (Stalk/Cob/Ear)	84
	12	Torrefied material	30
	13	Treated wood	61
	14	Untreated wood	270
	15	Char	4
	16	Biochar	26
NTA 8003	1	Wood/Forestry	336
	2	Biomass (Horticulture/Agriculture)	286
	3	Manure	29
	4	Sludge	57
	5	Biomass (Industry)	93
	6	Organic Residue	14
	7	Other	29
	8	Composite Streams	197
	9	Solid Recovered Fuels	40

4.2.2 Feature Selection and Assessment Methods

Feature selection can aid in data visualization and comprehension while reducing the requirements for measurement and storage, training and use times, and mitigating the challenges posed by high dimensionality to improve prediction accuracy (Nasiri & Alavi, 2022). Feature selection can address the issue by eliminating irrelevant and duplicated data, hence reducing computation time, and enhancing clustering performance (Hancer et al., 2020). Pearson Correlation (Williams et al., 2020) and Mutual Information Score (Pedregosa et al., 2011; Scikit-Learn, 2023c) are utilized in this study feature selection and assessment for the clustering of fuels, whose definitions are explained as follows.

4.2.2.1 Pearson Correlation

Pearson correlation is one of the most common method that is used to evaluate the strength of the linear relationship between two variables (Williams et al., 2020). It takes value in the range of [-1,1]. The closer the Pearson correlation value to -1, 0, and 1 means negative correlation, no correlation, and positive correlation, respectively (Nasir et al., 2020). In other words, the closer the Pearson correlation value to -1 or 1, the less information is lost when this feature is eliminated whilst for construction of the model (Nasir et al., 2020; Williams et al., 2020). Pearson correlation between two features X and Y is given by (Kotu & Deshpande, 2019):

$$PC(X,Y) = \frac{s_{xy}}{s_x \cdot s_y} \tag{4.1}$$

where s_{xy} is the covariance of X and Y, and s_x and s_y are the standard deviation of X and Y, respectively.

4.2.2.2 Mutual Information Score

The mutual information score is a measure of similarity between two discrete vectors (Pedregosa et al., 2011; Scikit-Learn, 2023c). It considers both linear and non-linear associations (Macedo et al., 2022). It takes value in the range of [0,1]. The closer the mutual information score to 0, the more dissimilar the two vectors, whereas the closer the mutual information score to 1, the more similar the two vectors. If the vectors are chosen as the one of the features and the actual classes, the similarity between the two may be utilized to assess the importance of the said

feature (Hoque et al., 2014). The mathematical evaluation of the mutual information score between the vectors U and V is given as (Scikit-Learn, 2023c):

$$MI(U,V) = \sum_{i=1}^{|U|}\sum_{j=1}^{|V|}\frac{\left|U_i \cap V_j\right|}{N} log\frac{N\left|U_i \cap V_j\right|}{|U_i| \cdot |V_i|} \quad (4.2)$$

where $|U_i|$ is the number of samples in cluster U_i and $\left|V_j\right|$ is the number of the samples in cluster V_j.

4.2.3 Clustering Methodology

Clustering is a crucial tool in unsupervised machine learning, where the task is to partition the given data into clusters of neighboring data points (Grunau et al., 2022). While there are several clustering methods available in the literature with different variations, the k-means is one of the most widely preferred and utilized clustering algorithm due to its simplicity, intuitive nature, and convergence properties (Aljabbouli et al., 2020; Amer, 2020). The goal of this algorithm is to choose k centers which minimizes the sum of the squared distances between each point and its closest center. The main drawback of the k-means algorithm was the random selection of the initial selection of the centers (Aljabbouli et al., 2020). This drawback was sufficiently addressed by Arthur & Vassilvitskii by the introduction of the 'k-means++' algorithm (Arthur & Vassilvitskii, 2007), which enabled the selection of the initial centers based on an empirical probability distribution of the points' contribution to the overall inertia (Pedregosa et al., 2011; Scikit-Learn, 2023a). In this study, the 'k-means++' algorithm is utilized for different cluster numbers in order to determine the clusters of the fuel samples, with and without utilizing the class information. This enables the proposition of novel fuel classes directly from the chemical and physical properties of the fuel.

4.2.4 Performance Metrics

The most commonly used performance metrics for the unsupervised k-means clustering algorithm are the internal metrics (inertia, silhouette score, Davies-Bouldin score, and Calinski-Harabasz score) which do not necessitate the ground true classes and can be computed directly from the features. When the actual class information of all samples are available, as is in this study, the computation of the external metrics (adjusted rand index, homogeneity, completeness, and v-measure)

are also utilizable. If C is the set of ground truth class assignment and K is the set resulted from the clustering, the definitions regarding these performance metrics are as follows:

4.2.4.1 Inertia

Inertia is the sum of squared distance of samples to their closest cluster center (Yellowbrick, 2023). As the number of clusters increase, the inertia decreases. While the lower inertia values are preferred, increasing the number of clusters does not always cooperate with the aim of clustering applications. Hence, the optimum number of clusters is determined by the 'elbow method', in which it is clearly observed on the graph that increasing the number of clusters does not yield a sufficient decrease of the inertia (Yellowbrick, 2023).

4.2.4.2 Silhouette Coefficient

Silhouette coefficient (s) is the most commonly used internal performance metric for all clustering applications. It yields results in the range of [-1, 1]. The closer the silhouette coefficient to 1, the better and highly denser clustering. The mathematical expression for the silhouette coefficient for a single sample is (Rousseeuw, 1987):

$$s = \frac{b - a}{\max(a, b)} \tag{4.3}$$

where a is the mean distance between a sample and all other points in the same class, and b is the mean distance between a sample and all other points in the next nearest cluster.

The silhouette coefficient of a set is computed by taking the average of the silhouette coefficient for each sample of the set (Rousseeuw, 1987).

4.2.4.3 Davies-Bouldin Index

Davies-Bouldin Index (DBI) is another internal metric that measures the separation between the clusters. The lowest possible value for the Davies-Bouldin index is zero. The lower the Davies-Bouldin index, the better the cluster partition. The mathematical relations for the Davies-Bouldin index are:

$$R_{ij} = \frac{S_i + S_j}{M_{ij}} \tag{4.4}$$

where S_i is the cluster diameter of cluster i, and M_{ij} is the Minkowski metric of the centroids i and j.

$$DBI = \frac{1}{k} \cdot \sum_{i=1}^{k} R_i \tag{4.5}$$

where k is the number of clusters, and R_i is the maximum of R_{ij} while i≠j.

4.2.4.4 Calinski-Harabasz Index

Calinski-Harabasz index (CHI), also known as variance ratio criterion, is the ratio of the sum between clusters dispersion and of within cluster dispersion for all clusters. The mathematical formulation is (Caliñski & Harabasz, 1974; Scikit-Learn, 2023a):

$$CHI = \frac{tr(B_k)}{tr(W_k)} \cdot \frac{n_E - k}{k - 1} \tag{4.6}$$

where n_E is the data size, k is the number of clusters, $tr(B_k)$ is the trace of the between group dispersion matrix, and $tr(W_k)$ is the trace of the within-cluster dispersion matrix.

4.2.4.5 Adjusted Rand Index

Rand Index (RI) measures the similarity of the two assignments, ignoring the permutations (Rand, 1971). However, it does not ensure to obtain a value close to zero for random labelling. The adjusted rand index (ARI) counters this issue and is widely used in clustering applications (Steinley, 2004). The mathematical relations for RI and ARI is as follow (Rand, 1971; Scikit-Learn, 2023a; Steinley, 2004):

$$RI(C, K) = \frac{a + b}{C_2^{n_{samples}}} \tag{4.7}$$

where a is the number of pairs of elements that are in the same set in C and in the same set in K, b is the number of pairs of elements that are in different sets in C and different sets in K, and $C_2^{n_{samples}}$ is the total number of possible pairs in the dataset.

$$ARI(RI) = \frac{RI - E[RI]}{\max(RI) - E[RI])} \tag{4.8}$$

where $E[RI]$ is the expected rand index.

4.2.4.6 Homogeneity

Homogeneity (h) is the measure of how many data belong to different classes within a cluster. It gives information regarding the homogeneity of the clusters. The value is closer to 1 as the clusters contain only one class type (Rosenberg & Hirschberg, 2007; Scikit-Learn, 2023a):

$$h = 1 - \frac{H(C|K)}{H(C)} \tag{4.9}$$

where $H(C|K)$ is the conditional entropy of the classes given the cluster assignments, and $H(C)$ is the entropy of classes.

4.2.4.7 Completeness

Completeness (c) is the measure of how many data from the given class is assigned to the same cluster. The value is closer to 1 as all the members of all classes are collected in the same cluster (Rosenberg & Hirschberg, 2007; Scikit-Learn, 2023a).

$$c = 1 - \frac{H(K|C)}{H(C)} \tag{4.10}$$

where $H(K|C)$ is the conditional entropy of the clusters given the classes, and $H(C)$ is the entropy of classes.

4.2.4.8 V-Measure

V-Measure (V) is the weighted harmonic mean of homogeneity and completeness (Rosenberg & Hirschberg, 2007; Scikit-Learn, 2023a):

$$V = \frac{(1+\beta) \cdot h \cdot c}{\beta \cdot h + c} \tag{4.11}$$

where β is the constant which to adjust the importance of homogeneity with respect to completeness. If $\beta > 1$, the completeness is weighted more strongly than homogeneity. If $\beta < 1$, the homogeneity is weighted more strongly instead. $\beta = 1$ is taken in this study, which is the default value and infer no preferences.

4.2.5 Analysis of Proposed Clusters and Defining the HOM Classification System

The analysis of the proposed clusters are conducted by several approaches. Binary plots of each feature against HHV is utilized to understand the individual cluster properties. Then, decision tree classification (Pedregosa et al., 2011) is carried out and the optimum resulted tree with lowest depth and high cross validation accuracy is illustrated in order to provide an easy and quantitative means of determination of the fuel cluster (HOM class). Contingency matrices between the proposed clusters and both ECN Phyllis and NTA 8003 CSs are constructed to gain insight into how the unsupervised clustering algorithm performed clustering compared to the conventional classes. 1st and 2nd principal component plots obtained from PCA (Jollife & Cadima, 2016), ternary plots (Basu, 2018), and Van-Krevelen diagrams (Van Krevelen, 1950) are also prepared to enhance the illustration of all CSs, and to gain insight about the proposed clusters for the most accurate analysis. All these analysis are utilized in order to assign the most appropriate names to the cluster sets, which finally provide a definition of the proposed HOM CS.

4.3 Results and Discussion

4.3.1 Data Preprocessing and Feature Selection

Prior to application of any kind of modeling, the data should be investigated in detail to investigate opportunities that may enhance the performance and validity of the models. In this study, we aim to utilize a large dataset of 1081 fuel samples for enhanced clustering, which enables the classification of any fuel, including composite streams, wastes, and fuels of unknown origins. The ultimate (C (%), H (%), O (%), N (%), S(%)) and proximate (MC (%), ASH (%)) analysis data is obtained directly from the literature for all fuel samples. However, HHV of 152 of these fuel samples, an important feature for the classification of fuels, was not present in the data. Luckily, there are several models produced in the literature that are successful in estimation of HHV from ultimate or proximate analysis (Dashti et al., 2019; Noushabadi et al., 2021; Xing et al., 2019a; Yaka et al., 2022). Thus, instead of removing the samples that have null HHVs, the HHVs are computed by using ultimate analysis data and the RFR model proposed in (Yaka et al., 2022). The RFR model was first validated with the fully collected 929 data and is found

successful in estimating the HHV of these samples with high R^2 (=0.9802) and low RMSE (=0.8015) values. Finally, the HHV of the 152 fuel samples is calculated and assigned. Hence, the finalized data contains 152 computed and 929 retrieved HHV. Statistical information regarding the calculated, calculated for validation, assigned, and finalized HHVs of all fuels is given in Table 4.3. As shown here, all the calculated HHV are within range of the collected and finalized data and yield similar statistical values (see also Table 4.2).

Table 4.3 Statistical information regarding calculated, calculated for validation, assigned, and finalized HHV feature.

index	HHV Calculated	HHV Validation	HHV Assigned	HHV Finalized
count	1081	929	152	1081
mean	19.99	20.18	18.80	19.98
std	5.17	5.30	4.12	5.38
min	8.36	8.36	9.53	4.22
25%	18.13	18.23	17.25	17.94
50%	19.23	19.29	18.74	19.29
75%	20.53	20.67	19.91	20.62
max	48.71	48.71	33.36	55.55

After the data curation, the Pearson correlation matrix is computed for each feature and illustrated in Figure 4.2a to further investigate the performance enhancement possibilities. The Pearson correlation matrix shows that all the features are independent. Only the C and H percentages show some correlation with the HHV, but these values are not sufficient for elimination of HHV or claiming direct dependency. This correlation is actually expected since the energy of fuels is generally released by breaking of the chemical bonds between the C and H. To further prove HHV is an independent and important feature for fuel classification, and to conclusively determine the features that is used in this study, the mutual information scores are evaluated for each feature with respect to ECN Phyllis and NTA 8003 CSs as well (see Figure 4.2b). Here, it is easily observable that all the features contribute sufficient information for the classification of fuels. The C (%) is the leading feature with the highest score, followed by HHV and O (%). Hence,

the importance of HHV is once more emphasized as a feature. When both Figure 1 and Figure 2 are investigated together, no further alteration in the finalized dataset is deemed necessary.

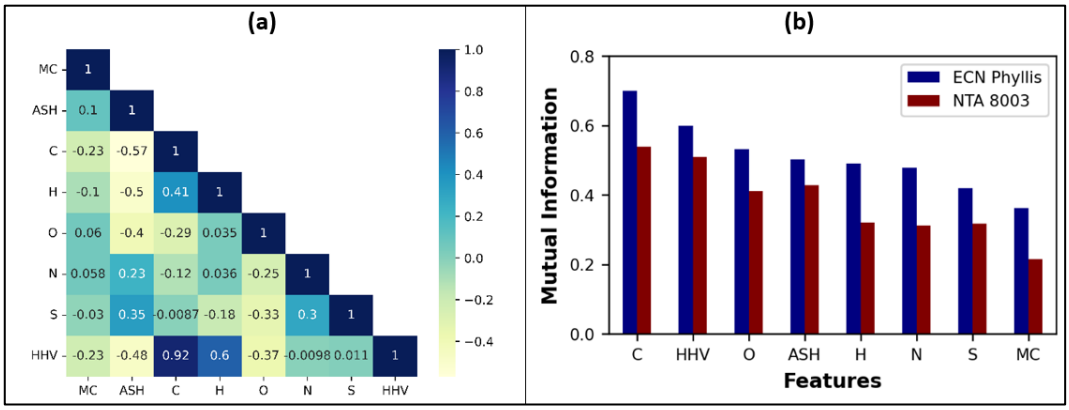

Figure 4.2 Pearson correlation of features (a) and mutual information scores of features according to ECN Phyllis and NTA 8003 CSs (b).

4.3.2 Unsupervised K-means Clustering of Fuel Samples

Determination of the number of clusters is crucial to cluster the fuel samples in the most accurate and reasonable manner. To this end, the optimum number of clusters for k-means clustering is determined by evaluating both unsupervised and supervised performance metrics. The metrics corresponding to the number of clusters are illustrated in Figure 4.3. Here, the optimum number of clusters is observed to be between 4 and 6 when the unsupervised performance metrics is considered. However, the supervised performance metrics for both ECN Phyllis and NTA 8003 CS agrees that the optimum number of clusters resides between 5 and 7. When we compare all the candidate cluster numbers, it is observed that 6 clusters is the best choice due to its exceptional completeness and silhouette coefficient values. Hence, separating the data into 6 clusters is determined to be the most suitable. From here on, the aim of this study becomes to determine if the 6 clusters obtained by the unsupervised k-means algorithm are logical and practical for fuel classification applications. After the analysis of these clusters, they will be defined as the classes of proposed HOM CS and each cluster will be named accordingly.

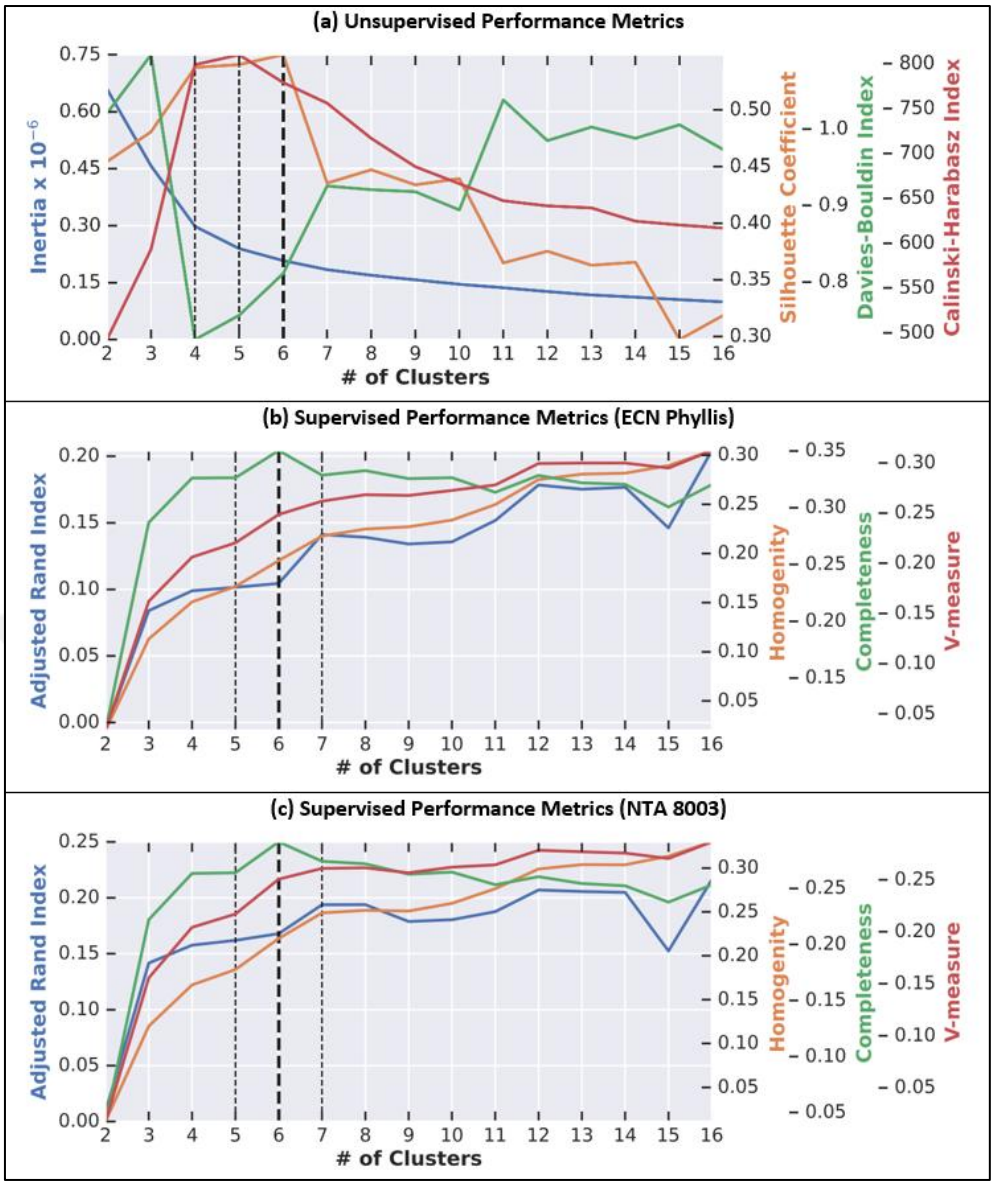

Figure 4.3 Performance metrics for k-means clustering with respect to clusters. The candidate cluster numbers are highlighted with black dashed lines. The most suitable number of clusters selected is shown by the bold dashed line.

4.3.3 Analysis of Proposed Clusters

Prior to comparing the proposed clusters with the conventional fuel classes, it is important to gain insight into the properties of each cluster. Thus, the binary plots of all features with respect to HHV is illustrated with the corresponding clusters in Figure 4.4. Here, it can easily be observed that the fuels are separated into the clusters according to their properties by the design of the k-means algorithm. The prominent properties of each cluster is observed as follows:

- **Cluster 1:** The fuels in this cluster have comparatively high O (%) but is low on MC (%) and Ash (%). It has average HHV, C (%), and H (%).
- **Cluster 2:** The fuels in this cluster have the highest C (%) and HHV. They may contain high levels of H, N, or S. They contain low amounts of MC or ash.
- **Cluster 3:** Having a high MC (%) is the most noticeable feature of the fuels in this cluster, compared to the other clusters. The HHV and C (%) of these fuels are comparatively low as well, and they are likely to contain ash.
- **Cluster 4:** The fuels belonging to this cluster have high Ash (%), resulting in the lowest HHVs. Unlike cluster 3, it has a low MC (%).
- **Cluster 5:** The fuels of this cluster have an average MC (%) (between 20% and 40%), and C (%). However, they are high in terms of O (%), which seem to lower their HHV.
- **Cluster 6:** The fuels in this cluster are observed to be low in terms of O (%) and ASH (%), and between HHVs of 10 and 30. This cluster is in similar behavior to cluster 5, excepting that cluster 5 has a high O (%).

While these descriptions of clusters provide insight and information about each cluster, they are not sufficiently deterministic for a class system. Furthermore, a rule based system is more conventional when an unlabeled sample is tried to be determined. Hence, a DTC algorithm is utilized to obtain these rules illustratively and conclusively for each clusters. The optimum maximum depth of the tree is determined by conducting 10-fold cross validation for each maximum depth of the tree from 1 to 9. The resulting accuracies are illustrated in Figure 4.5. Here, maximum depth of the tree is selected as 4, since further increase of this value do not significantly affect the cross validation performance of the classification and yields a complex tree which is hard to utilize sufficiently. Hence, the data is classified with maximum depth of 4, and the yielding decision tree is illustrated in Figure 4.6. The illustrated tree has an overall 10-fold cross validation accuracy of 97.7%. The application of cross validation method here ensures that the proposed decision tree is generalizable and able successfully to classify fuels of unknown origin. In the figure, if the check within the node is satisfied (True case), the next check flows to the left leaf, otherwise (False case) it continues to the right leaf. The process is terminated when an end node is reached. The results obtained here agrees

with the cluster descriptions above and provides deterministic results regarding which data corresponds with which cluster.

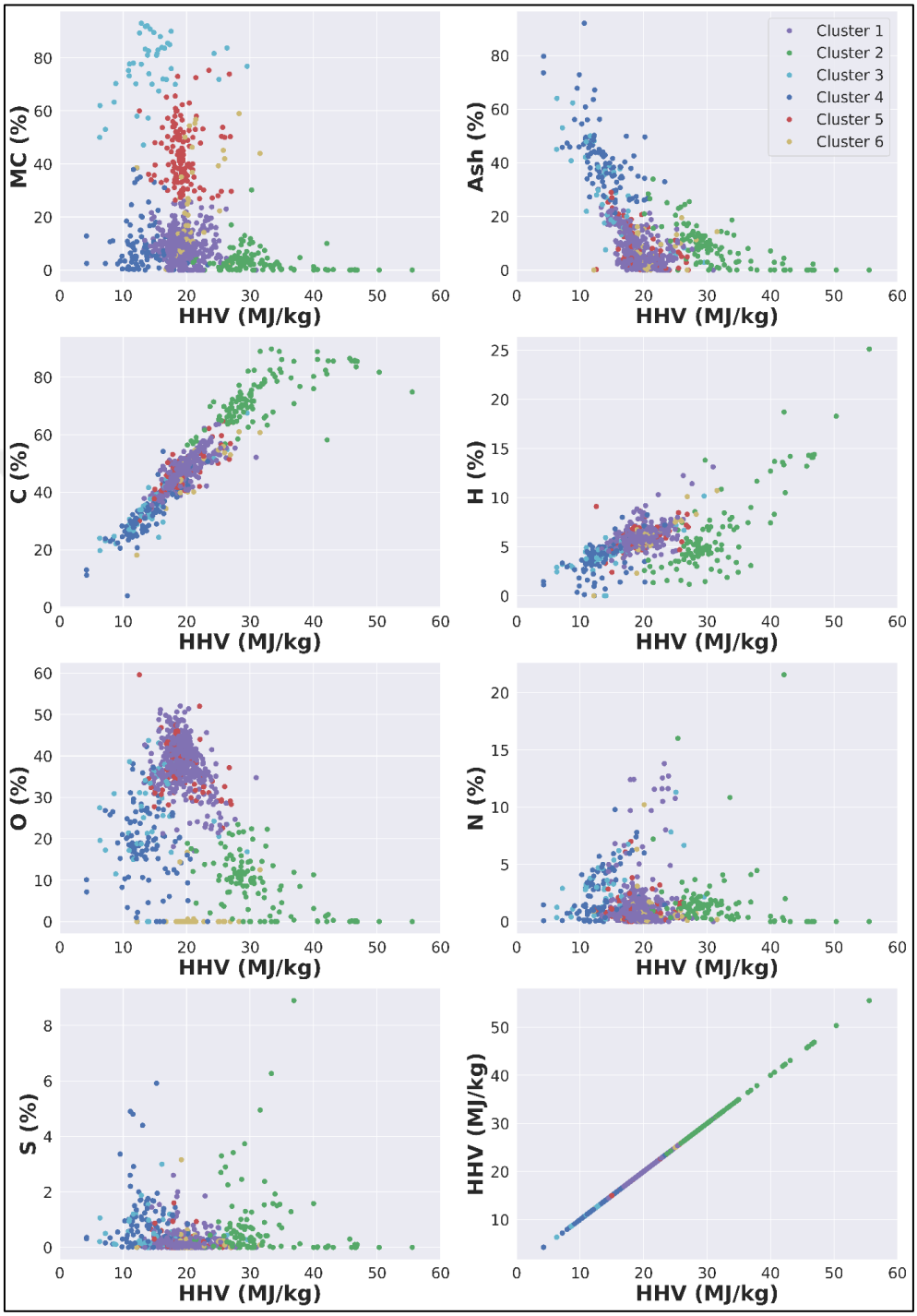

Figure 4.4 Binary plots of all features with respect to HHV, illustrating the proposed clusters.

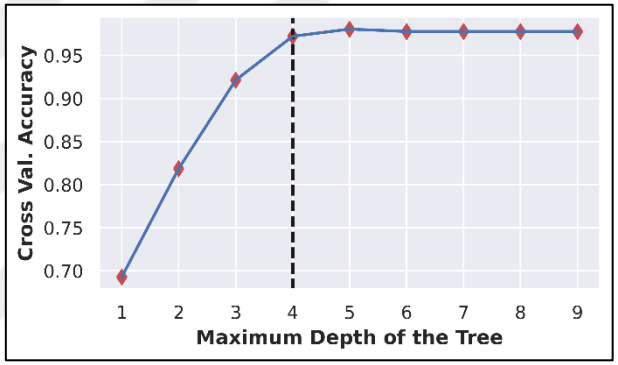

Figure 4.5 10-fold cross validation accuracy for each maximum depth of the tree.

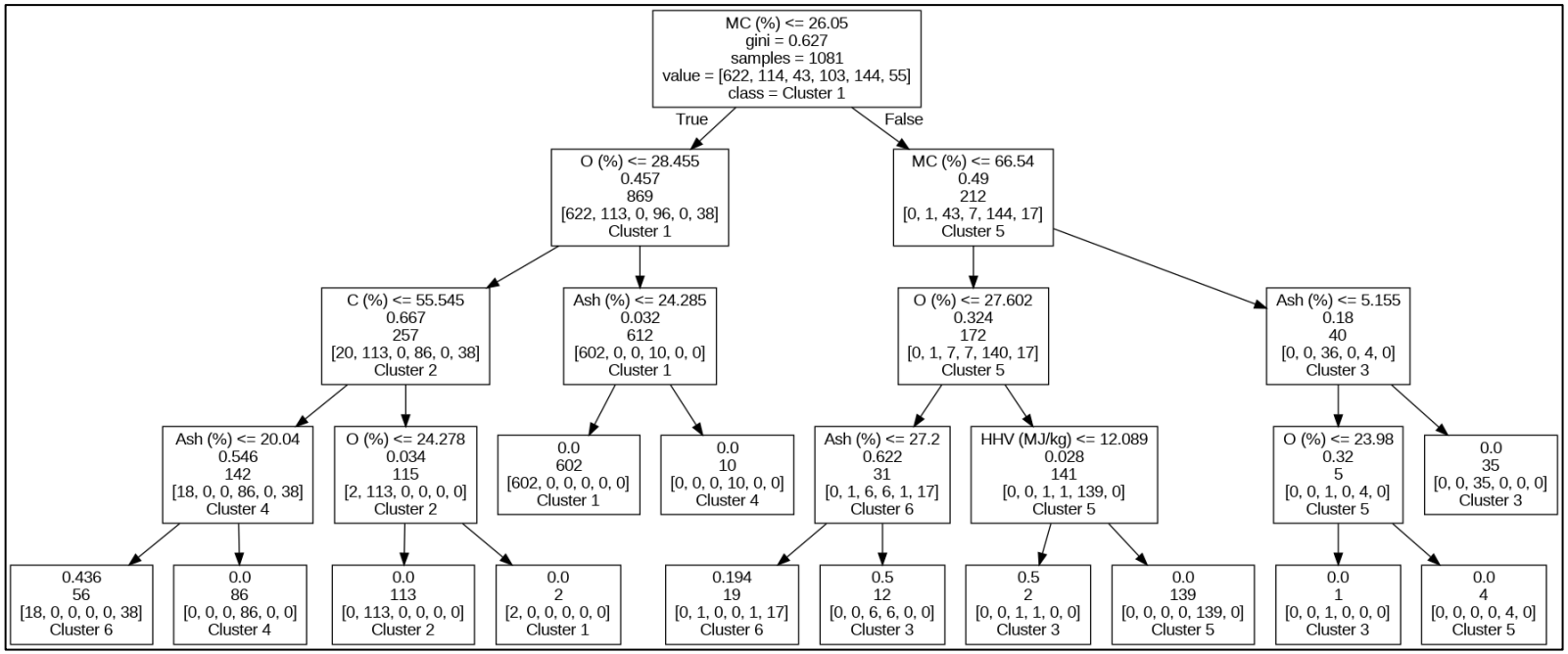

Figure 4.6 Decision tree classification applied to the data labeled with the proposed clusters.

4.3.4 Cluster – Conventional Class Relationships

While the clusters above are optimally determined directly from the fuel properties, it is crucial to show the relationship of these clusters with the established conventional classes. To this end, the proposed clusters are compared with both ECN Phyllis and NTA 8003 CSs in detail. Firstly, a cluster-wise class distribution analysis is conducted to gain insight regarding the cluster contents and class distributions. Then, principal component analysis (PCA) is applied with two principal components to illustrate the similarities between the classes and clusters on a plot corresponding to the maximum amount of variance. Finally, conventional plots, namely, the ternary plot analysis and Van-Krevelen diagram, are produced by using the atomic ratios of H/C, O/C, and H/O for each CS to better illustrate the similarities and differences between the proposed clustering based CS. All these results obtained here are discussed comparatively in detail in the following section.

4.3.4.1 Contingency Matrices

Here, the aim is to simply obtain the numbers of data that belong to each class type within the proposed clusters and then evaluate the class distributions in each cluster accordingly. Table 4.4 and Table 4.5 represent these values for ECN Phyllis and NTA 8003 CSs, respectively. In these tables, the "# Column" shows the number of fuel samples that belong to the corresponding cluster and class. The "D1 Column" shows the percentage of the fuel class with respect to all classes within the specified cluster. The "D2 Column" shows what percentage of the fuels that belong to the specified class are distributed to each cluster. In example, it can be seen from Table 4.4 that 62 fuel samples belong to cluster 1 and organic residue class of ECN Phyllis, 9% of the cluster 1 consists of organic residue, and 53% of the fuel samples in organic residue class belong to cluster 1.

Table 4.4 Distributions of each class type within each proposed cluster with respect to ECN Phyllis CS.

	Cluster 1			Cluster 2			Cluster 3			Cluster 4			Cluster 5			Cluster 6			Total	
	#	D1	D2	#	D1	D2	#	D1	D2	#	D1	D2	#	D1	D2	#	D1	D2	#	D2
Others	13	2	35	7	6	19	0	0	0	4	4	11	5	3	14	8	15	22	37	100
Fossil Fuel	12	2	14	58	51	69	0	0	0	3	3	4	6	4	7	5	9	6	84	100
Grass/Plant	95	15	66	0	0	0	9	21	6	0	0	0	38	26	26	3	5	2	145	100
Husk/Shell/Pit	65	10	94	0	0	0	0	0	0	0	0	0	2	1	3	2	4	3	69	100
Manure	9	1	31	0	0	0	5	12	17	8	8	28	5	3	17	2	4	7	29	100
Algae	8	1	62	0	0	0	5	12	38	0	0	0	0	0	0	0	0	0	13	100
Non-O. Residue	4	1	14	16	14	55	0	0	0	5	5	17	0	0	0	4	7	14	29	100
Organic Residue	57	9	52	1	1	1	5	12	5	20	19	18	23	16	21	4	7	4	110	100
RDF and MSW	18	3	60	2	2	7	0	0	0	7	7	23	3	2	10	0	0	0	30	100
Sludge	2	0	3	0	0	0	16	37	27	41	40	68	1	1	2	0	0	0	60	100
Straw	79	13	94	1	1	1	2	5	2	0	0	0	0	0	0	2	4	2	84	100
Torr. Material	21	3	70	9	8	30	0	0	0	0	0	0	0	0	0	0	0	0	30	100
Treated Wood	42	7	69	0	0	0	0	0	0	4	4	7	7	5	11	8	15	13	61	100
Untreated Wood	196	32	73	0	0	0	1	2	0	2	2	1	54	38	20	17	31	6	270	100
Char	0	0	0	0	0	0	0	0	0	4	4	100	0	0	0	0	0	0	4	100
Biochar	1	0	4	20	18	77	0	0	0	5	5	19	0	0	0	0	0	0	26	100
Total	622	100	-	114	100	-	43	100	-	103	100	-	144	100	-	55	100	-		

Table 4.5 Distribution of each class type within each proposed cluster with respect to NTA 8003 CS.

	Cluster 1			Cluster 2			Cluster 3			Cluster 4			Cluster 5			Cluster 6			Total	
	#	D1	D2	#	D1	D2	#	D1	D2	#	D1	D2	#	D1	D2	#	D1	D2	#	D2
Wood/Forestry	241	39	72	0	0	0	1	2	0	6	6	2	63	44	19	25	45	7	336	100
Biomass (H/A)	220	35	77	1	1	0	17	40	6	1	1	0	39	27	14	8	15	3	286	100
Manure	9	1	31	0	0	0	5	12	17	8	8	28	5	3	17	2	4	7	29	100
Sludge	1	0	2	0	0	0	15	35	26	40	39	70	1	1	2	0	0	0	57	100
Biomass (Ind.)	58	9	62	3	3	3	3	7	3	7	7	8	19	13	20	3	5	3	93	100
Organic Residue	0	0	0	0	0	0	2	5	14	8	8	57	3	2	21	1	2	7	14	100
Other	22	4	76	0	0	0	0	0	0	7	7	24	0	0	0	0	0	0	29	100
Comp. Streams	51	8	26	109	96	55	0	0	0	19	18	10	9	6	5	9	16	5	197	100
Solid Rec. Fuels	20	3	50	1	1	3	0	0	0	7	7	18	5	3	13	7	13	18	40	100
Total	622	100	-	114	100	-	43	100	-	103	100	-	144	100	-	55	100	-		

4.3.4.2 Principal Component Analysis

PCA is one of the most commonly used feature reduction algorithm which enables us to illustrate and gain insight about high dimensional data. Here, the data that contain 8 features are reduced to its first and second primary components, where the variance is maximized among these axes. The resulting data is illustrated in Figure 4.7, where different colors indicate different cluster or classes. In Figure 4.7c, since the clusters are obtained according to the physical properties of the fuel samples, the colors are distinctly distributed. When all the plots in Figure 4.7 is compared, it can be easily commented that the proposed clusters can form a CS that can perform significantly better in classification studies. Furthermore, the plots in Figure 4.7b and Figure 4.7c are quite similar, where both have a fewer number of class labels than ECN Phyllis CS. The similarity is especially obvious on the bottom-right corner and center-right of the plots, where clusters 2 and 5 are highly in-line with classes 8 and 1 of NTA 8003, respectively.

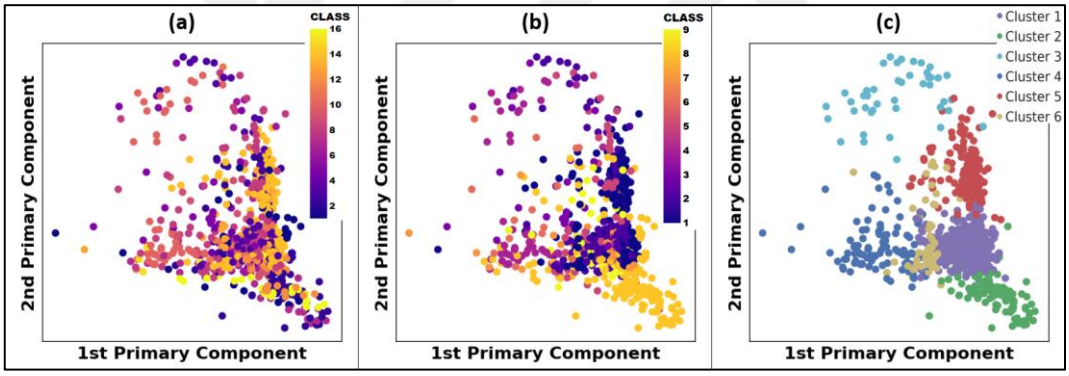

Figure 4.7 Primary component plots of the data for ECN Phyllis classes (a), NTA 8003 classes (b), and proposed clusters (c).

4.3.4.3 Ternary Plot Analysis

The ternary plots (see Figure 4.8) are obtained with the data of HHV and atomic ratios of C, O, and H, which were shown to be the most important features according to their mutual information scores. While the atomic ratios determine the position of the data on the plot, HHV determines the size of the datapoint. The colors of the data again indicate the cluster and class labels. The ternary plots show that the lower the atomic ratio of O, the greater the HHV. Here, the similarity that was observed in the primary component plots between the cluster 2 and NTA 8003 class 8 is shown even more clearly, where these share the common property that they are

comparatively low in terms of atomic ratio of O. Furthermore, it is more clearly seen here that cluster 2 and class 8 of NTA 8003 is also related with classes 1, 7, and 16 of ECN Phyllis.

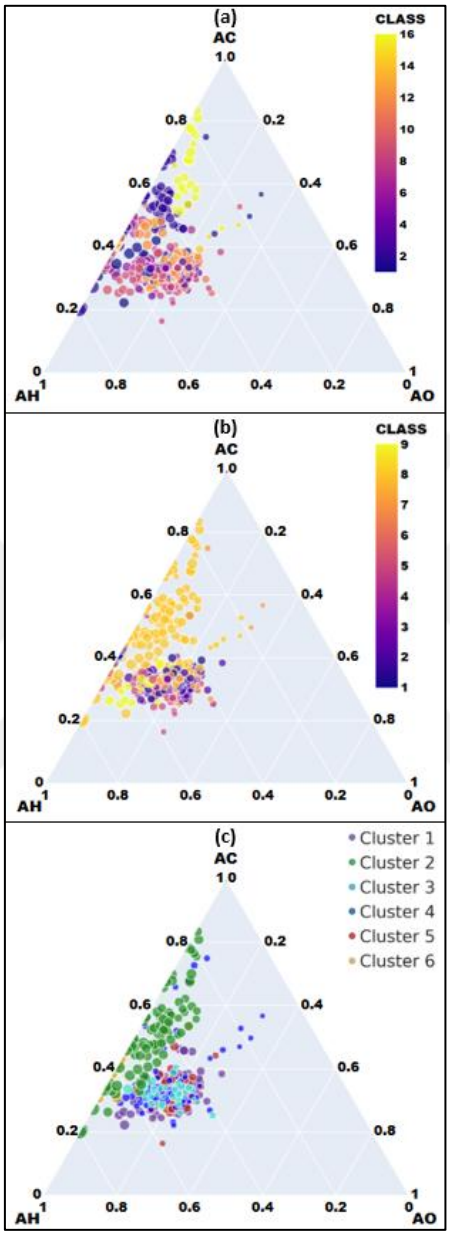

Figure 4.8 Ternary plots of the data for ECN Phyllis classes (a), NTA 8003 classes (b), and proposed clusters (c).

4.3.4.4 Van-Krevelen Diagrams

The afore mentioned similarities between the clusters and classes can further be observed in the Van-Krevelen diagrams (see Figure 4.9) as well. Furthermore, the defining properties of the clusters is represented much more distinctly here. It is once again shown that cluster 2 corresponds with low H/C and O/C rations and

cluster 6 has low O content (low O/C ratio). Since the clusters 1, 3, and 6 are mainly distinguished by their proximate analysis, they are clumped together in the diagram, where they exhibit moderate to high H/C and O/C ratios. It should also be noted that the diagrams agree with the literature for the classes of both ECN Phyllis and NTA 8003 CSs, which is expected since these are highly reputable databases.

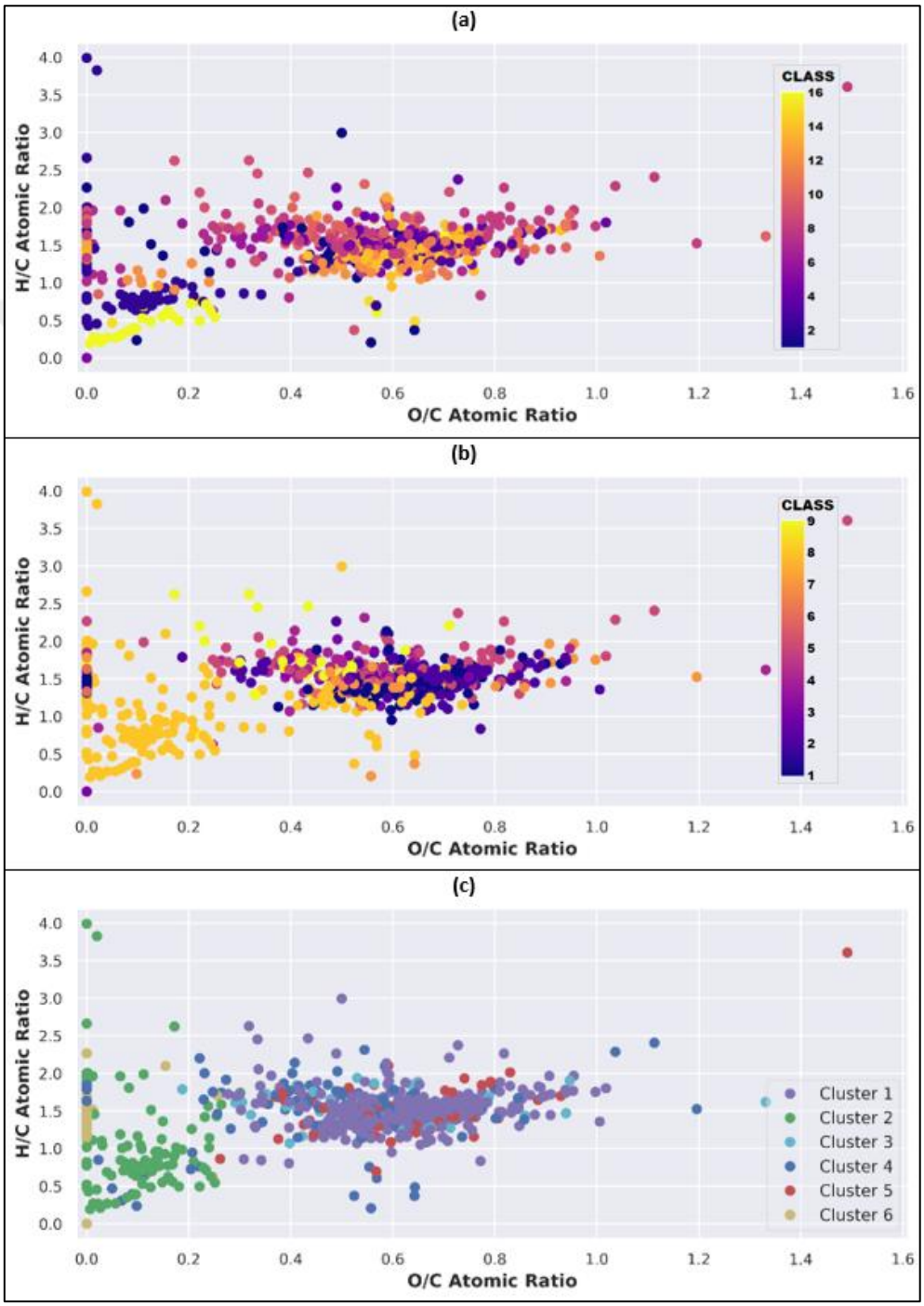

Figure 4.9 Van-Krevelen diagrams of the data for ECN Phyllis classes (a), NTA 8003 classes (b), and proposed clusters (c).

4.3.5 Defining the HOM Classification System and Overall Discussion

From the former analysis, Table 3.6 is constructed to clearly define the proposed HOM CS and provide a summary of the properties of the obtained clusters. The class names for the HOM CS is constructed by the defining properties, which are unique and informative for each cluster. The corresponding classes belonging to both ECN Phyllis and NTA 8003 CSs are also presented for each HOM class. These corresponding class information are determined mainly by utilizing Tables 4.4-4.5 and Figures 4.4-4.9, which prove to be useful for understanding the implications of the proposed HOM CS. Thus, the most common examples of fuels belonging to each HOM CS class is obtained and also presented in Table 4.3. Note that the HOM class of a fuel is determined best directly by the physical properties of the fuel, as explained in the previous sections. Here, it is observed that a particular HOM class contains several ECN Phyllis and NTA 8003 classes. This is expected, since there is a reduction in the number of total classes (from 16 and 9 classes to only 6 classes). However, understanding why these seemingly different classes should be considered as the same is crucial in the assessment of the importance of the proposed HOM CS. In fact, the new HOM CS facilitates the segregation of waste based on their specific utilization areas. It emphasizes the advantages of separating the biomass into woody biomass (HOM-1), high-energy density fuels (HOM-2), wet organic residues (HOM-3), ash-rich residues (HOM-4), moisture rich biomasses (HOM-5) and low-oxygen low-ash fuels (HOM-6).

The Woody Biomasses (HOM-1) class mainly consists of wood/forestry and biomass according to the NTA 8003 CS, which is also confirmed by the corresponding classes 4, 11-14 of the ECN Phyllis CS, as these in fact are all some kind of agricultural wastes or wood/forestry. Some fuel samples for this class can be exemplified as: wood- birch + maple (#70), sunflower seed husk (#378), wheat straw (#460), almond shells (#707), cacao (#884), hemp-fan dried (#1197), wood pellets from Labee- The Netherlands (#2244), Residual wood (#3186) etc. This class can also be called "Lignocellulosic Biomasses" highlighting their woody nature and the presence of complex polysaccharides. Woody biomasses are a significant feedstock for various applications such as biofuels, biopower, and bioproducts.

Table 4.6 Appropriate name assignments of the proposed clusters for HOM CS, and comparison of clusters with classes of the conventional CSs.

Cluster #	HOM CS Class Label	Defining Properties	Corresponding Classes		Most Common Examples
			ECN Phyllis #	NTA 8003 #	
1	**HOM-1**	High O (%), Low MC (%) and Ash (%)	4,11-14	1,2,7	Wood/forestry, agricultural wastes, woody wastes.
2	**HOM-2**	High C (%) and HHV (MJ/kg)	2,7,16	8	Fuels with high calories (HHV > 20 MJ/kg).
3	**HOM-3**	High MC (%), Low C (%) and HHV (%)	3,5,6,10	2-4	Wet biomass (MC > 50%), manure, sludge.
4	**HOM-4**	High Ash (%), Low HHV (MJ/kg)	5,8,10,15	3,4,6	Wastes with high ash content (Ash > 25%).
5	**HOM-5**	High O (%), Low Ash (%)	3,8,14	1,2,5	Green agricultural residues, untreated biomass (MC > 25%).
6	**HOM-6**	Low O (%) and Ash (%)	1,13-14	1,8	Fuels with low oxygen content.

The High-Energy Density Fuels (HOM-2) class consist of fuels that have high carbon content and HHV such as fossil fuels, non-organic residues, and composite streams. Some fuel examples of the HOM-2 class are petroleum coke (#919), methane 100% (#930), propane 100% (#931), coal- bituminous coal (#1145), coal-Iowa Rawhide coal (#1275), diesel oil (#1468) tyres (#1876) wood char (#2273) Biochar from oak wood 600/60/0 (#3506) etc. This description conveys the key attribute of these fuels, which is their ability to provide a substantial amount of energy in a relatively small quantity, making them efficient and desirable for various applications, including power generation, transportation, and industrial processes.

The Wet Organic Residues (HOM-3) class is observed to consist of biomass that have high moisture content (>50%) such as grass/plant, algae, manure, and sludge. Examples of this type of fuels can be given as: paper residue sludge (#681), rice straw- soaked (#736), sewage sludge (#1669), chicken manure (#1748), algae-Monodus Lipids extract- fraction-2 (#2325), cow manure (#2782), tomato plant (#2887), watermelon plant (#2890) etc. Wet Organic Residues emphasizes both the

organic nature of the materials and their moisture content, distinguishing them from other types of biomasses or organic waste. Biomass with very high moisture content, such as grass/plant, algae, manure, and sludge, can be utilized with various applications including anaerobic digestion, composting, fermentation to produce biofuels or biochemicals.

The Ash-Rich Residues (HOM-4) class contains manure, sludge, organic residues, and composite streams that are high (>20%) in ash content. Some examples of the HOM-4 class are: sewage sludge- dried (#960), char from carpet waste (#1356), black liquor (#1395), MSW (#1518), cattle manure- partially composted (#1883), humus from digested MSW (#2133), Straw pellets char 350 deg C (#2710), Mushroom manure (#3066), tomato plant, greenhouse waste (#3517) etc. This class indicates that these wastes contain a relatively high proportion of ash compared to other samples. This description is useful for distinguishing these materials from low-ash or ash-free organic wastes and helps communicate their potential implications for disposal, utilization, or further treatment.

The Moisture Rich Biomasses (HOM-5) class contains wet (MC>25%) agricultural residues and untreated biomass in general, whose oxygen content is high and ash content is low. These can be exemplified as: wood- mixed hardwood chips (#280), soft wood (#300), miscanthus (#596), under water wood (#877), banana grass (#1114), coffee grounds (#1769), spent coffee (#2190), Mango seeds (#2925) etc. Moisture-rich biomass is useful for differentiating biomass that requires special handling, processing, or drying techniques before it can be effectively used for energy generation or other applications.

The Low-Oxygen Low-Ash Fuels (HOM-6) class contains various fuels that have significantly low O and ash percentages. Some examples of this fuel type include PVC (#781), bone meal (#2239), Solid Recovered Fuel (#3103), Wood (#3114), Wood chips (#3178), Biodiesel (#3273), Used wood- chemically treated -class C- (#3279) Compost (#3488) etc. indicates that these wastes contain a relatively high proportion of ash compared to other components. Low-Oxygen Low-Ash Fuels description is useful for distinguishing these materials from low-ash or ash-free organic wastes and helps communicate their potential implications for disposal, utilization, or further treatment.

These descriptions and examples show that the proposed classification system emphasizes the properties of the fuels instead of the fuels' source & origin. Furthermore, the proposed HOM CS does not contain a class named "others" as opposed to the other CSs, which enables the classification of all types of fuels. This classification also offers the advantage of segregating fuels into distinct groups such as woody biomass (HOM-1), high-energy density fuels (HOM-2), wet organic residues (HOM-3), ash-rich residues (HOM-4), moisture rich biomasses (HOM-5), and low-oxygen low-ash fuels (HOM-6). This categorization is especially important for accurately determining the most efficient conversion methods for wastes, fuels of unknown origin, and fuel mixes that are most commonly utilized in waste-to-energy processes. Thus, the proposed HOM CS has the potential of becoming an impactful CS whilst deciding the appropriate fuel type or even the fuel mixture for a given process.

4.4 Conclusion

In this study, firstly a large dataset of 1081 fuel samples is constructed with the features determined as the ultimate and proximate analysis data and HHV, including class labels according to ECN Phyllis and NTA 8003 CSs. By using this data, it is shown that HHV is an important feature for classification of fuels, as well as the features obtained from the ultimate and proximate analysis. Then, k-means clustering is carried out to determine a novel CS that is based on the physical properties of the fuel rather than the conventional approaches where the origin or source of the fuels is utilized instead. Here, the optimum number of clusters is determined as 6 with respect to both unsupervised and supervised performance metrics. Then, to gain quantitative insight into the nature of the obtained clusters, decision tree classification is utilized and the optimum model is illustrated. Furthermore, advanced analysis of the proposed clusters is conducted in comparison with the conventional CSs by utilizing contingency matrices, ternary plots, and Van-Krevelen diagrams. Finally, the novel HOM CS is proposed as a result of the analysis by assigning appropriate class names to the proposed clusters.

Herein, the proposed HOM CS is shown to be advantageous to the conventional CSs due to its ability to classify any kind of fuel by using its physical properties. This is significantly important whilst classifying fuel mixtures and fuels of

unknown source or origin, or composite streams which are vaguely classified as “wastes,” “composite streams,” or “others” by the conventional CSs. The researchers may utilize any of the analysis methods presented here to obtain the HOM class of any fuel, but we recommend the utilization of decision tree classification whose rule based algorithm is illustrated in Figure 6, since it is the most convenient. Furthermore, the ternary plots and Van-Krevelen diagrams of all 1081 fuels are presented in this study for all the CSs as well, so the researchers may use them to determine or check their fuel’s class according to any CS. By understanding the characteristics of each fuel group, it becomes possible to optimize energy generation from waste resources. With the implementation of the new HOM CS, waste materials can now be categorized based on their specific applications. This categorization provides valuable insights into determining the most efficient conversion methods for waste-to-energy processes, including combustion, gasification, and biogas plants.

As a future direction, further classification studies may be conducted with more data considering the HOM CS as well as the conventional CSs and the performance of all advanced classification methods with respect to each CS can be further investigated. Determination of the HOM CS of fuels may be adapted as an in-between step to enhance performance of fuel recovery processes, recycling, composting etc. where the fuels are generally classified from visual data. Thus, the correct assignment of HOM class from images seems to be the one of the next natural steps in moving forward with respect to literature.

5
GENERALIZABLE WIND POWER ESTIMATION FROM HISTORIC METEOROLOGICAL DATA BY ADVANCED ARTIFICIAL NEURAL NETWORKS

5.1 Introduction

As the installation of wind power grows each year, the share of wind power (WP) in the power systems continues to increase (Tang et al., 2024). The unpredictability and instability caused by the widespread use of wind power at elevated levels poses significant difficulties for ensuring the secure and consistent functioning of the electricity grid (Ahmed et al., 2020). Accurately forecasting wind power output of the wind farms (WF) will successfully mitigate these negative consequences, further fostering the utilization of WP and diminishing the environmental contamination resulting from the use of fossil fuels.

There have been several recent studies conducted to advance WP prediction. The models employed by these studies are generally categorized as physical models, statistical models and machine learning models. Physical models primarily use numerical weather prediction (NWP) methods to obtain wind energy forecasts by solving differential equations based on the principles of wind energy conversion and meteorological knowledge (Nielsen et al., 2007; L. Wang et al., 2013). Statistical models generally use historical data to predict WP. Traditional statistical models, such as time series models like autoregressive (AR), autoregressive moving average (ARMA), and autoregressive integrated moving average (ARIMA) models, directly use historical WP data to predict future WP(Karakuş et al., 2017). However, their performance is shown to be highly affected by weather conditions (Liao et al., 2023).

With the developments in artificial intelligence (AI) methods, various machine learning algorithms such as artificial neural networks (ANN) , support vector machines (SVM) , and long short-term memory networks (LSTM) have been used to forecast WP (R. Yu et al., 2019; H. Zhang et al., 2014). These models are utilized to calculate WP based on numerical weather prediction and historical power data.

For example, a study proposed an improved radial basis function neural network-based model with error feedback scheme to forecast short-term wind speed and power where they showed with a numerical experiment based on a WF that the proposed method can achieve better accuracy and maintain computational efficiency (Rajagopalan & Santoso, 2009). Khosravi et al. combined decision trees and SVM and resulted that the prediction performance of the proposed method was improved by 37%, while the computation time was shorter than that of only utilizing SVM (Khosravi et al., 2018). Zhang et al. used LSTM to predict wind turbine power based on numerical weather prediction and historical power data (J. Zhang et al., 2019). As a result, a gaussian mixture model was used to analyze the uncertainty of WP. The effectiveness of the proposed model was verified by numerical experiments conducted in a real power plant.

When the latest studies on WP prediction are examined, it is observed that these studies emphasize the advantages of advanced ANN models such as Nonlinear Autoregressive with Exogenous Inputs (NARX) model, Elman model, and Long Short Term Memory (LSTM) model. Cadenas et al. compared the univariate ARIMA model and the multivariate NARX model for wind speed prediction and reported that the NARX model was superior to ARIMA (Cadenas et al., 2016). Gu et al. showed that the 4-hour, 24-hour and 72-hour wind power prediction accuracies of the LSTM model they developed were higher than other tested models (Gu et al., 2021). Cui et al. presented an advanced hybrid model using Long Short-Term Memory (LSTM) while considering wind power ramp events (WPREs). The results of the proposed model outperformed existing methods (Cui et al., 2023) Liao et al. proposed a new short-term wind power probabilistic prediction model based on MTGP using the idea of multi-task learning. The model demonstrated that GP performs well in wind power forecasting when sufficient training data is available (Liao et al., 2023). Gidom et al. collected data for a power plant in Kocaeli/Türkiye and showed the high performance of the NARX model in power prediction for this plant (Gidom et al., 2024). Liu et al., in their study, predicted wind power using Elman neural networks and showed the effectiveness and sophistication of the Elman model by having higher prediction accuracy compared to other prediction models (S. Liu et al., 2024)

All these studies emphasize that the accurate estimation of WP output of WFs is crucial for grid stability and optimization. However, the following research gaps still present challenges according to our literature review:

- Some of the features for prediction of the WP output are difficult to obtain or only available to the management of the particular WF, which undermines the collective effort for grid stability and optimization.
- The lookback period, that is, the duration which refers to the historical time frame of data that the model uses to make predictions, is undecided throughout literature.
- There is no generalizable model proposed that can be utilized by anyone and for any WF within a region. This causes each WF to obtain their prediction models by utilizing their own data, which may be challenging for well-established WFs and is impossible for newly-established WFs.

In this study, the meteorological and power data of four different WFs (three of which are well-established while one of which is newly-established) located at west of Türkiye was utilized to conduct a detailed analysis of the most prominent ANN models, namely NARX, Elman, and LSTM derivatives, to address these research gaps. Performances of these ANN models are investigated by utilizing expanding window validation method at the three of the WFs that are well-established. Here, the best performing advanced ANN method was selected considering both performance and computational load. Then, the best performing model for each WF was utilized, with slight modifications, firstly in prediction of power output of the remaining well-established WFs, and then in prediction of power output of a newly-established WF within the same region. The flowsheet of the study is illustrated as Figure 5.1 to clearly explain the organization of the paper. Overall, the novelties of this study can be summarized as follows:

- The most common and publicly available features for WF power output estimation is investigated.
- The optimum lookback period for the prediction models was determined.
- The performance of prevalent ANN models for WF power output are compared in detail by utilizing expanding window validation method.

- By using the best performing model determined on the previous step, a generalizable WF power prediction model that can utilize the data of different well-established WFs for training is proposed and cross-validated by the data of three different WFs in west of Türkiye.
- The performance of the generalizable model in estimating power output of a newly-established WF is showcased by validating the model on a WF that has only 2 months of power production data available.

Thus, by determining the best modeling approach for WP output forecasting of WFs and proposing a generalizable ANN model that can be utilized to estimate WP of any WF within a region, this study presents essential information for researchers, managers, and governmental offices who work on stabilization or optimization of the grid networks that are connected to WFs. This study will gain even greater significance as the global number of WFs increases and societies focus on the efficient utilization of WP in order to reduce environmental contamination caused by the utilization of fossil fuels.

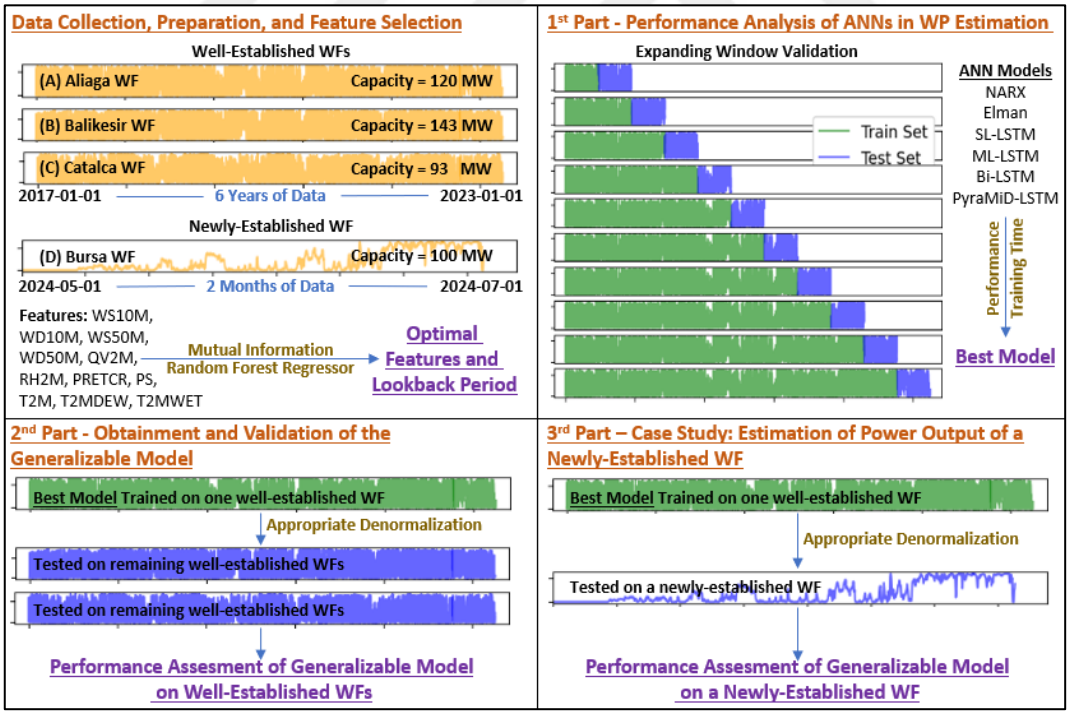

Figure 5.1 Flowsheet of this study: Generalizable Wind Power Estimation from Historic Meteorological Data by Advanced Artificial Neural Networks.

5.2 Methodology

5.2.1 Data Collection, Preparation, and Feature Selection

In this study, 11 features (independent variables), namely Wind Speed at 10 Meters (WS10M, m/s), Wind Direction at 10 Meters (WD10M, Degrees), Wind Speed at 50 Meters (WS50M, m/s), Wind Direction 50 Meters (WD50M, Degrees), Specific Humidity at 2 Meters (QV2M, g/kg), Relative Humidity at 2 Meters (RH2M, %), Precipitation Corrected (PRETCR, mm/hour), Surface Pressure (PS, kPa), Temperature at 2 Meters (T2M, °C), Dew/Frost Point at 2 Meters (T2MDEW, °C), Wet Bulb Temperature at 2 Meters (T2MWET, °C), were collected from NASA Power platform (NASA, 2024) to estimate the power output (dependent variable) of the three different WFs located in Türkiye. The specific locations of these WFs, which are Aliaga (A) WF, Balikesir (B) WF, and Catalca (C) WF are given in Figure 5.2. The power output data for all WFs is obtained from the government's EPIAS Transparency Platform (EPIAS, 2024). The data is collected from these WFs is on hourly basis for 6 years (between 2017.01.01 – 2023.01.01). Furthermore, to showcase the applicability of the proposed model when there is a lack of consistent power output data, a recently established WF (Bursa WF (D)) with only 2 months of data available (between 2024.05.07 – 2024.07.01), was also examined, whose location is also illustrated in Figure 5.2. These locations were selected for this study since the wind power capacity of regions Aegean and Marmara (which will be collectively referred to as west-Türkiye) consists of more than 70% of the total capacity of Türkiye (Arıcı et al., 2021). The statistical information regarding the data collected for this study is illustrated via violin plots in Figure 5.3. Here, it is observed that the trends of Balikesir, Catalca, and Bursa WFs seem similar whereas the wind direction statistics of Aliaga is significantly different since its west is open to the Aegean sea, which should be noted during feature preparation and selection.

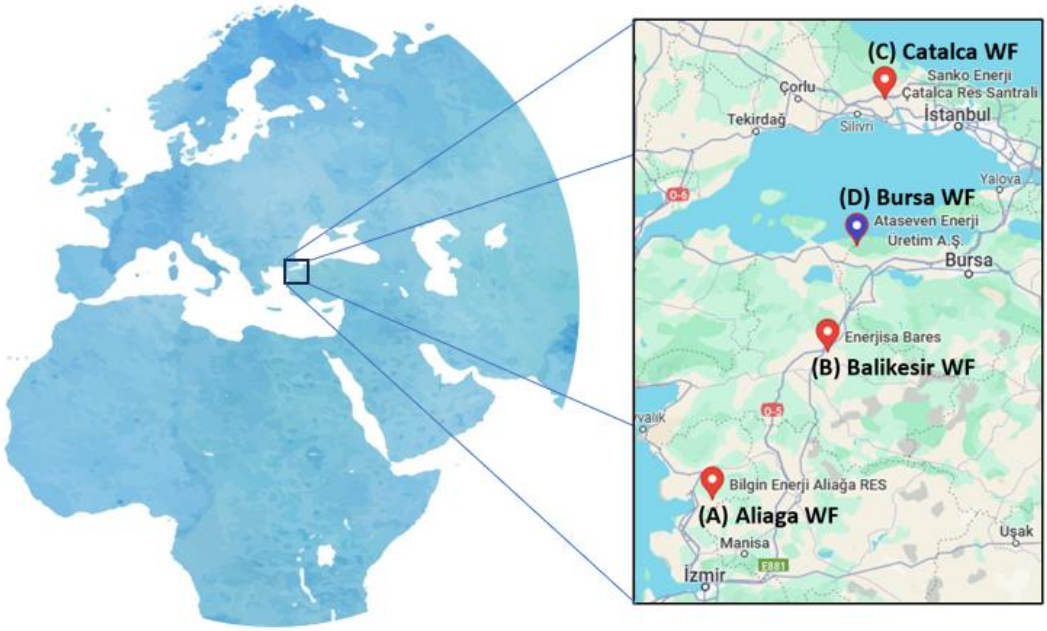

Figure 5.2 Locations of the WFs that are investigated in this study. The Aliaga, Balikesir, and Catalca WFs are well-established WFs whose 6 year data is available whereas the Bursa WF is a newly-established WF with only 2 months of data reported.

Before conducting any kind of modeling or estimation study, it is crucial to analyze the features' ability to estimate the output individually and eliminate the unnecessary features to both simplify the model and reduce the number of necessary inputs. Thus, before modeling, the correlations of features is investigated via the Pearson correlation matrix and their mutual information with respect to the output is investigated. The mutual information score for the feature selection is evaluated by utilizing a random forest regressor as explained in detail by Koeman & Heskes (Koeman Mikeand Heskes, 2014).

After determination of the optimal features that will be utilized in estimation of WP, the lookback period, which can be defined as amount of hours before the prediction of which the model will consider before performing the estimation, remains undecided for the modeling. While different studies utilized a range of lookback periods, there is no study we could find that determines the optimum lookback period for one-hour ahead prediction of the WP. Thus, we once again utilized a random forest regressor to estimate WP considering different lookback periods in the range of 1 hour to 36 hours. The performance of the random forest regressor is

evaluated for each well-established WF to determine the optimum lookback period, which is then utilized in estimation of the WP by the advanced ANN models.

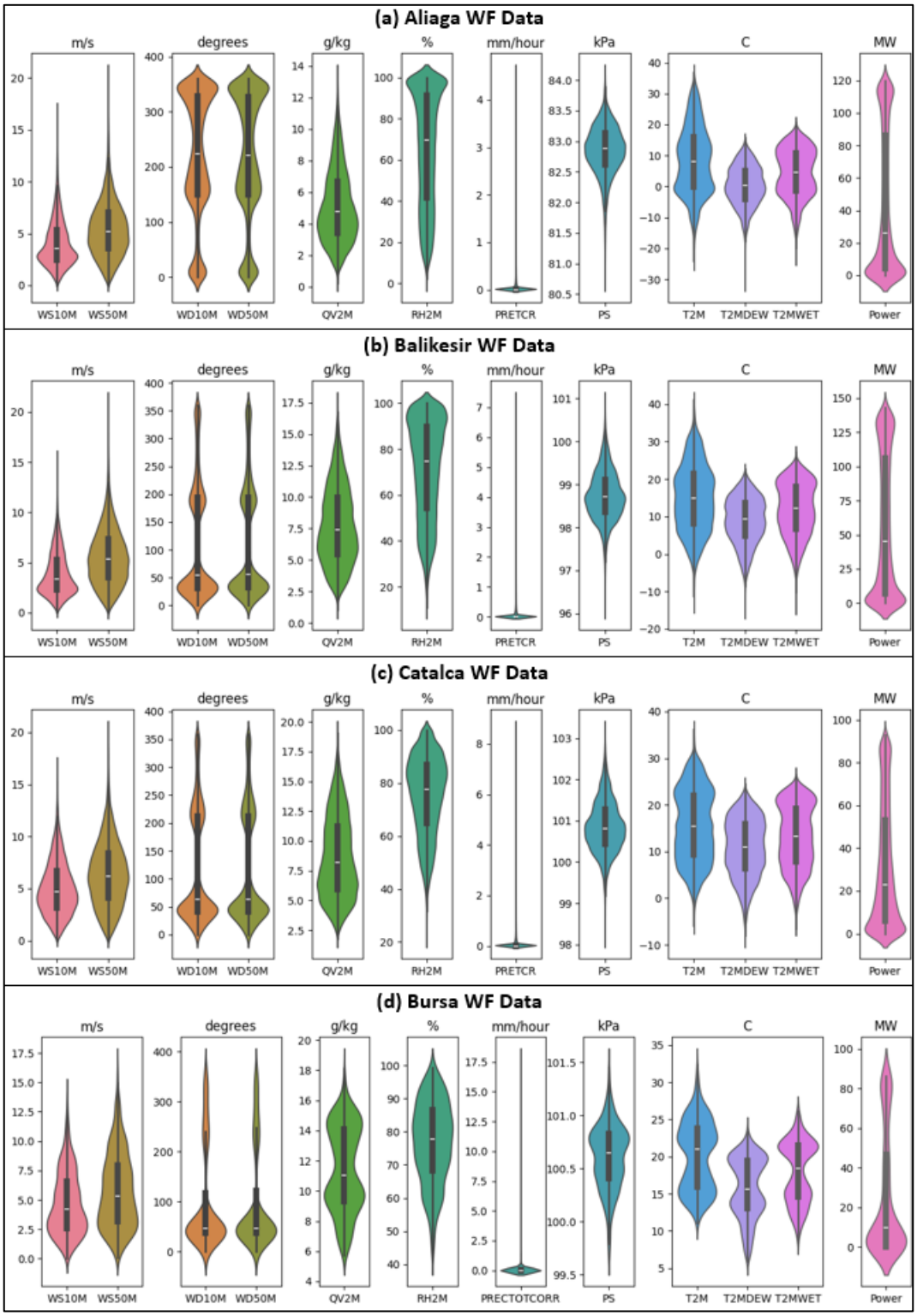

Figure 5.3 Violin plots of the data collected for each WF.

The seasonal trends of each well-established WF is also illustrated to validate our claims that the regional variability of the WP produced is similar, which shows the potential for the obtainment of the generalizable model for the region.

5.2.2 Artificial Neural Networks for Wind Power Projection

Artificial neural networks are a network simulation that imitates the neuron structure of the human brain. The reason why it has been preferred in various applications such as WP forecasting in recent years is that it can process multiple data simultaneously and easily learn the complexities between parameters. Artificial neural networks consist of 3 main parts: input layer, hidden layer and output layer (Shirazi et al., 2020). We first feed the data we obtain from the data source we use to the input layer. Then, the fed data passes to the hidden layer and is weighted. Input data is collected by multiplying it with the weight values attached to each hidden layer neuron. The sum of the products represents the neuron's input. Each input is processed through an activation function, producing a non-linear output. After the applied activation function, the output of the neuron is fed as input to the output layer. The weights are optimized to minimize the error in the output layer (Aguirre & Fuentes, 2019). It learns behaviors in complex relationships by updating weight values during the learning process. By propagating the error in the output layer backwards (back propagation), calculating the derivative according to the weights, placing a certain learning rate, partially adapting the weight updates from the previous update (momentum), or using regularization techniques to prevent the model from overlearning, the weights can be updated (Nøkland, 2016). Improved model performance is a measure of learning and generalization ability (Jin et al., 2022). Hereafter, we will be focusing on the NARX, Elman, and LSTM ANN models, whose network architectures is given in Figure 5.4, as these are the most prevalent ANN models to estimate wind power.

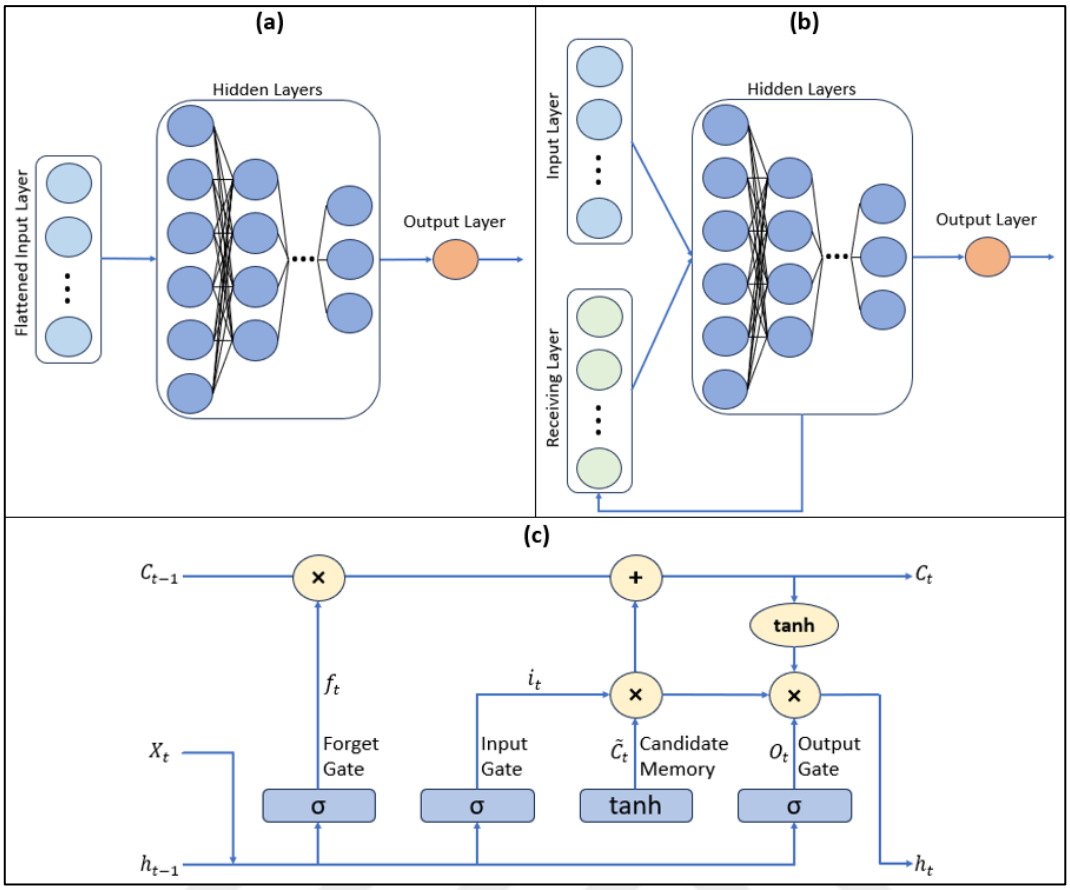

Figure 5.4 General illustrations for architecture of (a) NARX, (b) Elman, and (c) LSTM ANN models.

5.2.2.1 NARX ANN Model

The NARX model is a dynamic neural network model used for predicting nonlinear, time-dependent, and non-repetitive systems (Boussaada et al., 2018, p. 620). The effectiveness of the NARX model has been shown in simulating non-repetitive, unique, and stochastic systems without recurring patterns. This feature makes the NARX model an ideal choice for forecasting natural systems, such as wind energy applications. The NARX neural network architecture typically consists of two main components: the autoregressive(AR) part and the exogenous (X) part. The autoregressive part captures the system's past outputs as inputs to predict the current output (Badji et al., 2023). It includes feedback loops to account for temporal dependencies. The exogenous part includes additional external inputs that can affect the system but are not directly related to the system's past outputs. Unlike models that rely solely on historical data, the NARX model incorporates exogenous inputs to forecast future outputs (Xu & Zhang, 2021). The model's structure fundamentally

consists of a function that accounts for the system's past outputs and external inputs. The NARX model has two primary architectures: series-parallel (open-loop) and parallel (closed-loop). In the series-parallel architecture, previously predicted outputs are not reused for future predictions. The goal in the open-loop configuration is to maximize the model's stability, but this can limit its generalization ability. The open-loop model operates on real-world data and external inputs. Unlike the open-loop architecture, the closed-loop architecture feeds back previously predicted outputs as inputs for future predictions. This approach enhances the model's generalization capability compared to the open-loop architecture. This model can be algebraically expressed using Equation 1. In this context, y represents the variable of interest, u is the externally determined variable, and ε_t is the error term. This structure is capable of performing nonlinear modeling without any prior knowledge of the relationships between input and output variables (Kumar et al., 2017)**.**

$$Y_t = F(y_{t-1}, y_{t-2}, y_{t-3}, \dots, u_t, u_{t-1}, u_{t-2}, u_{t-3}, \dots) + \varepsilon_t \quad (5.1)$$

5.2.2.2 Elman ANN Model

Elman Neural Networks, a type of recurrent neural network (RNN), are designed to model sequential dependencies in data. The Elman neural network consists of four main layers: input layer, hidden layer, context layer, and output layer (H. Liu et al., 2015). The input layer receives the input data from the time series and transmits it to the network. The hidden layer processes the incoming data and directs it to the context units. Elman networks include a hidden layer that functions as a context layer, capturing information from the previous time step and feeding it back into the network for the current time step. The architecture of the Elman network allows it to capture temporal dependencies in sequential data, enabling a form of short-term memory. This memory mechanism distinguishes Elman networks from traditional feedforward neural networks and makes them particularly suitable for tasks such as time series forecasting, where understanding the temporal evolution of data is crucial. The model can establish nonlinear relationships because it learns the dependencies evolving over time by using past data and the hidden states from previous time steps. In Elman architecture, the parameters adjusted during the learning process enhance memory depth, referring to the quantity of

stored information, while reducing resolution, which pertains to the accuracy of the information (Alhmoud & Nawafleh, 2021b).

In the neural network model with $y(t)$ output nodes, the number of input nodes is denoted by (x), the number of hidden layer nodes is (m), and the number of output nodes is (Y). The weight matrices used in the model are defined as follows: (w^1) represents the weight matrix for the connection between the association layer and the hidden layer; (w^2) represents the weight matrix for the connection between the input layer and the output layer; and (w^3) represents the weight matrix for the connection between the hidden layer and the output layer. The transfer function of the output layer is denoted by (g), while the transfer function of the hidden layer is defined as the log-sigmoid transfer function (f) (Alhmoud & Nawafleh, 2021a).

$$y(t) = g(w^3 x(t) + b_2) \tag{5.2}$$

$$y(t) = f(w^1 x_c(t) + w^2\big(u(k-1)\big) + b_1 \tag{5.3}$$

$$x_c(t) = x(t-1) \tag{5.4}$$

5.2.2.3 LSTM ANN Models

Long Short-Term Memory (LSTM) neural networks are a type of recurrent neural network (RNN) that is designed to efficiently capture and model sequential dependencies in data (Shao et al., 2021). LSTM captures and processes long-term dependencies, allowing it to learn these dependencies effectively and thereby improve modeling performance. Long Short-Term Memory is a modified version of RNN that facilitates the retention of past data in memory and addresses the vanishing gradient problem. LSTMs overcome the vanishing gradient problem by combining memory cells equipped with input, forget, and output gates. These gates regulate the flow of information, allowing LSTMs to preserve significant context over extended sequences (Cui et al., 2023). The most significant advantage of LSTM is its special memory block structures located in the recurrent hidden layer. Memory blocks consist of small memory cells that preserve the temporal position and state of the LSTM network while processing information. The role of these memory cells is to store and update information. Within these memory cells, unique mechanisms known as "gates" are used. Focusing on the mathematical formulation

of the LSTM cell; in Equation (4.5), X_t represents the input vector, h_{t-1} the hidden state, and c_{t-1} the previous cell state. The hidden state output h_t is provided in Equation (4.7), while C_t represents the current cell state output as shown in Equation (9) (Lin et al., 2020). These equations represent the general architecture of the LSTM (see also Figure 5.4c). The LSTM can further be classified into more specific types, namely, single-layer LSTM, multi-layer LSTM, bidirectional LSTM, and PyraMiD-LSTM.

$$i_t = \sigma(X_t U^i + h_{t-1} W^i + b_i) \tag{5.5}$$

$$\tilde{C}_t = tanh(X_t U^c + h_{t-1} W^c + b_c) \tag{5.6}$$

$$C_t = C_{t-1} \cdot f_t + i_t \cdot \tilde{C}_t \tag{5.7}$$

$$O_t = \sigma(X_t U^o + h_{t-1} W^o + b_o) \tag{5.8}$$

$$h_t = O_t \cdot \tanh(C_t) \tag{5.9}$$

- **Single-Layer LSTM**

The single-layer LSTM (SL-LSTM) model is the most fundamental form of LSTM networks. It consists of a single LSTM cell, which enables the processing of long-term dependencies and facilitates the handling of contexts. The LSTM cell state is an advanced version, consisting of an input gate, output gate, forget gate, and memory cell. In the LSTM architecture, cellular processes are governed by gates and the sigmoid activation function. The first step in the LSTM mechanism is to decide which information from the cell state should be discarded. The forget gate determines which information from the previous cell state should be discarded, thereby reducing the information stored in the memory cell. The input gate decides the rate at which the cell should be updated, using the information from the previous hidden state and the current input data, and produces a weight value for this update. The cell state is then updated by evaluating the outputs of the input and forget gates. Finally, the output gate generates the hidden state based on the updated cell state (Salman et al., 2018).

- **Multi-Layer LSTM**

Multi-Layer LSTM (ML-LSTM) is an architecture that consists of multiple LSTM units stacked together. In this architecture, the output from the previous LSTM layer is fed synchronously as the input to the next LSTM layer. There are several LSTM layers that the input layer data passes through. Each LSTM layer generates its own hidden state (h_t) and cell state (c_t) outputs by utilizing the original input data (X_t) and the hidden state output (h_t-1) from the preceding layer (Y. Wang et al., 2023).

- **Bidirectional LSTM**

Bidirectional LSTM (Bi-LSTM) model is an advanced version of the unidirectional standard LSTM model. While the standard LSTM processes information in a single direction, focusing only on past data, the Bi-LSTM model provides a more comprehensive analysis by processing data in both forward and backward directions (Mohammadi et al., 2022). During model training, each time step is passed through two separate networks that process the data in both past and future contexts. The forward network operates similarly to a standard LSTM model, where the time series data is processed from t=1 to t=T, i.e., from past to future. Conversely, the backward network processes the data in the reverse order, from t=T to t=1. As a result, unlike the standard LSTM model, the Bi-LSTM model generates two different outputs by altering the context information (Alhussan et al., 2023).

- **PyraMiD-LSTM**

PyraMiD-LSTM is a model developed to enable traditional LSTM networks to more effectively capture patterns in real-world data. It processes data hierarchically and focuses on subjective representations of each data. In this way, it can read more complex data and establish the correlation in a hierarchical way. In PyraMiD-LSTM, each layer consists of different representations of the data. Thanks to these representations, the data is separated and achieves hierarchical harmony. As you move from the base of the pyramid to the top, the ability of the layers to simultaneously capture patterns in the data increases and continues to be transferred to the next layer. The hierarchical representation created as a whole enables learning long-term dependencies better and capturing complex patterns.

5.2.3 Performance Metrics

The correlation coefficient (R^2) explains the direction and strength of the relationship between variables. This value ranges from 0 to 1, with values closer to 1 indicating an increase in the model's success. It is calculated using the formula shown in Equation (4.10). The Mean Squared Error (MSE) and Root Mean Squared Error (RMSE) are commonly used to assess the accuracy of a proposed system. Both metrics measure the amount of error, but RMSE places greater emphasis on larger error values compared to MSE, making significant errors more noticeable. The closer the MSE and RMSE values are to zero, the closer the model's predictions are to the actual values, and the better the performance. The mathematical equations of the performance metrics to be used in this study, where P_p is the predicted power output and P_m is the measured power output, are as follows:

$$R^2 = 1 - \frac{\sum_{i=1}^{n}\left(P_m - P_p\right)^2}{\sum_{i=1}^{n}\left(P_m - \bar{P}_p\right)^2} \tag{5.10}$$

$$MSE = \frac{1}{N}\sum_{i=1}^{N}\left(P_m - P_p\right)^2 \tag{5.11}$$

$$RMSE = \sqrt{\frac{1}{N}\sum_{i=1}^{N}\left(P_m - P_p\right)^2} \tag{5.12}$$

5.2.4 Hypothesis Testing

Considering the crucial importance of predictive accuracy, assessing the forecasting accuracy of forecasting models holds a key place in WP estimation. Nevertheless, it is not sufficient to only utilize the conventional performance metrics for comparison of the forecasting models (Wu et al., 2020a). The Diebold-Mariano (DM) test, introduced by Diebold and Marino (Diebold & Mariano, 2002), is also used in this study to evaluate the predicting accuracy of the proposed hybrid system in comparison to other models. The DM score is evaluated as in Equation (4.13) as follows (Diebold & Mariano, 2002):

$$DM = \frac{\frac{\sum d_i}{n}}{\sqrt{s^2/n}} s^2 \tag{5.13}$$

where s^2 the estimator of the variance and d_i is the difference between the forecasting error of the tested model ($L(Error^1)$) and the benchmark model ($L(Error^2)$).

Then, defining the hypothesis test as:

$$H_0: E[L(Error^1)] = E[L(Error^2)] \tag{5.14}$$

$$H_1: E[L(Error^1)] \neq E[L(Error^2)] \tag{5.15}$$

where H_0 indicates the null hypothesis, that the error of the models are the same, and H_1 represents the alternative hypothesis, that the performance of models are different.

In order to verify the acceptability of the hypothesis ascertain the outcome, the DM score is compared with $Z_{\alpha/2}$, where Z_α is the standard normal random variable with significance α. If the DM score falls within the interval [-$Z_{\alpha/2}$, $Z_{\alpha/2}$], the null hypothesis is rejected and the models are said to show no significance. When the DM score falls out of the range [-$Z_{\alpha/2}$, $Z_{\alpha/2}$], the null hypothesis is rejected and it is concluded that the models are significantly different with the confidance α. In this study, we compared the models with respect to $\alpha = 0.01$ and $\alpha = 0.05$, with the corresponding $Z_{\alpha/2}$ values of 1.96 and 2.58, respectively.

5.2.5 Model Validation

This study includes strategies such as the sliding window and expanding window approaches to evaluate the performance of the models. The sliding window method divides time series data into training and validation sets by using a fixed-size window that moves sequentially across the dataset. In each iteration, the model is trained on the data within the window and validated on the subsequent time steps. This process allows for the assessment of the model's generalization ability as it encounters new data points over time. The sliding window approach is particularly suitable for applications with evolving temporal dynamics, as it captures changes in patterns and ensures the model remains adaptable to the most recent information. In contrast, the expanding window method gradually increases the training set over time. It starts with an initial subset of data and progressively includes additional observations for training while maintaining a fixed validation set. This method is

beneficial when it is desired to evaluate how the model performs as more historical data becomes available. The expanding window approach provides a dynamic evaluation that reflects the model's performance as it adapts to a growing dataset. Thus, the expanding window validation was utilized determine the best performing models for the estimation of the WP output for individual WFs at the 1st part of this study (see Figure 4.1). A validation method similar to hold-out validation was carried out for the 2nd and 3rd parts of this study but note that the "held-out" data for the validation belonged to different WFs than the model is trained on (see again Figure 4.1).

5.3 Results and Discussion

5.3.1 Data Preparation & Feature Selection

Adequate preparation of data and feature selection is essential before any mathematical modeling application. In this study, we have investigated the Pearson correlation and mutual information of the features (see **Figure 5.5**) to determine the necessary features to be utilized in estimating WP output of the WFs. As can be seen from **Figure 5.5**, the QV2M is highly correlated with T2MDEW, and it has the least mutual information in determining the WP in accordance with the RFR. Thus, we eliminate the QV2M from the set of features and determine the power outputs of WFs from the remaining 10 features.

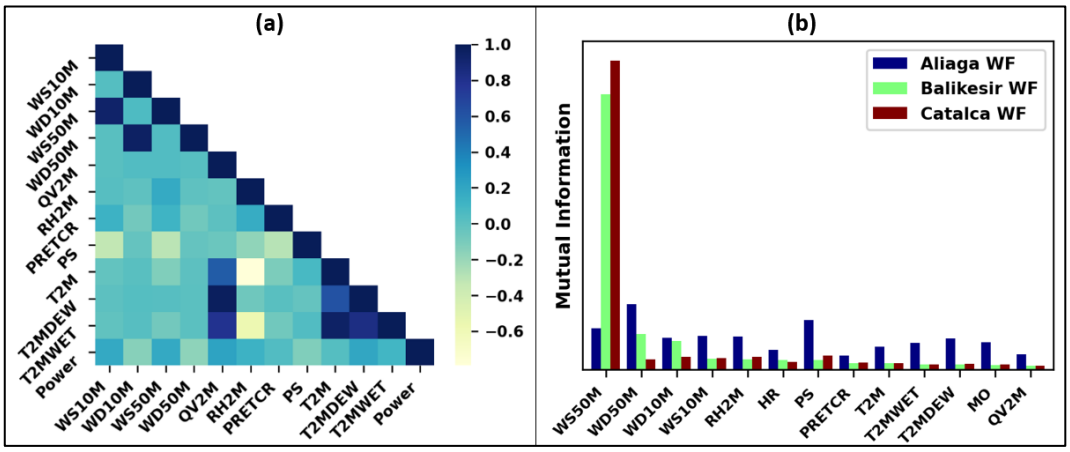

Figure 5.5 Pearson correlation (a) and mutual information (b) of features.

Before continuing on with the modeling study, however, we have noticed that the lookback period (amount of hours before the prediction of which the model will consider before performing the estimation) for estimation of power output of the

WFs is not clear in the literature. Thus, we utilized a simple RFR to determine the optimum number of hours for the lookback period in our modeling and recorded the MSE values as in Figure 5.6. Here, it can be observed that there are several candidates for the selection of lookback period. By investigating this plot, the optimum lookback period was determined as 8 hours, since that is where the MSE_{AVG} value has obtained the lowest value.

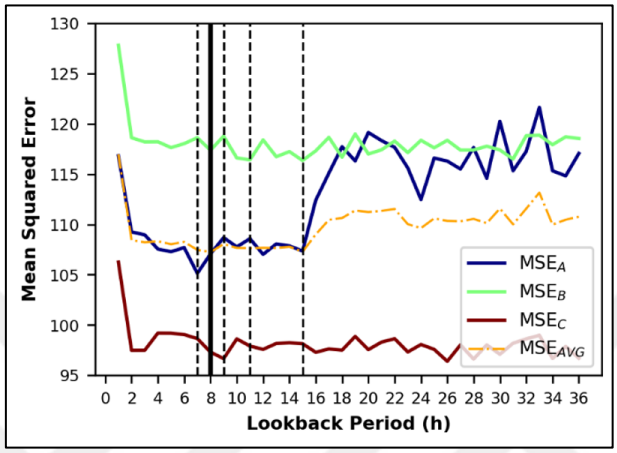

Figure 5.6 Hold-out (90%/10%) validation results by using an RFR for different lookback periods. Dashed black lines indicate the candidate lookback periods while straight black line show the optimum lookback period.

Investigating the power output of different facilities at different seasons (see Figure 5.7) is also important to gain insight regarding the generalizability of the obtained ANN models, that is, predicting the power output of different WFs from the model obtained from a particular WF data. While some studies proposed different models for different seasons (Niu et al., 2024; Wu et al., 2020b), Figure 5.7 shows that there is no significant difference between the WP output data trends of the WFs selected for this study. Thus, in-line with the generalizability mindset, the models obtained in this study are aimed to be utilized any time of the year, regardless of the season. One of the concerns regarding the generalizability of such models we have encountered was the assumption that the importance of features for each WF is significantly different from each other, and predicting the power output would not be as easy as predicting the power output of solar power facilities. However, as Figure 5.5b shows, the important features are observed to be similar in each WFs. Moreover, Figure 5.7 shows that the power output of these WFs show a similar trend, even though they are at least 100s of kilometers apart with mountains and

even small seas in between. This observation has led us to the possibility of a generalizable model that can be utilized to predict the power output of any WF, at least, around the area of the west of Türkiye, which we will be discussing in detail in the following sections.

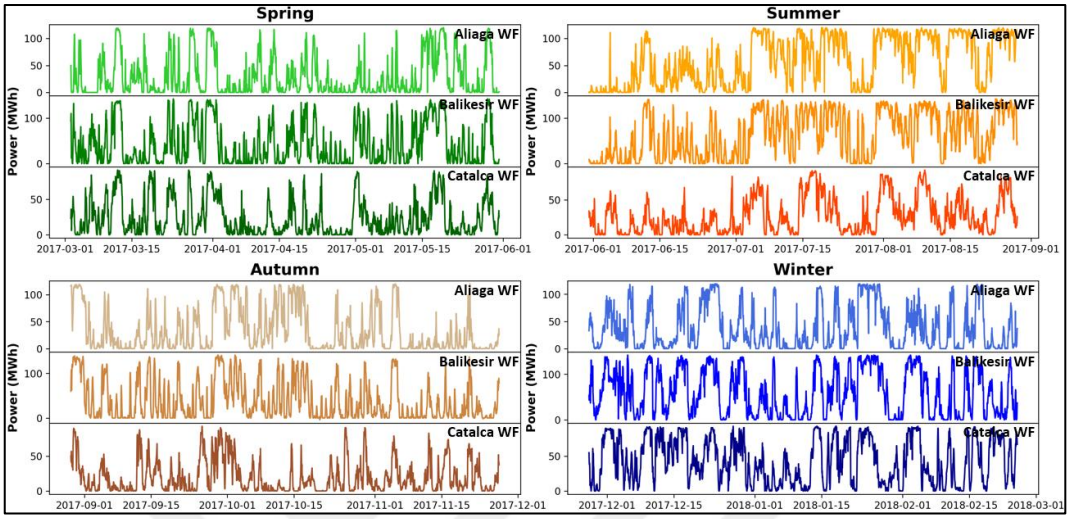

Figure 5.7 Hourly power output of Aliaga, Balikesir, and Catalca WFs at different seasons.

5.3.2 Performance Analysis of ANNs in WP Estimation

In this section, the aim is to determine the best ANN structure for estimation of hourly WP output of the WFs among the most commonly utilized ANNs, namely, NARX, Elman, SL-LSTM, ML-LSTM, Bi-LSTM, and PyraMiD-LSTM. Here, the expanding window validation is utilized for evaluating the performance metrics by using each WF data to determine the most suitable model (see Table 5.1). Furthermore, the performance at each expanding window iteration is also illustrated in Figure 5.8 along with the average and maximum training time information for each WFs. It is observed from Table 5.1 and Figure 5.8 that while NARX and Elman are computationally efficient, they yield higher MSE values when compared to the remaining models. PyraMiD-LSTM, being the most complex ANN structure among these, obtained high training times for each WF consistently, while not performing well at some training/test splits during the validation. The SL-LSTM, ML-LSTM, and Bi-LSTM models has shown consistent similarity in terms of performance, among them ML-LSTM being the most computationally expensive. The choice between SL-LSTM and Bi-LSTM was less clear, due to their similar results in terms of both performance and computation time, but since the Bi-LSTM

obtained slightly better metrics consistently, we conclude from these tables that Bi-LSTM is the best model for predicting WF power output for these facilities.

Table 5.1 Expanding window validation results of models for each WF.

Model	WF	R^2 Train	R^2 Test	MSE Train	MSE Test
NARX	(A)	0.9190	0.9253	142.438	137.450
	(B)	0.9351	0.9340	155.892	163.820
	(C)	0.9343	0.9305	53.700	55.570
Elman	(A)	0.9091	0.9348	140.679	124.339
	(B)	0.9326	0.9399	148.532	145.640
	(C)	0.9362	0.9312	51.754	56.771
SL-LSTM	(A)	0.9289	0.9378	124.880	114.146
	(B)	0.9370	0.9370	151.834	156.702
	(C)	0.9363	0.9337	52.054	53.017
ML-LSTM	(A)	0.9284	0.9358	125.690	117.780
	(B)	0.9378	0.9385	149.943	152.802
	(C)	0.9357	0.9327	52.537	53.824
Bi-LSTM	(A)	0.9280	0.9365	126.326	116.541
	(B)	0.9368	0.9366	152.438	157.585
	(C)	0.9361	0.9331	52.218	53.321
PyraMiD-LSTM	(A)	0.9256	0.9324	130.292	124.242
	(B)	0.9354	0.9354	155.525	160.241
	(C)	0.9322	0.9291	55.383	56.658

The actual and prediction plots of the test set from the last iteration of expanding window validation for Bi-LSTM is presented in Figure 5.9 to clearly illustrate the successful prediction of the model. Note that there are some limited over/under shootings present in the model predictions. While an adjusted Relu activation function may be utilized to eliminate these noise, limiting the output of the models to be within the WF capacity range, we have observed some non-convergence behaviors at some training/test sets when this was implemented. This instability stems from the non-derivability of the Relu (or similar) activation functions (Hu et al., 2018; Sankaranarayanan & Rengaswamy, 2022). Thus, instead of trying to limit the output, the default linear activation function was utilized at the output node for all models, which converge consistently and do not hinder the assessment of the models and their comparison in the scope of this study. In real life applications,

these over/under shootings can be neglected since the performance of the models are unaffected or may be corrected easily with simple rule based controls.

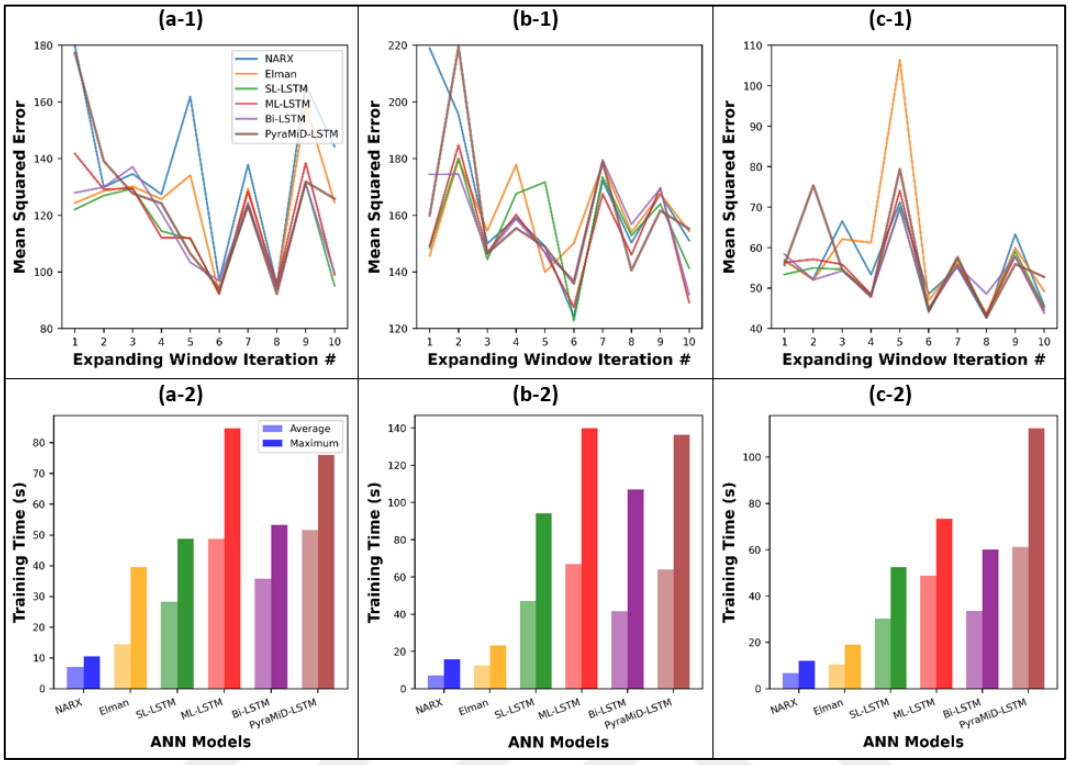

Figure 5.8 The MSE performance metric and training time of each model is illustrated for each expanding window iteration number for Aliaga WF (a-1, a-2), Balikesir WF (b-1, b-2), and Catalca WF (c-1, c-2), respectively.

While from performance metrics in Table 5.1 and Figure 5.8 it can be deduced that Bi-LSTM is the superior model, this claim still needs to be proven statistically. In Table 5.2 the DM test results are computed to show that Bi-LSTM is indeed statistically different from the remaining models in prediction of the WP output of WFs. The Bi-LSTM model was selected as the benchmark model and the DM scores were computed. The values show that while some models behave similarly from season to season with the LSTM model, these resemblance is not consistent. Overall, the SL-LSTM and ML-LSTM behaves most similarly with the Bi-LSTM, as was also deduced from former analysis, but in the end, all models are different from the Bi-LSTM when different WFs are also considered. Due to the abundance of the critical values of both 1% and 5% significance levels, the alternative hypothesis can be accepted, that the Bi-LSTM model is different from the remaining models.

Table 5.2 DM test of different models in four seasons for each well-established WF.

Models	Spring			Summer			Autmn			Winter			Overall		
	A	B	C	A	B	C	A	B	C	A	B	C	A	B	C
NARX	10.9[1]	0.5[3]	-3.0[1]	20.2[1]	-0.3[3]	2.2[2]	11.7[1]	-0.8[3]	-4.6[1]	4.4[1]	-0.6[3]	-9.3[1]	47.6[1]	53.7[1]	-18.7[1]
Elman	-2.4[2]	22.9[1]	-2.4[2]	-3.8[1]	24.2[1]	-4.3[1]	-2.5[2]	24.5[1]	-5.2[1]	-2.7[1]	26.4[1]	-9.4[1]	-7.8[1]	69.2[1]	-25.0[1]
SL-LSTM	0.2[3]	61.7[1]	-0.5[3]	-1.2[3]	65.7[1]	0.7[3]	-0.5[3]	62.5[1]	-2.2[2]	-1.1[3]	50.0[1]	-5.5[1]	3.7[1]	-59.2[1]	-9.4[1]
ML-LSTM	1.0[3]	65.5[1]	2.7[1]	1.7[3]	65.2[1]	2.2[2]	0.9[3]	63.1[1]	0.3[3]	-0.2[3]	52.9[1]	-0.9[3]	7.7[1]	-34.1[1]	3.2[1]
Bi-LSTM	-	-	-	-	-	-	-	-	-	-	-	-	-	-	-
PyraMiD-LSTM	3.6[1]	5.5[1]	7.4[1]	3.3[1]	6.5[1]	4.4[1]	4.8[1]	8.0[1]	8.1[1]	5.4[1]	13.8[1]	7.0[1]	10.6[1]	88.7[1]	25.5[1]

[1:] Indicates %1 significance level, [2:] Indicates %5 significance level, [3:] Indicates no significance

Ultimately, the developed Bi-LSTM stands out notably from the remaining models. Incorporating the performance metrics from former analysis, it is shown that the proposed Bi-LSTM ANN model demonstrates superior performance, surpassing the other models in WP estimation. Table 5.2 also shows that there is no consistent change with respect to seasons in terms of model comparison when different WFs are also considered. Thus, in-line with the analysis of Figure 5.7 in the former section, seasonal effects will be neglected whilist the obtainment of the generalizable models.

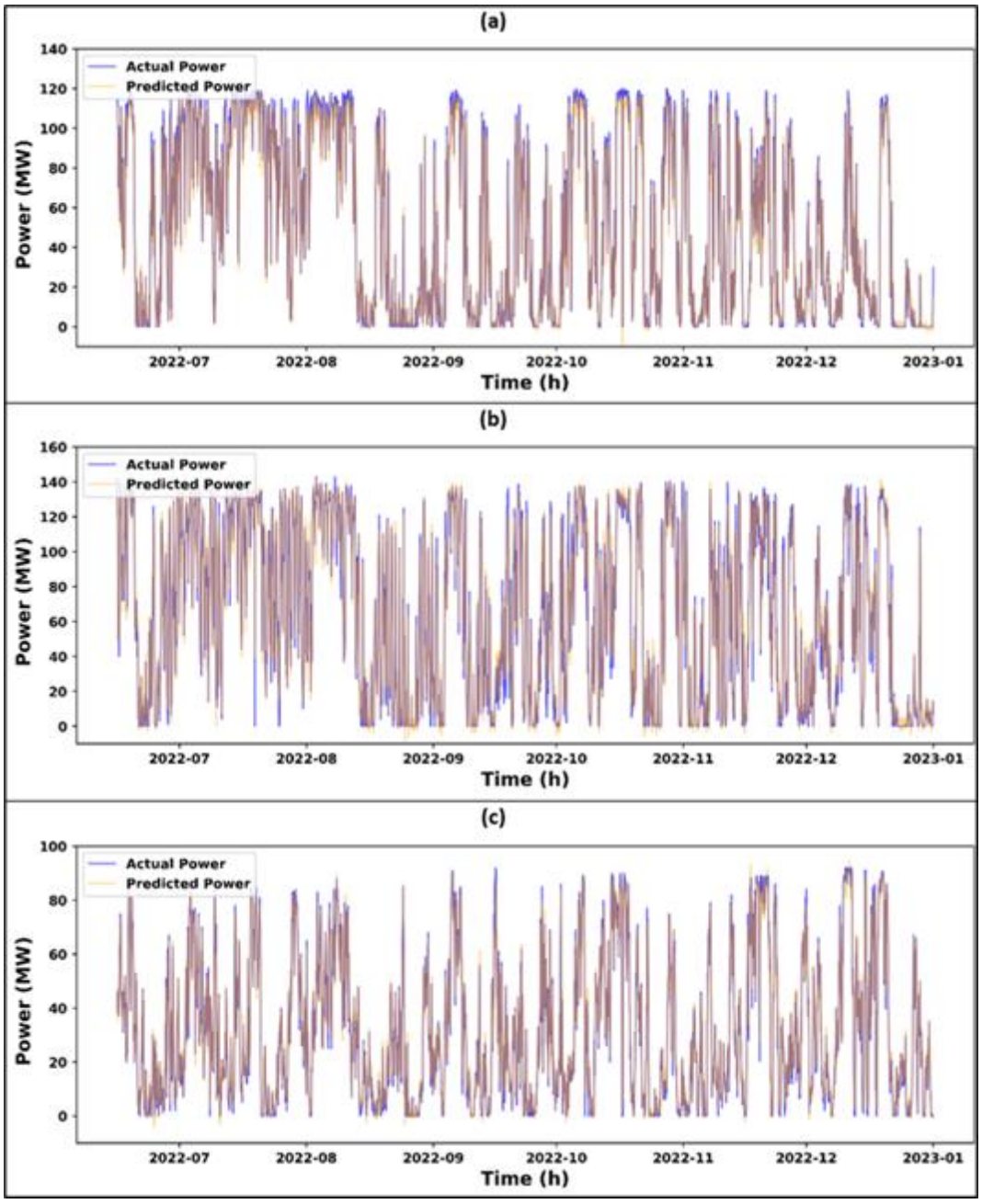

Figure 5.9 Actual and predicted power output of Aliaga (a), Balikesir (b), and Catalca (c) WFs considering the test set of the last iteration of the expending window validation (90% train, 10% test) for the respective Bi-LSTM models.

5.3.3 Obtainment and Validation of the Generalizable Model

In this section, we will focus on how a model constructed at one WF can be utilized in a different WFs and how significant is the performance loss for such applications. As discussed before, the data is normalized to 0-1 scale for all features and output before the ANN modelling. Thus, when we obtain the "predicted power" by de-normalizing the actual output of the ANN model. In terms of the power output of a WF, this de-normalizing is carried out with respect to capacity of the WF, mapping the 0 to 1 output of the ANN model to 0 to capacity of the WF. Thus, whilst estimating the power output of a different WF, one can simply de-normalize with respect to the predicted WF's capacity to estimate the power output of that facility. That is the methodology carried out in this study to estimate the power output of the other WFs. Figure 5.10 showcases the performances of Bi-LSTM models trained on entire data of Aliaga (Figure 5.10a), Balikesir (Figure 5.10b), and Catalca (Figure 5.10c) WFs and tested on the entire data of the remaining WFs. As expected, the models best perform at the WFs that they were constructed from. However, it is clear that the decrease in the performance when estimating the power output of other WFs are acceptable with similar R^2 and RMSE values obtained even though the test sets consist of 52573 data each. Thus, it is concluded that the Bi-LSTM models can successfully be utilized in estimation of any WF in the region of West-Türkiye. This is significant since the proposed model can be utilized not only by the management of the WFs, but also by third parties like government agencies or competitors, which would enable enhanced optimization for balancing the supply and demand for the grid. Furthermore, as will be demonstrated in the next section, the models can successfully be utilized for newly established WFs that don't have adequate number of data for obtainment of sufficient ANN models

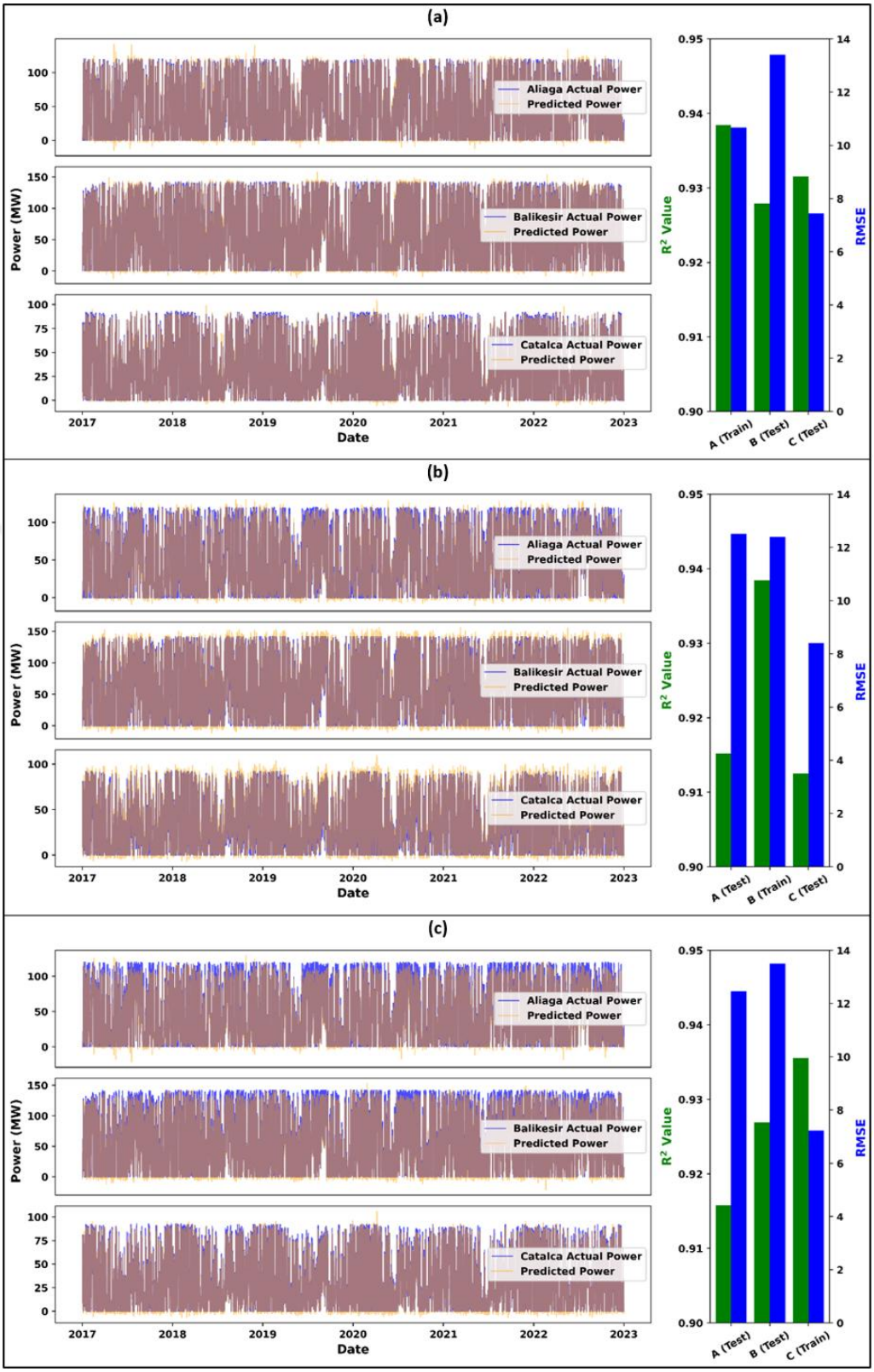

Figure 5.10 Actual and predicted power output of WFs and their performance metrics. The Bi-LSTM models are obtained by utilizing the entire data of Aliaga (a), Balikesir (b), and Catalca (c) WFs as training sets, and testing them on the remaining WFs respectively.

5.3.4 Estimation of Power Output of a Newly-Established WF

While the ability to predict the power output of a WF by utilizing the generalizable model addresses several limitations that the WP production inherits, such as eliminating its unpredictive nature and providing means to optimize the grid, better models can be obtained by training them on the WFs' own data. What is more interesting, however, is being able to estimate newly-established WFs with limited data and unstable nature. To exemplify such an application, we have selected a WF in the region, the Bursa WF, and predicted its power output by utilizing the Bi-LSTM model trained on the Aliaga WF data. Thus, the data from the Aliaga WF can be considered as the train set whereas the data of the Bursa WF can be considered as the test set. The results of the model in estimating the power output of the Bursa WF is illustrated in Figure 5.11. The model performed extremely well for predicting the power output of the Bursa WF, with R^2=0.9633, MSE=33.917, and RMSE=5.823. In Figure 5.11, at the beginning of May, before the WF began power production, there is some deviations from zero. These can be considered as expectations of trend, however, since the WF does not produce any power, it checks the last 8 hours (the lookback period) being zero and corrects itself. In fact, the real operational estimations are conducted after 7th of May, since this is the date the first power output data is reported. And, as can be clearly observed from Figure 5.11 and the performance metrics, the generalizable model can satisfactorily be utilized in estimation of a newly-established WF, proving its usefulness for any WF around the region of West-Türkiye.

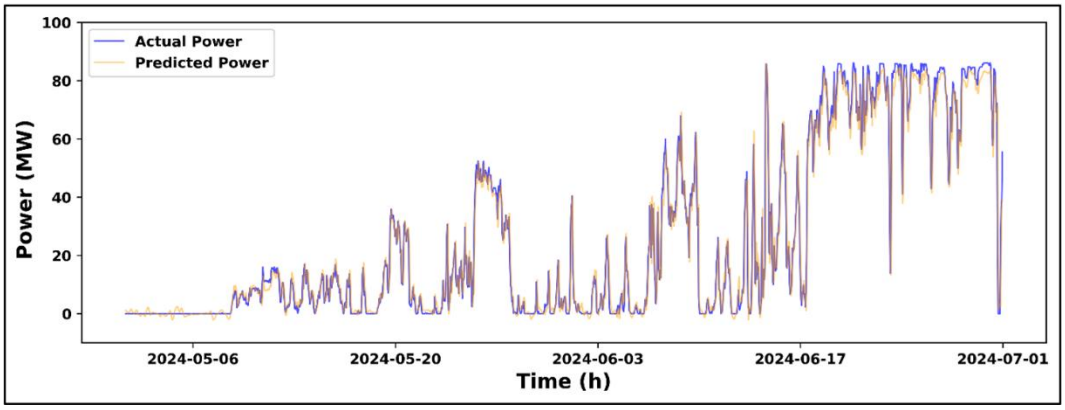

Figure 5.11 Actual and predicted power of the newly-established Bursa WF.

5.3.5 Overall Comparison of the Obtained Models

There are numerous studies conducted for very short (less than an hour) and short (hourly) term WP forecasting studies that can be found in the literature. Table 5.3 provides a summary of the results of the most recent principal studies. Here, it can be observed that the power prediction has started with simple models like SVR, NARX, and Elman moved on to more advanced models consisting of LSTM derivatives. Indeed, in the first part of this study, we have shown that LSTM derivatives, especially SL-LSTM and Bi-LSTM, are superior to the remaining models in terms of model performance and necessary training duration. By utilizing an expanding window validation, Bi-LSTM is shown to be the best model when predicting the power output of the same WFs, where the model is trained and tested on the same WF data, in line with the literature.

While the first part of this study presents novelty in decidedly suggesting the best modeling approach for these applications, the main novelty of this study lies on its second and third parts, where generalizable Bi-LSTM models obtained by the data of one WF which is then utilized in estimating the power output of other WFs. On the second part of the study, it is shown that the proposed model can successfully be utilized in estimating power production of other well-established WFs, whose entire data was utilized as the test sets. These results indicate that these models can satisfactorily be utilized by both managers of these WFs and by third parties including government agencies, which poses crucial grid optimization potential. In the third part of this study, the generalizable Bi-LSTM model is utilized to estimate the power output of a newly-established WF with limited data. This showcased the ability of the generalizable model performing satisfactorily even if the actual data of the WF is limited or unavailable. The results of the second and third parts of this study are of greatest importance for enhancing the optimization of the grid by addressing the inherent uncertainty of the WP output, one of the most challenging problems in WP applications. Table 5.3 also shows the performance of the best obtained models for each part of this study. Here, it can be observed that the most trending and up-to-date models and validation methods are utilized in this study to estimate the power output of the WFs. The performance metrics are well in range when compared to the literature, and the application of the models obtained one

WF, and tested on other WFs are reported for the first time in the literature for WP estimation.

Table 5.3 Comparison of the performance of the obtained models with the literature.

Aim	Utilized Models	Data Type / Size	Prediction Interval	Validation Method	Model Performances	Ref.
WPF	SVR	3min / 5 days	VST	Cross Validation	RMSE=1.0887 MAE=0.6336 RMAE=0.064	(H. Zhang et al., 2014)
WSF	NARX, ARIMA	10 min, Hourly /16 months	VST & ST	Holdout Validation	MAE=0.43 MSE=0.34	(Cadenas et al., 2016)
WPF	PAR, ANN-ANFIS	Hourly /1-2 years	ST	Holdout Validation	NRMSE=0.05 0 NMAPE=3.96	(Karakuş et al., 2017)
WPSDF	MLFFN, SVR-RBF, ANFIS-PSO	5-60 min /1 years	VST & ST	Holdout Validation	RMSE=0.3651 MSE=0.1333	(Khosravi et al., 2018)
WPF	LSTM-EFG	10min /3 years	VST	Holdout Validation	MSE=5.5311	(R. Yu et al., 2019)
WPF	LSTM-GMM	15min /3 months	VST	Holdout Validation	RMSE=6.37	(J. Zhang et al., 2019)
WPF	LSTM, SVR&GPR	10min, Hourly /1 year	VST / ST	Holdout Validation	R^2=0.89	(Gu et al., 2021)
ELP	NARX, ARMA, ELMAN	Hourly/1 years	ST	Holdout Validation	MAPE=3.42%	(Alhmoud & Nawafleh, 2021a)
WPF	MTGP	Hourly /100 days	ST	Holdout Validation	RMSE=0.1255 MAE=0.0936	(Liao et al., 2023)
WPF	LSTM-WPRE	15min /2 years	VST	Holdout Validation	MAPE=0.094 rRMSE=0.112	(Cui et al., 2023)
WSF	NARNN, NARXNN	Hourly /1 year	ST	Holdout Validation	MSE=0.2253 R^2=0.904	(Gidom et al., 2024)
WPF	Elman	Hourly /1 year	ST	Holdout Validation	MSE=4.7141 rRMSE=0.069 MAPE=11.777	(S. Liu et al., 2024)
SIF	HFF based SA-CNN-LSTM	Hourly /3,4,5 years	ST	Sliding Window Validation	RMSE=42.132 MAE=20.412 R^2=0.979	(Xiao et al., 2024)

Table 5.4 Comparison of the performance of the obtained models with the literature. (continues)

WPF	NARX, Elman, SL-LSTM, ML-LSTM, Bi-LSTM, PyraMiD-LSTM	3 WFs / Hourly / 6 Years	ST	Expanding Window Validation for Each WF	R^2=0.9366 MSE=53.321 RMSE=10.198	**This Study 1st Part**
WPF of Different Well-Established WFs	Bi-LSTM	3 WFs / Hourly / 6 Years	ST	Train: 1 WF Test: Remaining 2 WFs	R^2=0.9294 MSE=57.177 RMSE=7.562	**This Study 2nd Part**
WPF of a Newly-Established WF	Bi-LSTM	2 WF / Hourly / 6 Years, 2 Months	ST	Train: 1 WF Test: Newly-Established WF	R^2=0.9633 MSE=33.917 RMSE=5.823	**This Study 3rd Part**

5.4 Limitations

While this study fills crucial knowledge gaps present in the literature, it has some limitations that should be highlighted. First of all, while obvious, the generalizable models obtained here are limited to the region that the model is tested. Thus, while the generalizable model proposed in this study is shown to be able to forecast the WP output of WFs located in the region of west-Türkiye, it should be used with care elsewhere. Since there are generally well established WFs in most of the regions, similar methodology can be utilized to obtain a generalizable model in these regions for the best practice. Moreover, this study has focused on the estimation of the WP only on an hourly basis, which is generally utilized in most grid optimization applications, but interval predictions should still be investigated in detail. Finally, it should also be noted that the hyperparameters of the models presented here can further be optimized to obtain slightly improved predictions for the WFs, but our experience whilst analyzing the models is that the effect of the hyperparameters is minimal in estimating the WP output of different WFs, which was the main focus of this study.

5.5 Conclusion

As the energy transition towards green energy continues, it is obvious that the accurate estimation of WP output of WFs around the world will gain more and more significance to balance the supply and demand and optimize the grid. While there have been numerous studies conducted to estimate the WP of well-established individual WFs, limited studies carried out for the obtainment of a generalizable model that can be utilized in estimation of WP of any WF. Furthermore, as far as we know, there were no study conducted with the aim of estimating the WP of newly-established WFs with limited data. To this end, we firstly showed that among several prevalent ANN models, Bi-LSTM is superior for WP estimation of WFs with good performance and low computational load. Then, we provided examples to demonstrate that the Bi-LSTM trained on a WF can be utilized in estimating the WP of other WFs. Moreover, we tested the generalizable model with a newly-established WF, showcasing that it is indeed possible to estimate the WP of any WF around the same region by using the generalizable model. The utilization of the model in different regions, while possible, is not tested in the scope of this study. Even so, the methodology presented here can be utilized anywhere in the world, enabling anyone to accurately estimate the WP output of any WF, including the engineers and managers of the WFs, consumers, government agencies, grid managers etc. Thus, the methodology showcased here has the potential to be applied anywhere in the world for maintenance planning in WFs, optimization of power dispatch, reduction of operational costs, and assurance of safe and stable operation of the power system.

6
CONCLUSION

6.1 Summary and Implications

This thesis provides an essential guide for applications of energy production by challenging and solving three major problems of the available literature. As a regression problem, a higher heating value estimation study was conducted in the 3rd chapter of the thesis. Here, the best ANN models are obtained by hyperparameter optimization, which yielded high correlation coefficient and low error values when compared to the literature, proving their ability in accurate HHV estimation. This study's findings assist researchers and managers in optimizing fuel processing and waste management by facilitating the calculation of the most accurate HHV for fuels of any kind. In the 4th chapter, as both classification and clustering study, we have proposed the HOM classification system. Here, the proposed HOM classification system is indeed unique since it is based on properties of the fuels, rather than their origin or source. It also enables the accurate classification of wastes, which are in many cases ambigiously classified as “other” or “waste”. Thus, this study will enable researchers and policy-makers to utilize the wastes or fuels in the most optimum manner. Finaly, in the 5th chapter, forecasting of wind power output of the wind farms is studied as a time-series problem. Here, most notably, a generalizable ANN model is proposed that can be utilized in different wind farms. the methodology presented here can be utilized anywhere in the world, enabling anyone to accurately estimate the WP output of any WF, including the engineers and managers of the WFs, consumers, government agencies, grid managers etc. Consequently, the technique presented herein may be implemented globally for maintenance planning in wind farms, optimization of power dispatch, reduction of operating expenses, and ensuring the safe and stable functioning of the power system. Overall, this thesis challenges the most prevalent problems in applications of artificial intelligence in energy production and provides unique insights regarding both the theoretical foundations and practical implementations of AI-driven solutions in the energy sector.

6.2 Curent Challenges and Future Directions

When the literature is observed, there are numerous AI studies in the topic of energy production, conducted with the aim of improving the models previously proposed, especially in the last five years. Thus, with this kind of collective focus on the topic, it is difficult to highlight current challenges that will be long-lasting and thus be meaningful. The most obvious one may be considered availability of reliable, accurate, and ethically collected data – as in common with most AI applications – but the energy sector has become more and more transparent in recent years, providing many opportunities for applications. After the successful collection of the data, the literature showcases that the data is generally directly utilized for applications with minimal feature analysis or data processing. While the AI models obtained in such a direct manner still performed well for most applications, the future improvements will likely be from improved data pre-processing techniuqes rather than utilization of more advanced or optimized AI models. Even so, there are still some gaps in some topics where the hyperparameters of AI models utilized are not optimized sufficiently. Furthermore, future studies should make sure that they are utilizing the most up-to-date validation methods, since some even recent studies still utilize only hold-out validation, which lacks the ability to demonstrate the AI models competence in estimating the output due to its lack of generalizability and openness to malpractices. While hold-out validation is a crucial tool in optimizing hyperparameters and proving that there is no overfitting/underfitting problem, it should be utilized with validation methods like cross-validation or sliding/expanding window validation that clearly showcases the model's ability in estimating the output is showcased by advanced. Finally, it should also be underlined that, especially in energy demand forecasting applications with the advancing internet of things technologies, the laws and regulations regarding data privacy and security should be up-to-date with these applications, preventing any unethical behavior.

6.3 Final Remarks

It is evident that AI applications will shape the future of energy production since there is already abundant data that has already been collected and utilized in the sector. With the widespread attention AI gets, collecting and storing any use-case specific data has also attained significance for possible AI applications. Thus, as the large datasets are collectively constructed, the AI models trained on these data will be more and more successful. As discussed previously, the problems in the energy sector that are generally tried to be addressed by utilizing AI models can be classified into four main groups: regression problems, classification problems, clustering problems, and time-series problems. By challenging three of these problems that encompass these problem classes, this thesis provides an in-depth methodological analysis and innovative solutions which can be applied to a wide range of applications. Together, these studies lay the foundation for advancing artificial intelligence applications in energy production, ultimately improving efficiency and sustainability. Thus, while the issues addressed in this thesis have contributed to the literature on fuel utilization enhancement and power plant performance prediction, the methodologies developed for these solutions will persist in aiding researchers, engineers, and policymakers in undertaking analogous studies with their own data and for their specific challenges.

REFERENCES

Acharya, B., & Marhold, K. (2019). Determinants of household energy use and fuel switching behavior in Nepal. *Energy*, *169*, 1132–1138. https://doi.org/10.1016/j.energy.2018.12.109

Adomako, A. B., Jamshidi, E. J., Yusup, Y., Elsebakhi, E., Jaafar, M. H., Ishak, M. I. S., Lim, H. S., & Ahmad, M. I. (2024). Deep learning approaches for bias correction in WRF model outputs for enhanced solar and wind energy estimation: A case study in East and West Malaysia. *Ecological Informatics*, *84*. https://doi.org/10.1016/j.ecoinf.2024.102898

Aguirre, D., & Fuentes, O. (2019). Improving Weight Initialization of ReLU and Output Layers. *Lecture Notes in Computer Science (Including Subseries Lecture Notes in Artificial Intelligence and Lecture Notes in Bioinformatics)*, *11728 LNCS*. https://doi.org/10.1007/978-3-030-30484-3_15

Ahmed, S. D., Al-Ismail, F. S. M., Shafiullah, M., Al-Sulaiman, F. A., & El-Amin, I. M. (2020). Grid Integration Challenges of Wind Energy: A Review. In *IEEE Access* (Vol. 8, pp. 10857–10878). Institute of Electrical and Electronics Engineers Inc. https://doi.org/10.1109/ACCESS.2020.2964896

Alam, M. M., Rahman, M. H., Ahmed, M. F., Chowdhury, M. Z., & Jang, Y. M. (2022). Deep learning based optimal energy management for photovoltaic and battery energy storage integrated home micro-grid system. *Scientific Reports*, *12*(1). https://doi.org/10.1038/s41598-022-19147-y

Alhmoud, L., & Nawafleh, Q. (2021a). Short-Term Load Forecasting for Jordan Power System Based on NARX-ELMAN Neural Network and ARMA Model. *IEEE Canadian Journal of Electrical and Computer Engineering*, *44*(3). https://doi.org/10.1109/icjece.2021.3076124

Alhmoud, L., & Nawafleh, Q. (2021b). Short-Term Load Forecasting for Jordan Power System Based on NARX-ELMAN Neural Network and ARMA Model Prévision de la charge à court terme du système électrique jordanien basée sur le réseau neuronal NARX-ELMAN et le modèle ARMA. *IEEE Canadian Journal of Electrical and Computer Engineering*, *44*(3). https://doi.org/10.1109/icjece.2021.3076124

Alhussan, A. A., M. El-Kenawy, E. S., Abdelhamid, A. A., Ibrahim, A., Eid, M. M., & Khafaga, D. S. (2023). Wind speed forecasting using optimized bidirectional LSTM based on dipper throated and genetic optimization algorithms. *Frontiers in Energy Research*, *11*. https://doi.org/10.3389/fenrg.2023.1172176

Ali, M., Prakash, K., Hossain, M. A., & Pota, H. R. (2021). Intelligent energy management: Evolving developments, current challenges, and research

directions for sustainable future. *Journal of Cleaner Production*, *314*. https://doi.org/10.1016/j.jclepro.2021.127904

Aljabbouli, H., Albizri, A., & Harfouche, A. (2020). Tree-Based Algorithm for Stable and Efficient Data Clustering. *Informatics*, *7*(4). https://doi.org/10.3390/informatics7040038

Almalaq, A., & Edwards, G. (2017). A review of deep learning methods applied on load forecasting. *Proceedings - 16th IEEE International Conference on Machine Learning and Applications, ICMLA 2017*, *2017-December*, 511–516. https://doi.org/10.1109/ICMLA.2017.0-110

Al-Sheikh, H., & Moubayed, N. (2012). Fault detection and diagnosis of renewable energy systems: An overview. *2012 International Conference on Renewable Energies for Developing Countries (REDEC)*, 1–7. https://doi.org/10.1109/REDEC.2012.6416687

Amer, A. A. (2020). On K-means clustering-based approach for DDBSs design. *Journal of Big Data*, *7*(1). https://doi.org/10.1186/s40537-020-00306-9

Amin, S. Bin, Chang, Y., Khan, F., & Taghizadeh-Hesary, F. (2022). Energy security and sustainable energy policy in Bangladesh: From the lens of 4As framework. *Energy Policy*, *161*. https://doi.org/10.1016/j.enpol.2021.112719

Antonio De Rose, Marina Buna, Carlo Strazza, Nicolo Olivieri, Tine Stevens, Leen Peeters, & Daniel Tawil-Jamault. (2017). *Technology Readiness Level: Guidance Principles for Renewable Energy Technologies*. https://doi.org/10.2777/863818

Arıcı, E., Ellez, F., İçten, K. C., Kaynak, İ. E., & Tosuner, Ö. (2021). *İzmir İli, Menemen İlçesi Yilmaz Rüzgar Enerji Santrali 3. Derece Arkeolojik Sit Alani 1/1000 Ölçekli Koruma Amaçli Uygulama İmar Plani Değişikliği Ve Yol İlavesi Plan Araştirma Ve Açiklama Raporu*.

Arthur, D., & Vassilvitskii, S. (2007). k-means++: The Advantages of Careful Seeding. *Proceedings of the Eighteenth Annual ACM-SIAM Symposium on Discrete Algorithms*.

Arun, M., Le, T. T., Barik, D., Sharma, P., Osman, S. M., Huynh, V. K., Kowalski, J., Dong, V. H., & Le, V. V. (2024). Deep learning-enabled integration of renewable energy sources through photovoltaics in buildings. *Case Studies in Thermal Engineering*, *61*. https://doi.org/10.1016/j.csite.2024.105115

Badji, A., Benseddik, A., Bensaha, H., Boukhelifa, A., Bouhoun, S., Nettari, C., Kherrafi, M. A., & Lalmi, D. (2023). Experimental assessment of a greenhouse with and without PCM thermal storage energy and prediction their thermal behavior using machine learning algorithms. *Journal of Energy Storage*, *71*. https://doi.org/10.1016/j.est.2023.108133

Balakumar, P., Vinopraba, T., & Chandrasekaran, K. (2023). Deep learning based real time Demand Side Management controller for smart building integrated with renewable energy and Energy Storage System. *Journal of Energy Storage*, *58*. https://doi.org/10.1016/j.est.2022.106412

Basu, P. (2018). Chapter 3 - Biomass Characteristics. In P. Basu (Ed.), *Biomass Gasification, Pyrolysis and Torrefaction (Third Edition)* (Third Edition, pp.

49–91). Academic Press. https://doi.org/https://doi.org/10.1016/B978-0-12-812992-0.00003-0

Better Biomass. (2019). *Impact assessment NTA 8003 conversion*.

Blagrave, P., & Furceri, D. (2021). The macroeconomic effects of electricity-sector privatization. *Energy Economics*, *100*. https://doi.org/10.1016/j.eneco.2021.105245

Bordass, B. (2020). Metrics for energy performance in operation: the fallacy of single indicators. *Buildings and Cities*, *1*(1), 260–276. https://doi.org/10.5334/bc.35

Boumanchar, I., Charafeddine, K., Chhiti, Y., M'hamdi Alaoui, F. E., Sahibed-dine, A., Bentiss, F., Jama, C., & Bensitel, M. (2019a). Biomass higher heating value prediction from ultimate analysis using multiple regression and genetic programming. *Biomass Conversion and Biorefinery*, *9*(3), 499–509. https://doi.org/10.1007/s13399-019-00386-5

Boumanchar, I., Charafeddine, K., Chhiti, Y., M'hamdi Alaoui, F. E., Sahibed-dine, A., Bentiss, F., Jama, C., & Bensitel, M. (2019b). Biomass higher heating value prediction from ultimate analysis using multiple regression and genetic programming. *Biomass Conversion and Biorefinery*, *9*(3), 499–509. https://doi.org/10.1007/s13399-019-00386-5

Boussaada, Z., Curea, O., Remaci, A., Camblong, H., & Bellaaj, N. M. (2018). A nonlinear autoregressive exogenous (NARX) neural network model for the prediction of the daily direct solar radiation. *Energies*, *11*(3). https://doi.org/10.3390/en11030620

Büyükkanber, K., Haykiri-Acma, H., & Yaman, S. (2023). Calorific value prediction of coal and its optimization by machine learning based on limited samples in a wide range. *Energy*, *277*. https://doi.org/10.1016/j.energy.2023.127666

Cadenas, E., Rivera, W., Campos-Amezcua, R., & Heard, C. (2016). Wind speed prediction using a univariate ARIMA model and a multivariate NARX model. *Energies*, *9*(2). https://doi.org/10.3390/en9020109

Cakman, G., Gheni, S., & Ceylan, S. (2021). Prediction of higher heating value of biochars using proximate analysis by artificial neural network. *Biomass Conversion and Biorefinery*. https://doi.org/10.1007/s13399-021-01358-4

Caliński, T., & Harabasz, J. (1974). A Dendrite Method Foe Cluster Analysis. *Communications in Statistics*, *3*(1), 1–27. https://doi.org/10.1080/03610927408827101

Chi, P., Liang, R., Hao, C., Li, G., & Xin, M. (2025). Cable fault diagnosis with generalization capability using incremental learning and deep convolutional neural network. *Electric Power Systems Research*, *241*. https://doi.org/10.1016/j.epsr.2024.111304

Cordeiro-Costas, M., Villanueva, D., Eguía-Oller, P., & Granada-Álvarez, E. (2023). Intelligent energy storage management trade-off system applied to Deep Learning predictions. *Journal of Energy Storage*, *61*. https://doi.org/10.1016/j.est.2023.106784

Cordeiro-Costas, M., Villanueva, D., Eguía-Oller, P., Martínez-Comesaña, M., & Ramos, S. (2023). Load Forecasting with Machine Learning and Deep Learning Methods. *Applied Sciences (Switzerland)*, *13*(13). https://doi.org/10.3390/app13137933

Cordero, T., Marquez, F., Rodriguez-Mirasol, J., & Rodriguez, J. (2001). Predicting heating values of lignocellulosics and carbonaceous materials from proximate analysis. *Fuel*, *80*(11), 1567–1571. https://doi.org/10.1016/S0016-2361(01)00034-5

Cui, Y., Chen, Z., He, Y., Xiong, X., & Li, F. (2023). An algorithm for forecasting day-ahead wind power via novel long short-term memory and wind power ramp events. *Energy*, *263*. https://doi.org/10.1016/j.energy.2022.125888

Dashti, A., Noushabadi, A. S., Raji, M., Razmi, A., Ceylan, S., & Mohammadi, A. H. (2019). Estimation of biomass higher heating value (HHV) based on the proximate analysis: Smart modeling and correlation. *Fuel*, *257*(August), 115931. https://doi.org/10.1016/j.fuel.2019.115931

Deka, P., & Saha, U. (2023). Introduction of k-means clustering into random cascade model for disaggregation of rainfall from daily to 1-hour resolution with improved preservation of extreme rainfall. *Journal of Hydrology*, *620*, 129478. https://doi.org/https://doi.org/10.1016/j.jhydrol.2023.129478

Diebold, F. X., & Mariano, R. S. (2002). Comparing Predictive Accuracy. *Journal of Business & Economic Statistics*, *20*(1), 134–144. https://doi.org/10.1198/073500102753410444

Dinesh, L. P., Khafaf, N. Al, & McGrath, B. (2025). A short term multistep forecasting model for photovoltaic generation using deep learning model. *Sustainable Operations and Computers*, *6*, 34–46. https://doi.org/10.1016/j.susoc.2024.11.003

Dodo, U. A., Ashigwuike, E. C., & Abba, S. I. (2022). Machine learning models for biomass energy content prediction: A correlation-based optimal feature selection approach. *Bioresource Technology Reports*, *19*, 101167. https://doi.org/10.1016/j.biteb.2022.101167

Dubey, R., & Guruviah, V. (2023). Predictive Modeling of Higher Heating Value of Biomass Using Ensemble Machine Learning Approach. *Arabian Journal for Science and Engineering*, *48*(7), 9329–9338. https://doi.org/10.1007/s13369-022-07346-8

Duca, D., Mancini, M., Rossini, G., Mengarelli, C., Foppa Pedretti, E., Toscano, G., & Pizzi, A. (2016). Soft Independent Modelling of Class Analogy applied to infrared spectroscopy for rapid discrimination between hardwood and softwood. *Energy*, *117*, 251–258. https://doi.org/10.1016/j.energy.2016.10.092

Duhirwe, P. N., Hwang, J. K., Ngarambe, J., Kim, S., Kim, K., Song, K., & Yun, G. Y. (2021). A novel deep learning-based integrated photovoltaic, energy storage system and electric heat pump system: Optimising energy usage and costs. *International Journal of Energy Research*, *45*(6), 9306–9325. https://doi.org/10.1002/er.6462

Elgowainy, A., Han, J., Cai, H., Wang, M., Forman, G. S., & DiVita, V. B. (2014). Energy Efficiency and Greenhouse Gas Emission Intensity of Petroleum Products at U.S. Refineries. *Environmental Science & Technology*, *48*(13), 7612–7624. https://doi.org/10.1021/es5010347

Elmaz, F., Büyükçakır, B., Yücel, Ö., & Mutlu, A. Y. (2020). Classification of solid fuels with machine learning. *Fuel*, *266*. https://doi.org/10.1016/j.fuel.2020.117066

EPIAS. (2024). *EPIAS Transparency Platform*. https://seffaflik.epias.com.tr/home

Eren, Y., & Küçükdemiral, İ. (2024). A comprehensive review on deep learning approaches for short-term load forecasting. *Renewable and Sustainable Energy Reviews*, *189*, 114031. https://doi.org/https://doi.org/10.1016/j.rser.2023.114031

Fang, J., Li, S., Wu, Y., He, M., & Xu, F. (2025). Research on an intelligent fault diagnosis method for nuclear power plants based on ETCN-SSA combined algorithm. *Annals of Nuclear Energy*, *213*, 111138. https://doi.org/https://doi.org/10.1016/j.anucene.2024.111138

Gaboitaolelwe, J., Zungeru, A. M., Yahya, A., Lebekwe, C. K., Vinod, D. N., & Salau, A. O. (2023). Machine Learning Based Solar Photovoltaic Power Forecasting: A Review and Comparison. In *IEEE Access* (Vol. 11, pp. 40820–40845). Institute of Electrical and Electronics Engineers Inc. https://doi.org/10.1109/ACCESS.2023.3270041

Gerassimidou, S., Velis, C. A., Williams, P. T., & Komilis, D. (2020). Characterisation and composition identification of waste-derived fuels obtained from municipal solid waste using thermogravimetry: A review. In *Waste Management and Research* (Vol. 38, Issue 9, pp. 942–965). SAGE Publications Ltd. https://doi.org/10.1177/0734242X20941085

Ghugare, S. B., & Tambe, S. S. (2017). Genetic programming based high performing correlations for prediction of higher heating value of coals of different ranks and from diverse geographies. *Journal of the Energy Institute*, *90*(3), 476–484. https://doi.org/10.1016/j.joei.2016.03.002

Gidom, M., Kökçam, A. H., & Uyaroğlu, Y. (2024). Short-Term Wind Speed Forecasting Using Nonlinear Autoregressive Neural Network: A Case Study in Kocaeli-Türkiye. *Electric Power Components and Systems*, *52*(3). https://doi.org/10.1080/15325008.2023.2220688

Grunau, C., Özüdoğru, A. A., Rozhoň, V., & Tětek, J. (2022). *A Nearly Tight Analysis of Greedy k-means++*. arXiv. https://doi.org/10.48550/ARXIV.2207.07949

Gu, B., Zhang, T., Meng, H., & Zhang, J. (2021). Short-term forecasting and uncertainty analysis of wind power based on long short-term memory, cloud model and non-parametric kernel density estimation. *Renewable Energy*, *164*. https://doi.org/10.1016/j.renene.2020.09.087

Güleç, F., Pekaslan, D., Williams, O., & Lester, E. (2022). Predictability of higher heating value of biomass feedstocks via proximate and ultimate analyses – A comprehensive study of artificial neural network applications. *Fuel*, *320*. https://doi.org/10.1016/j.fuel.2022.123944

Guo, B., Walter, V., Hornung, U., & Dahmen, N. (2019). Hydrothermal liquefaction of Chlorella vulgaris and Nannochloropsis gaditana in a continuous stirred tank reactor and hydrotreating of biocrude by nickel catalysts. *Fuel Processing Technology*, *191*, 168–180. https://doi.org/10.1016/j.fuproc.2019.04.003

Ha, B., Nam, S., Byun, J., Han, J., & Hwangbo, S. (2024). Stochastic techno-economic assessment of future renewable energy networks based on integrated deep-learning framework: A case study of South Korea. *Chemical Engineering Journal*, *485*. https://doi.org/10.1016/j.cej.2024.150050

Hancer, E., Xue, B., & Zhang, M. (2020). A survey on feature selection approaches for clustering. *Artificial Intelligence Review*, *53*(6), 4519–4545. https://doi.org/10.1007/s10462-019-09800-w

Harris, S. J., Harris, D. J., & Li, C. (2017). Failure statistics for commercial lithium ion batteries: A study of 24 pouch cells. *Journal of Power Sources*, *342*, 589–597. https://doi.org/10.1016/j.jpowsour.2016.12.083

Hippert, H. S., Pedreira, C. E., & Souza, R. C. (2001). Neural networks for short-term load forecasting: A review and evaluation. *IEEE Transactions on Power Systems*, *16*(1), 44 – 55. https://doi.org/10.1109/59.910780

Hissel, D., Candusso, D., & Harel, F. (2007). Fuzzy-Clustering Durability Diagnosis of Polymer Electrolyte Fuel Cells Dedicated to Transportation Applications. *IEEE Transactions on Vehicular Technology*, *56*(5), 2414–2420. https://doi.org/10.1109/TVT.2007.898389

Hoque, N., Bhattacharyya, D. K., & Kalita, J. K. (2014). MIFS-ND: A mutual information-based feature selection method. *Expert Systems with Applications*, *41*(14), 6371–6385. https://doi.org/10.1016/j.eswa.2014.04.019

Hosseinpour, S., Aghbashlo, M., & Tabatabaei, M. (2018). Biomass higher heating value (HHV) modeling on the basis of proximate analysis using iterative network-based fuzzy partial least squares coupled with principle component analysis (PCA-INFPLS). *Fuel*, *222*, 1–10. https://doi.org/10.1016/j.fuel.2018.02.126

Hu, Z., Li, Y., & Yang, Z. (2018). Improving Convolutional Neural Network Using Pseudo Derivative ReLU. *2018 5th International Conference on Systems and Informatics (ICSAI)*, 283–287. https://doi.org/10.1109/ICSAI.2018.8599372

Huang, Q., Li, J., & Zhu, M. (2020). An improved convolutional neural network with load range discretization for probabilistic load forecasting. *Energy*, *203*. https://doi.org/10.1016/j.energy.2020.117902

Ighalo, J. O., Igwegbe, C. A., & Adeniyi, A. G. (2021). Multi-layer perceptron artificial neural network (MLP-ANN) prediction of biomass higher heating value (HHV) using combined biomass proximate and ultimate analysis data. *Modeling Earth Systems and Environment*. https://doi.org/10.1007/s40808-021-01276-4

Insel, M. A., Sadikoglu, H., & Melikoglu, M. (2022). Assessment and determination of 2030 onshore wind and solar PV energy targets of Türkiye considering several investment and cost scenarios. *Results in Engineering*, *16*. https://doi.org/10.1016/j.rineng.2022.100733

Jiang, L., Du, H., Bu, Y., Zhao, C., Lu, H., & Yan, J. (2024). Deep learning-based multilabel compound-fault diagnosis in centrifugal pumps. *Ocean Engineering*, *314*. https://doi.org/10.1016/j.oceaneng.2024.119697

Jin, J., Yin, F., Xu, Y., & Zhang, J. (2022). Learning a Model with the Most Generality for Small-Sample Problems. *ACM International Conference Proceeding Series*. https://doi.org/10.1145/3579731.3579814

Jollife, I. T., & Cadima, J. (2016). Principal component analysis: A review and recent developments. In *Philosophical Transactions of the Royal Society A: Mathematical, Physical and Engineering Sciences* (Vol. 374, Issue 2065). Royal Society of London. https://doi.org/10.1098/rsta.2015.0202

Kampker, A., Heimes, H., Offermanns, C., Wennemar, S., Robben, T., & Lackner, N. (2023). Optimizing the Cell Finishing Process: An Overview of Steps, Technologies, and Trends. In *World Electric Vehicle Journal* (Vol. 14, Issue 4). MDPI. https://doi.org/10.3390/wevj14040096

Karakuş, O., Kuruoğlu, E. E., & Altinkaya, M. A. (2017). One-day ahead wind speed/power prediction based on polynomial autoregressive model. *IET Renewable Power Generation*, *11*(11). https://doi.org/10.1049/iet-rpg.2016.0972

Karthikeyan, M., Manimegalai, D., & Rajagopal, K. (2025). Enhancing voltage control and regulation in smart micro-grids through deep learning - optimized EV reactive power management. *Energy Reports*, *13*, 1095–1107. https://doi.org/10.1016/j.egyr.2024.12.072

Khan, M., Raza Naqvi, S., Ullah, Z., Ali Ammar Taqvi, S., Nouman Aslam Khan, M., Farooq, W., Taqi Mehran, M., Juchelková, D., & Štěpanec, L. (2023). Applications of machine learning in thermochemical conversion of biomass-A review. *Fuel*, *332*. https://doi.org/10.1016/j.fuel.2022.126055

Khosravi, A., Koury, R. N. N., Machado, L., & Pabon, J. J. G. (2018). Prediction of wind speed and wind direction using artificial neural network, support vector regression and adaptive neuro-fuzzy inference system. *Sustainable Energy Technologies and Assessments*, *25*. https://doi.org/10.1016/j.seta.2018.01.001

Kim, D., Ryu, G., Moon, C., & Kim, B. (2024). Accuracy of a short-term wind power forecasting model based on deep learning using LiDAR-SCADA integration: A case study of the 400-MW Anholt offshore wind farm. *Applied Energy*, *373*. https://doi.org/10.1016/j.apenergy.2024.123882

Kocer, A. (2024). Prediction of the higher heating values of biomass using machine learning methods based on proximate and ultimate analysis. *Journal of Mechanical Science and Technology*, *38*(3), 1569–1574. https://doi.org/10.1007/s12206-024-0247-1

Koeman Mike and Heskes, T. (2014). Mutual Information Estimation with Random Forests. In K. S. and W. K. W. and T. A. and H. K. Loo Chu Kiong and Yap (Ed.), *Neural Information Processing* (pp. 524–531). Springer International Publishing.

Kotu, V., & Deshpande, B. (2019). Chapter 4 - Classification. In V. Kotu & B. Deshpande (Eds.), *Data Science (Second Edition)* (Second Edition, pp. 65–

163). Morgan Kaufmann. https://doi.org/https://doi.org/10.1016/B978-0-12-814761-0.00004-6

Kumar, V., Singhal, V. K., Kushwaha, A., Agarwal, M., & Gupta, A. (2017). Wind Speed & Power Forecasting using Artificial Neural Network (NARX) for new York Wind Energy Farm. *Journal for Research*.

Lakshmanaprakash, S., Abirami, A., Madanachitran, R., Mekala, R., & Vaishali, V. H. (2025). DON: Deep Optimized Network model based on Coot and Convoluted Recurrent learning algorithms for healthcare monitoring in IoMT systems. *Measurement: Journal of the International Measurement Confederation*, *242*. https://doi.org/10.1016/j.measurement.2024.116226

Laszakovits, J. R., & MacKay, A. A. (2022). Data-Based Chemical Class Regions for Van Krevelen Diagrams. *Journal of the American Society for Mass Spectrometry*, *33*(1), 198–202. https://doi.org/10.1021/jasms.1c00230

Le, T., Vo, M. T., Kieu, T., Hwang, E., Rho, S., & Baik, S. W. (2020). Multiple electric energy consumption forecasting using a cluster-based strategy for transfer learning in smart building. *Sensors (Switzerland)*, *20*(9). https://doi.org/10.3390/s20092668

Lee, H., Bere, G., Kim, K., Ochoa, J. J., Park, J., & Kim, T. (2020). Deep Learning-Based False Sensor Data Detection for Battery Energy Storage Systems. *2020 IEEE CyberPELS (CyberPELS)*, 1–6. https://doi.org/10.1109/CyberPELS49534.2020.9311542

Lee, J., Lin, K.-Y. A., Jung, S., & Kwon, E. E. (2022). Hybrid Renewable Energy Systems Involving Thermochemical Conversion Process for Waste-to-Energy Strategy. *Chemical Engineering Journal*, 139218. https://doi.org/10.1016/j.cej.2022.139218

Li, P., Yang, H., Wu, H., Wang, Y., Su, H., Zheng, T., Zhu, F., Zhang, G., & Han, Y. (2024). Deep learning model for solar and wind energy forecasting considering Northwest China as an example. *Results in Engineering*, *24*. https://doi.org/10.1016/j.rineng.2024.102939

Liao, Q., Cao, D., Chen, Z., Blaabjerg, F., & Hu, W. (2023). Probabilistic wind power forecasting for newly-built wind farms based on multi-task Gaussian process method. *Renewable Energy*, *217*. https://doi.org/10.1016/j.renene.2023.119054

Lin, H., Sun, Q., & Chen, S. Q. (2020). Reducing exchange rate risks in international trade: A hybrid forecasting approach of CEEMDAN and multilayer LSTM. *Sustainability (Switzerland)*, *12*(6). https://doi.org/10.3390/su12062451

Liu, H., Liu, Y., Guo, X., Wu, H., Wang, H., & Liu, Y. (2023). An energy consumption prediction method for HVAC systems using energy storage based on time series shifting and deep learning. *Energy and Buildings*, *298*. https://doi.org/10.1016/j.enbuild.2023.113508

Liu, H., Tian, H. Q., Liang, X. F., & Li, Y. F. (2015). Wind speed forecasting approach using secondary decomposition algorithm and Elman neural networks. *Applied Energy*, *157*. https://doi.org/10.1016/j.apenergy.2015.08.014

Liu, H., Zhao, Y., Zaporowska, A., & Skaf, Z. (2023). A machine learning-based clustering approach to diagnose multi-component degradation of aircraft fuel systems. *Neural Computing and Applications*, *35*(4), 2973–2989. https://doi.org/10.1007/s00521-021-06531-4

Liu, S., Sun, Z., Sun, Y., & Kong, D. (2024). Short-term prediction of wind power based on grey wolf optimization Elman neural network algorithm. *Journal of Physics: Conference Series*, *2703*(1). https://doi.org/10.1088/1742-6596/2703/1/012043

Luo, X., & Oyedele, L. O. (2022). A self-adaptive deep learning model for building electricity load prediction with moving horizon. *Machine Learning with Applications*, *7*. https://doi.org/10.1016/j.mlwa.2022.100257

Lv, X., Chen, S., Zeng, W., Liu, Y., Wang, C., Zhou, S., Song, S., & Shi, B. (2024). Study of hydrate generation risk in gas-saturated oil-water emulsion system based on artificial intelligence. *Chemical Engineering Research and Design*, *204*, 137–146. https://doi.org/10.1016/j.cherd.2024.02.034

Ma, L., Tian, J., Zhang, T., Guo, Q., & Hu, C. (2024). Accurate and efficient remaining useful life prediction of batteries enabled by physics-informed machine learning. *Journal of Energy Chemistry*, *91*, 512–521. https://doi.org/10.1016/j.jechem.2023.12.043

Macedo, F., Valadas, R., Carrasquinha, E., Oliveira, M. R., & Pacheco, A. (2022). Feature selection using Decomposed Mutual Information Maximization. *Neurocomputing*, *513*, 215–232. https://doi.org/10.1016/j.neucom.2022.09.101

Majumder, A. K., Jain, R., Banerjee, P., & Barnwal, J. P. (2008). Development of a new proximate analysis based correlation to predict calorific value of coal. *Fuel*, *87*(13–14), 3077–3081. https://doi.org/10.1016/j.fuel.2008.04.008

Masdoua, Y., Boukhnifer, M., Adjallah, K. H., & Benterki, A. (2023). Fault detection and diagnosis in AHU system using deep learning approach. *Journal of the Franklin Institute*, *360*(17), 13574–13595. https://doi.org/10.1016/j.jfranklin.2023.09.046

MathWorks. (2022a). *Assess and improve predictive performance of models*. https://www.mathworks.com/discovery/cross-validation.html#:~:text=Holdout%3A%20Partitions%20data%20randomly%20into,caution%20on%20small%20data%20sets.

MathWorks. (2022b). *Bayesian Optimization Algorithm*. https://www.mathworks.com/help/stats/bayesian-optimization-algorithm.html#bvaz8tr-1

MathWorks. (2022c). *Choose a Multilayer Neural Network Training Function*. https://www.mathworks.com/help/deeplearning/ug/choose-a-multilayer-neural-network-training-function.html

MathWorks. (2022). *Relieff*. https://www.mathworks.com/help/stats/relieff.html

Mishra, L., Dinesh, B., Kavyassree, P. M., & Mishra, N. (2024). *A Google Trend enhanced deep learning model for the prediction of renewable energy asset price*. https://doi.org/10.5281/zenodo.1

Mohammadi, H., Jokar, S., Mohammadi, M., Kavousifard, A., & Dabbaghjamanesh, M. (2022). AI-based Optimal scheduling of Renewable AC Microgrids with bidirectional LSTM-Based Wind Power Forecasting. *Electrical Engineering and Systems Science*.

Mohseni, S., Brent, A. C., Kelly, S., & Browne, W. N. (2022). Demand response-integrated investment and operational planning of renewable and sustainable energy systems considering forecast uncertainties: A systematic review. *Renewable and Sustainable Energy Reviews*, *158*. https://doi.org/10.1016/j.rser.2022.112095

Muench, S., & Guenther, E. (2013). A systematic review of bioenergy life cycle assessments. In *Applied Energy* (Vol. 112, pp. 257–273). Elsevier Ltd. https://doi.org/10.1016/j.apenergy.2013.06.001

Napitupulu, H. Y. P., Nugraha, I. G. D., & Sari, R. F. (2024). Development of optimization control system for chiller plant based on a predictive model with Multi Stack LSTM and Deep Learning Neural Network Multi Output. *Journal of Building Engineering*, *98*. https://doi.org/10.1016/j.jobe.2024.111029

NASA. (2024). *NASA Power DAV*. https://power.larc.nasa.gov/data-access-viewer/

Nasir, I. M., Khan, M. A., Yasmin, M., Shah, J. H., Gabryel, M., Scherer, R., & Damaševičius, R. (2020). Pearson Correlation-Based Feature Selection for Document Classification Using Balanced Training. *Sensors*, *20*(23). https://doi.org/10.3390/s20236793

Nasiri, H., & Alavi, S. A. (2022). A Novel Framework Based on Deep Learning and ANOVA Feature Selection Method for Diagnosis of COVID-19 Cases from Chest X-Ray Images. *Computational Intelligence and Neuroscience*, *2022*. https://doi.org/10.1155/2022/4694567

Naveed, M. H., Khan, M. N. A., Mukarram, M., Naqvi, S. R., Abdullah, A., Haq, Z. U., Ullah, H., & Mohamadi, H. Al. (2024). Cellulosic biomass fermentation for biofuel production: Review of artificial intelligence approaches. In *Renewable and Sustainable Energy Reviews* (Vol. 189). Elsevier Ltd. https://doi.org/10.1016/j.rser.2023.113906

Netherlands Enterprise Agency. (2019). *Guidance on the classification of biomass: categories and NTA 8003 codes under the SDE+ scheme*.

Nielsen, H. A., Nielsen, T. S., Madsen, H., San Isidro Pindado, M. J., & Marti, I. (2007). Optimal combination of wind power forecasts. *Wind Energy*, *10*(5). https://doi.org/10.1002/we.237

Niu, Z., Han, X., Zhang, D., Wu, Y., & Lan, S. (2024). Interpretable wind power forecasting combining seasonal-trend representations learning with temporal fusion transformers architecture. *Energy*, *306*. https://doi.org/10.1016/j.energy.2024.132482

Nøkland, A. (2016). Direct feedback alignment provides learning in deep neural networks. *Advances in Neural Information Processing Systems*.

Noushabadi, A. S., Dashti, A., Ahmadijokani, F., Hu, J., & Mohammadi, A. H. (2021). Estimation of higher heating values (HHVs) of biomass fuels based on ultimate analysis using machine learning techniques and improved equation.

Renewable Energy, *179*, 550–562. https://doi.org/10.1016/j.renene.2021.07.003

Nunes, L. J. R., De Oliveira Matias, J. C., & Da Silva Catalão, J. P. (2018). Chapter 1 - Introduction. In L. J. R. Nunes, J. C. De Oliveira Matias, & J. P. Da Silva Catalão (Eds.), *Torrefaction of Biomass for Energy Applications* (pp. 1–43). Academic Press. https://doi.org/https://doi.org/10.1016/B978-0-12-809462-4.00001-8

Pagoni, I., & Psaraki-Kalouptsidi, V. (2017). Calculation of aircraft fuel consumption and CO2 emissions based on path profile estimation by clustering and registration. *Transportation Research Part D: Transport and Environment*, *54*, 172–190. https://doi.org/10.1016/j.trd.2017.05.006

Pedregosa, F., Varoquaux, G., Gramfort, A., Michel V. and Thirion, B., Grisel, O., Blondel, M., Prettenhofer P. and Weiss, R., Dubourg, V., Vanderplas, J., Passos, A., Cournapeau, D., Brucher, M., Perrot, M., & Duchesnay, E. (2011). Scikit-learn: Machine Learning in Python. *Journal of Machine Learning Research*, *12*, 2825–2830.

Phyllis2. (2023). Database for (treated) biomass, algae, feedstocks for biogas production and biochar. In *TNO Biobased and Circular Technologies*. https://phyllis.nl/

Podlasek, S., Jankowski, M., Bałazy, P., Lalik, K., & Figaj, R. (2024). Application of ANN control algorithm for optimizing performance of a hybrid ORC power plant. *Energy*, *306*, 132082. https://doi.org/https://doi.org/10.1016/j.energy.2024.132082

Poudel, J., Karki, S., & Oh, S. C. (2018). Valorization of waste wood as a solid fuel by torrefaction. *Energies*, *11*(7). https://doi.org/10.3390/en11071641

Pouliezos A. D. and Stavrakakis, G. S. (1994). Fault Diagnosis Using Artificial Neural Networks (ANNs). In *Real Time Fault Monitoring of Industrial Processes* (pp. 369–429). Springer Netherlands. https://doi.org/10.1007/978-94-015-8300-8_5

Qiu, W., Yang, Y., Song, J., Que, W., Liu, Z., Weng, H., Wu, J., & Wu, J. (2025). A deep-learning-based multiobjective optimization for the design of in-situ uranium leaching system under multiple uncertainties. *Journal of Hydrology*, *651*. https://doi.org/10.1016/j.jhydrol.2024.132576

Rajagopalan, S., & Santoso, S. (2009). Wind power forecasting and error analysis using the autoregressive moving average modeling. *2009 IEEE Power and Energy Society General Meeting, PES '09*. https://doi.org/10.1109/PES.2009.5276019

Ramesh, S., Manikandan, T., Gnanajeyaraman, R., Arul, U., Michael, G., & Selvakumar, A. (2023). Vehicular network energy storage system with renewable analysis using deep learning architectures. *Computers and Electrical Engineering*, *110*. https://doi.org/10.1016/j.compeleceng.2023.108801

Rand, W. M. (1971). Objective Criteria for the Evaluation of Clustering Methods. *Journal of the American Statistical Association*, *66*(336), 846–850. https://doi.org/10.1080/01621459.1971.10482356

Ricci, L., & Martínez, R. (2008). Adjusted R2-type measures for Tweedie models. *Computational Statistics and Data Analysis*, *52*(3), 1650–1660. https://doi.org/10.1016/j.csda.2007.05.017

Robnik-Sikonja, M., & Kononenko, I. (2003). *Theoretical and Empirical Analysis of ReliefF and RReliefF* (Vol. 53).

Rosenberg, A., & Hirschberg, J. (2007). *V-Measure: A Conditional Entropy-Based External Cluster Evaluation Measure. Multi-Objective Genetic Programming for Visual Analytics View project V-Measure: A conditional entropy-based external cluster evaluation measure*. https://www.researchgate.net/publication/221012656

Ross, A. B., Jones, J. M., Kubacki, M. L., & Bridgeman, T. (2008). Classification of macroalgae as fuel and its thermochemical behaviour. *Bioresource Technology*, *99*(14), 6494–6504. https://doi.org/10.1016/j.biortech.2007.11.036

Rousseeuw, P. J. (1987). Silhouettes: A graphical aid to the interpretation and validation of cluster analysis. *Journal of Computational and Applied Mathematics*, *20*, 53–65. https://doi.org/https://doi.org/10.1016/0377-0427(87)90125-7

Ruiz-Moreno, S., Gallego, A. J., & Camacho, E. F. (2023). Artificial neural network-based fault detection and isolation in a parabolic-trough solar plant with defocusing strategy. *Solar Energy*, *262*. https://doi.org/10.1016/j.solener.2023.111909

Salman, A. G., Heryadi, Y., Abdurahman, E., & Suparta, W. (2018). Single Layer & Multi-layer Long Short-Term Memory (LSTM) Model with Intermediate Variables for Weather Forecasting. *Procedia Computer Science*, *135*. https://doi.org/10.1016/j.procs.2018.08.153

Sancho, A., Ribeiro, J. C., Reis, M. S., & Martins, F. G. (2022). Cluster analysis of crude oils with k-means based on their physicochemical properties. *Computers and Chemical Engineering*, *157*. https://doi.org/10.1016/j.compchemeng.2021.107633

Sankaranarayanan, P., & Rengaswamy, R. (2022). CDiNN – Convex difference neural networks. *Neurocomputing*, *495*, 153–168. https://doi.org/10.1016/j.neucom.2022.01.024

Schmuch, R., Wagner, R., Hörpel, G., Placke, T., & Winter, M. (2018). Performance and cost of materials for lithium-based rechargeable automotive batteries. In *Nature Energy* (Vol. 3, Issue 4, pp. 267–278). Nature Publishing Group. https://doi.org/10.1038/s41560-018-0107-2

Scikit-Learn. (2023a). *Clustering*. https://scikit-learn.org/stable/modules/clustering.html#clustering

Scikit-Learn. (2023b). *sklearn.cluster.KMeans*. https://scikit-learn.org/stable/modules/generated/sklearn.cluster.KMeans.html

Scikit-Learn. (2023c). *sklearn.metrics.mutual_info_score*. https://scikit-learn.org/stable/modules/generated/sklearn.metrics.mutual_info_score.html

Sethi, M. R., Subba, A. B., Faisal, M., Sahoo, S., & Koteswara Raju, D. (2024a). Fault diagnosis of wind turbine blades with continuous wavelet transform

based deep learning model using vibration signal. *Engineering Applications of Artificial Intelligence*, *138*. https://doi.org/10.1016/j.engappai.2024.109372

Sethi, M. R., Subba, A. B., Faisal, M., Sahoo, S., & Koteswara Raju, D. (2024b). Fault diagnosis of wind turbine blades with continuous wavelet transform based deep learning model using vibration signal. *Engineering Applications of Artificial Intelligence*, *138*. https://doi.org/10.1016/j.engappai.2024.109372

Sezer, S., Kartal, F., & Özveren, U. (2022). Prediction of combustion reactivity for lignocellulosic fuels by means of machine learning. *Journal of Thermal Analysis and Calorimetry*. https://doi.org/10.1007/s10973-022-11208-8

Shadangi, K. P., Sarangi, P. K., & Behera, A. K. (2023). Chapter 3 - Characterization techniques of biomass: physico-chemical, elemental, and biological. In K. P. Shadangi, P. K. Sarangi, K. Mohanty, I. Deniz, & A. R. Kiran Gollakota (Eds.), *Bioenergy Engineering* (pp. 51–66). Woodhead Publishing. https://doi.org/https://doi.org/10.1016/B978-0-323-98363-1.00022-3

Shao, B., Song, D., Bian, G., & Zhao, Y. (2021). Wind Speed Forecast Based on the LSTM Neural Network Optimized by the Firework Algorithm. *Advances in Materials Science and Engineering*, *2021*. https://doi.org/10.1155/2021/4874757

Shirazi, Z. A., de Souza, C. P. E., Kashef, R., & Rodrigues, F. F. (2020). Deep learning in the healthcare industry: Theory and Applications. In *Computational Intelligence and Soft Computing Applications in Healthcare Management Science*. https://doi.org/10.4018/978-1-7998-2581-4.ch010

Simsek, A. I., Koç, E., Desticioglu Tasdemir, B., Aksöz, A., Turkoglu, M., & Sengur, A. (2024). Deep Learning Forecasting Model for Market Demand of Electric Vehicles. *Applied Sciences (Switzerland)*, *14*(23). https://doi.org/10.3390/app142310974

Srinivasan, C., & Sheeba Joice, C. (2025). Bio-inspired optimizer with deep learning model for energy management system in electric vehicles. *Sustainable Computing: Informatics and Systems*, *45*. https://doi.org/10.1016/j.suscom.2025.101082

Steinley, D. (2004). Properties of the Hubert-Arabie adjusted Rand index. *Psychological Methods*, *9*(3), 386–396. https://doi.org/10.1037/1082-989X.9.3.386

Subhash, G. v., Sivapirakasam, S. P., Mohan, S., & Harisivasri Phanindra, K. (2021). Production, characterization and assessment of reformulated bio-mixture fuel from a mixture of various raw feedstock's and the effect of n-butanol as an additive on bio-mixture blends. *Biomass and Bioenergy*, *154*. https://doi.org/10.1016/j.biombioe.2021.106246

Tang, M., Wang, W., Zhen, X., An, B., Zhang, Y., & Yan, Y. (2024). Robust control of wind turbines to reduce wind power fluctuation. *Energy Science & Engineering*, *12*(5), 1818–1834. https://doi.org/https://doi.org/10.1002/ese3.1680

Tiwari, A., & Kumar, A. (2018). Comparative Analysis of Optimized Algorithms for Ontology Clustering. *2018 5th IEEE Uttar Pradesh Section International*

Conference on Electrical, Electronics and Computer Engineering (UPCON), 1–7. https://doi.org/10.1109/UPCON.2018.8597150

Ullah, Z., Khan, M., Naqvi, S. R., Khan, M. N. A., Farooq, W., Anjum, M. W., Yaqub, M. W., AlMohamadi, H., & Almomani, F. (2022). An integrated framework of data-driven, metaheuristic, and mechanistic modeling approach for biomass pyrolysis. *Process Safety and Environmental Protection*, *162*, 337–345. https://doi.org/10.1016/j.psep.2022.04.013

United Nations. (2015). *Sustainable Developement Goals*. https://sdgs.un.org/goals#goals

Uzun, H., Yıldız, Z., Goldfarb, J. L., & Ceylan, S. (2017). Improved prediction of higher heating value of biomass using an artificial neural network model based on proximate analysis. *Bioresource Technology*, *234*, 122–130. https://doi.org/10.1016/j.biortech.2017.03.015

Van Krevelen, D. W. (1950). Graphical-statistical method for the study of structure and reaction processes of coal. *Fuel*, *29*, 269–284.

Vandeginste, B. G. M., Massart, D. L., Buydens, L. M. C., De Jong, S., Lewi, P. J., & Smeyers-Verbeke, J. (1998). Chapter 30 - Cluster analysis. In B. G. M. Vandeginste, D. L. Massart, L. M. C. Buydens, S. De Jong, P. J. Lewi, & J. Smeyers-Verbeke (Eds.), *Handbook of Chemometrics and Qualimetrics: Part B* (Vol. 20, pp. 57–86). Elsevier. https://doi.org/https://doi.org/10.1016/S0922-3487(98)80040-3

Venkatasubramanian, V., Rengaswamy, R., Yin, K., & Kavuri, S. N. (2003). A review of process fault detection and diagnosis Part I: Quantitative model-based methods. *Computers and Chemical Engineering*, *27*, 293–311.

Vounatsos, P., Atsonios, K., Itskos, G., Agraniotis, M., Grammelis, P., & Kakaras, E. (2016). Classification of Refuse Derived Fuel (RDF) and Model Development of a Novel Thermal Utilization Concept Through Air-Gasification. *Waste and Biomass Valorization*, *7*(5), 1297–1308. https://doi.org/10.1007/s12649-016-9520-6

Walczak, S., & Cerpa, N. (2003). Artificial Neural Networks. In R. A. Meyers (Ed.), *Encyclopedia of Physical Science and Technology (Third Edition)* (Third Edition, pp. 631–645). Academic Press. https://doi.org/https://doi.org/10.1016/B0-12-227410-5/00837-1

Wang, H., Zhou, H., Chen, Y., Yang, L., & Bi, W. (2025). Deep learning GAN-based fault detection and diagnosis method for building air-conditioning systems. *Sustainable Cities and Society*, *118*. https://doi.org/10.1016/j.scs.2024.106068

Wang, L., Gao, Z., Pan, Z., Guo, X., & Bou-Zeid, E. (2013). Evaluation of turbulent surface flux parameterizations over tall grass in a beijing suburb. *Journal of Hydrometeorology*, *14*(5). https://doi.org/10.1175/JHM-D-12-0103.1

Wang, P., Cui, Y., Tao, H., Xu, X., & Yang, S. (2025). Machining parameter optimization for a batch milling system using multi-task deep reinforcement learning. *Journal of Manufacturing Systems*, *78*, 124–152. https://doi.org/10.1016/j.jmsy.2024.11.013

Wang, Q., Chen, S., Zeng, J., Du, W., & Wei, L. (2024). A deep learning fault diagnosis method for metro on-board detection on rail corrugation. *Engineering Failure Analysis*, *164*. https://doi.org/10.1016/j.engfailanal.2024.108662

Wang, Q., Li, Y., & Li, R. (2025). Integrating artificial intelligence in energy transition: A comprehensive review. In *Energy Strategy Reviews* (Vol. 57). Elsevier Ltd. https://doi.org/10.1016/j.esr.2024.101600

Wang, S., Rodriguez Alejandro, D. A., Kim, H., Kim, J. Y., Lee, Y. R., Nabgan, W., Hwang, B. W., Lee, D., Nam, H., & Ryu, H. J. (2022). Experimental investigation of plastic waste pyrolysis fuel and diesel blends combustion and its flue gas emission analysis in a 5 kW heater. *Energy*, *247*. https://doi.org/10.1016/j.energy.2022.123408

Wang, W., & Lu, Y. (2018). Analysis of the Mean Absolute Error (MAE) and the Root Mean Square Error (RMSE) in Assessing Rounding Model. *IOP Conference Series: Materials Science and Engineering*, *324*(1). https://doi.org/10.1088/1757-899X/324/1/012049

Wang, Y., Jiang, W., Wang, C., Song, Q., Zhang, T., Dong, Q., & Li, X. (2023). An electricity load forecasting model based on multilayer dilated LSTM network and attention mechanism. *Frontiers in Energy Research*, *11*. https://doi.org/10.3389/fenrg.2023.1116465

Wang, Y., Li, D., Li, L., Sun, R., & Wang, S. (2024). A novel deep learning framework for rolling bearing fault diagnosis enhancement using VAE-augmented CNN model. *Heliyon*, *10*(15). https://doi.org/10.1016/j.heliyon.2024.e35407

Williams, B., Halloin, C., Löbel, W., Finklea, F., Lipke, E., Zweigerdt, R., & Cremaschi, S. (2020). Data-Driven Model Development for Cardiomyocyte Production Experimental Failure Prediction. *30th European Symposium on Computer Aided Process Engineering*, *48*, 1639–1644. https://doi.org/https://doi.org/10.1016/B978-0-12-823377-1.50274-3

Wu, C., Wang, J., Chen, X., Du, P., & Yang, W. (2020a). A novel hybrid system based on multi-objective optimization for wind speed forecasting. *Renewable Energy*, *146*, 149–165. https://doi.org/10.1016/j.renene.2019.04.157

Wu, C., Wang, J., Chen, X., Du, P., & Yang, W. (2020b). A novel hybrid system based on multi-objective optimization for wind speed forecasting. *Renewable Energy*, *146*, 149–165. https://doi.org/10.1016/j.renene.2019.04.157

Xiao, Z., Gao, B., Huang, X., Chen, Z., Li, C., & Tai, Y. (2024). An interpretable horizontal federated deep learning approach to improve short-term solar irradiance forecasting. *Journal of Cleaner Production*, *436*. https://doi.org/10.1016/j.jclepro.2024.140585

Xing, J., Luo, K., Wang, H., Gao, Z., & Fan, J. (2019a). A comprehensive study on estimating higher heating value of biomass from proximate and ultimate analysis with machine learning approaches. *Energy*, *188*. https://doi.org/10.1016/j.energy.2019.116077

Xing, J., Luo, K., Wang, H., Gao, Z., & Fan, J. (2019b). A comprehensive study on estimating higher heating value of biomass from proximate and ultimate

analysis with machine learning approaches. *Energy*, *188*, 116077. https://doi.org/10.1016/j.energy.2019.116077

Xu, Z., & Zhang, X. (2021). Short-Term wind power prediction of wind farms based on LSTM+NARX neural network. *Proceedings - 2021 International Conference on Computer Engineering and Application, ICCEA 2021*. https://doi.org/10.1109/ICCEA53728.2021.00035

Xue, X., Lv, J., Chen, H., Xu, G., & Li, Q. (2022). Thermodynamic and economic analyses of a new compressed air energy storage system incorporated with a waste-to-energy plant and a biogas power plant. *Energy*, *261*, 125367. https://doi.org/10.1016/j.energy.2022.125367

Yaka, H., Insel, M. A., Yucel, O., & Sadikoglu, H. (2022). A comparison of machine learning algorithms for estimation of higher heating values of biomass and fossil fuels from ultimate analysis. *Fuel*, *320*, 123971. https://doi.org/10.1016/j.fuel.2022.123971

Yan, T., Rashid, J., Saleem, M. S., Ahmad, S., & Faheem, M. (2024). A Hybrid Deep Learning Approach for Green Energy Forecasting in Asian Countries. *Computers, Materials and Continua*, *81*(2), 2685–2708. https://doi.org/10.32604/cmc.2024.058186

Yang, F., Cho, H., Zhang, H., Zhang, J., & Wu, Y. (2018). Artificial neural network (ANN) based prediction and optimization of an organic Rankine cycle (ORC) for diesel engine waste heat recovery. *Energy Conversion and Management*, *164*, 15–26. https://doi.org/10.1016/j.enconman.2018.02.062

Yates, L. A., Aandahl, Z., Richards, S. A., & Brook, B. W. (2023). Cross validation for model selection: A review with examples from ecology. *Ecological Monographs*, *93*(1), e1557. https://doi.org/https://doi.org/10.1002/ecm.1557

Yellowbrick. (2023). *Elbow Method*. https://www.scikit-yb.org/en/latest/api/cluster/elbow.html

Yin, W., Xia, H., Wang, Z., Yang, B., Zhang, J., Jiang, Y., & Miyombo, M. E. (2023). A fault diagnosis of nuclear power plant rotating machinery based on multi-sensor and deep residual neural network. *Annals of Nuclear Energy*, *185*, 109700. https://doi.org/https://doi.org/10.1016/j.anucene.2023.109700

Yu, L., Qin, S., Zhang, M., Shen, C., Jiang, T., & Guan, X. (2021). A Review of Deep Reinforcement Learning for Smart Building Energy Management. *IEEE Internet of Things Journal*, *8*(15), 12046–12063. https://doi.org/10.1109/JIOT.2021.3078462

Yu, R., Gao, J., Yu, M., Lu, W., Xu, T., Zhao, M., Zhang, J., Zhang, R., & Zhang, Z. (2019). LSTM-EFG for wind power forecasting based on sequential correlation features. *Future Generation Computer Systems*, *93*. https://doi.org/10.1016/j.future.2018.09.054

Zandie, M., Ng, H. K., Gan, S., Muhamad Said, M. F., & Cheng, X. (2023). Multi-input multi-output machine learning predictive model for engine performance and stability, emissions, combustion and ignition characteristics of diesel-biodiesel-gasoline blends. *Energy*, *262*. https://doi.org/10.1016/j.energy.2022.125425

Zhang, H., Chen, L., Qu, Y., Zhao, G., & Guo, Z. (2014). Support vector regression based on grid-search method for short-term wind power forecasting. *Journal of Applied Mathematics, 2014*. https://doi.org/10.1155/2014/835791

Zhang, J., Yan, J., Infield, D., Liu, Y., & Lien, F. sang. (2019). Short-term forecasting and uncertainty analysis of wind turbine power based on long short-term memory network and Gaussian mixture model. *Applied Energy*, *241*. https://doi.org/10.1016/j.apenergy.2019.03.044

Zhou, H., Long, Y., Meng, A., Li, Q., & Zhang, Y. (2015). Classification of municipal solid waste components for thermal conversion in waste-to-energy research. *Fuel*, *145*, 151–157. https://doi.org/10.1016/j.fuel.2014.12.015

Zhu, Y., Niu, Y., Tan, H., & Wang, X. (2014). Short review on the origin and countermeasure of biomass slagging in grate furnace. *Frontiers in Energy Research*, *2*, 7.

Zou, J., Gao, Y., Frieges, M. H., Börner, M. F., Kampker, A., & Li, W. (2024). Machine learning for battery quality classification and lifetime prediction using formation data. *Energy and AI*, *18*, 100451. https://doi.org/https://doi.org/10.1016/j.egyai.2024.100451

A
HIGHER HEATING VALUE ESTIMATION OF WASTES AND FUELS BY UTILIZING ARTIFICIAL NEURAL NETWORKS

All the supporting files of this section (S.F.E.1-5, Tables S.I.1-7, and Figures S.I.1-5) are available online at https://doi.org/10.1016/j.wasman.2024.05.044.

PUBLICATIONS FROM THE THESIS

Conference Paper

1. Insel, M. A., Yucel, O., & Sadikoglu, H. (2024). Wind Power Forecasting by using Advanced Artificial Neural Networks. 7th International Conferance on Engineering Sciences, Book of Abstracts, 11.

Papers

1. Insel, M. A., Yucel, O., & Sadikoglu, H. (2024). Higher heating value estimation of wastes and fuels from ultimate and proximate analysis by using artificial neural networks. *Waste Management*, *185*, 33–42. https://doi.org/10.1016/j.wasman.2024.05.044

2. Insel, M. A., Yucel, O., & Sadikoglu, H. (2024). Optimizing waste-to-energy conversion: Unveiling the potential of unsupervised clustering through the new HOM classification system. *Sustainable Energy Technologies and Assessments*, *65*, *103796*. https://doi.org/10.1016/j.seta.2024.103796